ABSTRACT

PALMIERI, RICHARD DARREN. Development and evaluation of a weather-based epidemiological model for the prediction of brown patch in creeping bentgrass. (Under the direction of Dev Niyogi.)

The turfgrass industry is one of the largest agricultural industries in the United States. The nature of turfgrass favors the long-term buildup of pests, including many fungi that cause disease (including *Rhizoctonia solani*, the causal agent of the brown patch turfgrass disease). To combat these diseases, turfgrass managers must frequently apply expensive, harmful fungicides to their turf. Previous studies have shown that fungal infections of turfgrass are related to meteorological conditions, and that weather-based epidemiological models can be used to help turfgrass managers reduce the number of fungicide applications they are required to make, while maintaining the aesthetic quality of their turf. However, these previously-developed epidemiological models had not been tested in North Carolina, and their efficacy in this state was in question. Therefore, this study was undertaken to determine if the Schumann and Fidanza epidemiological models for brown patch could be used in North Carolina.

Disease observations and weather data collected over the summers of 2003 and 2004 at the NC State Faculty Club Turfgrass Field Laboratory were combined, and resulted in the conclusion that both the Schumann and the Fidanza epidemiological models met only with very limited success in predicting brown patch outbreaks. However, several other conclusions were reached by the end of the study, including:

- The most accurate method for measuring brown patch activity is uncertain, as a smaller data set of disease incidence measures disagreed frequently with the once-daily observations of brown patch activity.

- Weather data from regional-scale observational networks, and from operational numerical weather prediction (NWP) models, can likely be used as a proxy for on-site weather measurements. When weather data from the Raleigh-Durham International Airport, and from the operational run of the then National Centers for Environmental Prediction Eta model were used as inputs into the epidemiological models above, the results varied little as compared to the results using weather data from an on-site observation station.

After determining that no existing epidemiological model provided accurate predictions of brown patch (assuming that the disease activity observations were sufficient; an assumption in question), an effort was made to develop a new epidemiological model was undertaken. Several statistical methods were used, including an autoregressive model and a logistic regression model, but neither was able to accurately explain brown patch activity. A process-based epidemiological model was also developed, under the assumption that hot, humid conditions are a necessary condition for the development of brown patch disease. While this model did not lead to an accurate predictive index, it was the most promising effort, typically hampered by high false alarm ratios. This leads to the conclusion that an investigation into those meteorological conditions that are unfavorable for disease development, when all other factors appear favorable, is likely in order.

Finally, a NWP model sensitivity study was undertaken using the Pennsylvania State University-National Center for Atmospheric Research Mesoscale Model (MM5). Two cases were chosen to represent two very different summertime regimes for North Carolina, and for each case, two MM5 runs were performed; one using a 5-layer soil model, the other using the NOAH land-surface model (LSM). It was found that large variability can exist between

model runs based on the land-surface parameterizations used (especially in convective regimes), and that in this study, these differences can be of a greater magnitude than those differences seen using varying sources of weather data as inputs for the epidemiological models.

# DEVELOPMENT AND EVALUATION OF A WEATHER-BASED EPIDEMIOLOGICAL MODEL FOR THE PREDICTION OF BROWN PATCH IN CREEPING BENTGRASS

by
**RICHARD DARREN PALMIERI**

A thesis submitted to the Graduate Faculty of
North Carolina State University
in partial fulfillment of the
requirement for the Degree of
Master of Science

**ATMOSPHERIC SCIENCES**

Raleigh, North Carolina

2005

**APPROVED BY:**

| | |
|---|---|
| _____ | _____ |
| Co-Chair of Advisory Committee | Co-Chair of Advisory Committee |
| *Dr. Dev Niyogi* | *Dr. Lane Tredway* |

_____
Member of the Advisory Committee
*Dr. Gary Lackmann*

## PERSONAL BIOGRAPHY

Richard Darren Palmieri was born on July 6, 1981 in Honolulu, Hawaii. Because his father was a member of the United States Army, he has had the pleasure of living in many parts of the country, including Massachusetts, New York, and Virginia, and Augsburg, Germany for a little over three years before finally moving to Fort Bragg, North Carolina. Richard graduated from Seventy-First High School in Fayetteville, North Carolina in May of 1999, and moved to Raleigh soon thereafter to attend North Carolina State University as an undergraduate student studying meteorology. He obtained his Bachelor of Science degree in Meteorology with a minor in Parks, Recreation, and Tourism Management in May 2003, and was admitted to pursue his Masters of Science degree in Atmospheric Sciences that August.

## ACKNOWLEDGEMENTS

This research was supported primarily by the Center for Turfgrass Environmental Research and Education (CENTERE). Additional support was also provided through: a NC State University Faculty Professional Development Award; the National Science Foundation ATM 0233780 (Dr. S. Nelson), the National Aeronautics and Space Administration (NASA) – Terrestrial Hydrology Program (NNG04GI84G, Dr. J. Entin), the NASA – Interdisciplinary Sciences Program (NNG04GL61G, Drs. J. Entgin and G. Gutman), the Naval Research Laboratory (NRL) Program Element 0602435 of the NRL Base Program project number BE-435-003 (Dr. T. Holt), and the United State Department of Agriculture (USDA) National Research Initiative Competitive Grants Program – Watershed Processes and Water Resources (Dr. Nancy Cavallaro, USDA; Dr. S. Islam, Tufts University). Meteorological observations from the Raleigh-Durham International Airport ASOS site were obtained through the State Climate Office of North Carolina's Climate Retrieval and Observations Network of the Southeast (CRONOS) Database, available online at www.nc-climate.ncsu.edu. Eta/NAM data was obtained from the National Climatic Data Center (NCDC)'s NOAA Operational Model Archive and Distribution System (NOMADS), available online at www.ncdc.noaa.gov. Thanks also to the University Consortium for Atmospheric Research – Constellation Observing System for Meteorology Ionosphere and Climage (Dr. B. Kuo and F. Chen), and the NSP – American Workforce and Research and Education Program through the Office of International Science and Engineering, for providing an opportunity to add an international component to my research by supporting a collaborative visit to the Institute of Urban Meteorology, and the Chinese Meteorological Administration, in Beijing, China.

It seems only appropriate to me to first and foremost thank my committee, starting with my co-advisor, Dr. Dev Niyogi. He took a chance with a kid that didn't exactly have the most prestigious undergraduate academic record, and I only hope that over the course of the last two or so years that I haven't let him down. Next, Dr. Lane Tredway, my co-advisor in Plant Pathology, has been incredibly helpful throughout the process of this work. Any knowledge I have of anything plant-pathology related is solely attributable to him. And, he got me a really nice computer to work on! Finally (but certainly not least), Dr. Gary Lackmann provided me a place to work, and had the unparalleled honor of dealing with me on a day-to-day basis. Don't underestimate the strength that must have taken.

Since grouping people will help me give this section some semblance of order, I'll next acknowledge several members of the Forecasting Research Lab. In looking at other masters' thesis lately, it seems almost obligatory to acknowledge Mike Brennan, and my thesis will be no exception. I lost count of the number of times he helped me with a computing problem somewhere around 127. I can almost guarantee I would have had to pay to replace a computer or two if it weren't for his help. Continuing, I'd definitely be remiss if I didn't thank Kelly Mahoney for all her help. The summer I started working on my research, I don't think I even knew what a c-shell script (or, for that matter, what a c-shell) was, so she wrote scripts for me to do data collection and manipulation, along with some FORTRAN programs. Having those programs to start with really got me over the learning curve, and even though she'll probably completely dismiss how helpful I'm making her out to be here as libel, her help really was instrumental in my success. I'm not trying to exclude anyone that works in that lab; every one of you were helpful along the way, and at the very

least had opportunity to listen to many, many stories about my life that you probably had little or no real interest in. But you all acted interested, and I appreciate it.

Three people that deserve recognition here defy a grouping other than "Other People that Helped Me." First, Chris Lauer, who developed a pretty extensive FORTRAN program to manipulate model grids and produce several turfgrass disease indices. It was work that took him a week or so in his spare time, that would've taken me months to figure out. Srikant Nalatwad put together our first attempt at a web site in support of the project, and his tireless work on that project is much appreciated. Finally, Eren Demirhan, a graduate student in the Department of Statistics here at NC State, was of immeasurable help while performing the statistical analysis presented in Section 5. His knowledge of both statistical methods and the SAS suite of programs is really what made that section possible.

Finally, I have to acknowledge my personal friends. While most of them had absolutely no impact on my actual thesis, and many of them probably don't even know what my research is on, they all made my complete college experience what it was, and I'll remember it for the rest of my life. People like Scott Barnes, Michelle Goff, and Brandon Scott, who helped me through those times as an undergraduate that I became completely disenfranchised with the whole idea of school, and contemplated a career in the fast food industry. People like Justin Ford and David Parker, who introduced me to the world of sports officiating, a hobby that I have been pursuing for nearly six years now, and that got me to New Orleans for New Years three years in a row. There's no better stress reliever than New Orleans at New Years. People like Zach Brown and Meredith Croke, two of the first people I met that came here from other schools for grad school. I think sometimes we all wondered if we were in grad school or in high school. And then there are people like Jackie Avise and

Melissa Rountree, who made very sure that I never took myself too seriously. I'll never forget my times with them…at least, not the ones that I have recollection of in the first place.

I'll inevitably leave about ten people off of this list that will come back later and say, "Hey, what about me? Remember when I showed you where you forgot to put a space in line 67 of that one program, and that's why it wouldn't work?" My bad. If I listed every person that helped me with my thesis in one way or another, I'd have the longest acknowledgements section in history. Hopefully the knowledge that I truly appreciated your help will suffice.

## TABLE OF CONTENTS

## LIST OF FIGURES

## LIST OF TABLES

## 1. Introduction

The turfgrass industry is one of the largest agricultural industries in the United States. From sports fields to golf courses to landscaping, the turfgrass industry is an integral party of society. In North Carolina alone, turfgrass is grown on over two million acres, with annual maintenance costs exceeding $1 billion. The total annual economic impact of the turfgrass industry in North Carolina's was $4.7 billion in 1999, including the economic effects of both maintenance costs and maintenance equipment costs [North Carolina Department of Agriculture and Consumer Services (NCDA&CS) 2000].

Turfgrass is a perennial agricultural product, often being grown in the same location for many years. This situation favors the long-term buildup of turfgrass pests, including many fungi that cause diseases. Due to the importance of aesthetic quality in turfgrass stands, tolerance for disease outbreaks is very low, and pesticides are applied frequently to reduce or eliminate the risk of infection. Currently, most turfgrass managers use a calendar-based pesticide application schedule. The applications are based principally on the manufacturer's recommendations related to the duration of the pesticide's effectiveness.

Turfgrass pesticides have evolved in recent years. Previous generations of pesticides were designed to provide long-term protection for a variety of turfgrass diseases. These pesticides, however, were toxic in nature, and posed both environmental and human health risks. The US Food Quality Protection Act (FQPA) of 1996 was written into law in order to regulate pesticide use. Specifically, the Act amended the Federal Insecticide, Fungicide, and Rodenticide Act, allowing the US Environmental Protection Agency to prescribe labeling and other regulatory requirements to prevent unreasonable adverse effects on health or the environment. In response to the FQPA, pesticide managers developed a new generation of

pesticides. While the newer pesticides are safer for the environment and have longer periods of efficacy than many of their predecessors, they are highly expensive, making a calendar-based application schedule impractical for many turfgrass managers. Accordingly, the accurate timing of pesticide applications has become much more critical than in the past.

In addition to the environmental considerations described above, the application of pesticides also represents a substantial portion of total turfgrass maintenance costs. In 1999, pesticide costs accounted for 5.7% of total maintenance costs (not including labor costs for pesticide application), or a cost of over $68 million (NCDA&CS 2000). When considering that nearly 50% of turfgrass maintenance costs are labor costs, and that a portion of these expenses are for the application of pesticides, the costs of pesticide application are even larger. If considering only those turfgrass industries for which disease control is essential (golf courses, professional sports, etc.) the non-labor costs for pesticide application are much higher. A large portion of this pesticide expense goes toward the purchase of fungicides to ward off fungal turfgrass diseases. For example, in 1993, nearly half of all U.S. golf course pesticide budgets were spent on fungicides (Jackson 1994). While there are a variety of fungicides available, per application costs can range from nearly $100/acre to in excess of $500/acre.

The combination of environmental and economic concerns detailed above has created pressure within the turfgrass industry to find ways to reduce the number of fungicide applications required to maintain high-quality turf. Weather-based decision aids for the timing of fungicide applications represent one such method of disease control (Tredway et al. 2004). Nutter et al. (1983) showed that fungal pathogens of turfgrasses are omnipresent, but the pathogens require favorable meteorological conditions in order to infect the turfgrass. By

identifying the meteorological factors that trigger disease development, it is possible to develop systems for the prediction of turfgrass disease development. Schumann et al. (1994) developed one such weather-based disease prediction system, and demonstrated that up to 50% of fungicide applications could be avoided while still providing adequate protection against disease.

One important turfgrass disease is *Rhizoctonia* blight, more commonly referred to as brown patch (Burpee and Martin 1992). *Rhizoctonia* blight is caused by *Rhizoctonia solani* (Piper and Coe 1919), and all cool-season turfgrasses cultivated in the United States are susceptible to infection by this pathogen (Smiley et al. 1992). One result of the general susceptibility of cool-season turfgrasses to *R. solani* is that large portions of fungicide expenditures are for control of this one disease. In 1993, for example, 30% of all fungicide expenditures for turfgrasses were for brown patch control (Jackson 1994).

The purpose of this study is to develop a weather-based epidemiological model for use as a decision aid to assist turfgrass managers in determining when to apply fungicides to prevent brown patch outbreaks. To do this:

- Several epidemiological models developed for other regions in the United States will be tested for their accuracy in central North Carolina (a secondary goal of this initial effort will be to determine if existing weather observation networks can be used as proxies for on-site measurements).
- Current epidemiological models will be modified, or new models will be developed, based on the skill they demonstrate forecasting brown patch infection.

- A meteorological model will be employed to test the sensitivity of the model's prediction of those meteorological parameters thought to be most related with disease activity to changes in model physics.

The remainder of this thesis is organized as follows: Chapter 2 will be a literature review, containing information on previously developed weather-based epidemiological models for brown patch. Chapter 3 will describe the experimental setup and methodology. Results describing the performance of two currently available epidemiological models will be presented in Chapter 4. In Chapter 5, observed weather conditions will be used in an attempt to develop a new weather-based epidemiological model for North Carolina. Tests on the sensitivity of model-forecasted output for the epidemiological models will be presented in Chapter 6. Conclusions will be presented in Chapter 7, followed by references and appendices.

## 2. Literature Review

### *2.1 Plant disease epidemiology*

Plant disease epidemiology (or, for the strict etymologists, epiphytology), is the study of disease development in plants. At its simplest, plant disease epidemiologists have defined two different categories of disease progress: monocyclic (those plant diseases that undergo one infection cycle per plant cycle) and polycyclic (those that undergo multiple infection cycles per plant cycle). Simple models can be defined to mathematically quantify the progress of disease (Amerson 2001). These models incorporate three of the four elements of the "disease tetrahedron," (which shows two-way interactions between man, pathogen, host, and environment) including pathogen, host, and environment (Zadoks and Schein 1979).

For monocyclic diseases, research has shown that disease progress is typically linear:

$$x = QRt, \quad (2.1)$$

where x represents a proportion of diseased plants to disease-free plants, t represents a time increment, Q is the amount of initial inoculum, and R is a proportionality constant that represents rate of disease progress per unit of inoculum, with units of per unit initial inoculum per unit time (Vanderplank 1963). For polycyclic diseases:

$$x = x_0 e^{rt} . \quad (2.2)$$

In Equation (2.2), $x_0$ is the proportion of disease at the start of the epidemic, r is a proportionality constant defined as the rate of disease increase per unit disease (units are per unit time), and t represents a time increment (Vanderplank 1963). In Equations (2.1) and (2.2), R and r, respectively, incorporate many factors, including the virulence of the pathogen in question, the resistance to infection inherent to the plant species in question, and other environmental factors (including meteorological).

Equations (2.1) and (2.2) are most representative of disease progress during early stages of an epidemic, as one would expect the rates to slow as the proportion of plants infected approaches 100%. Because the purpose of this study is to prevent the proportion of diseased turfgrass from reaching values anywhere near 100%, the above equations are adequate.

The mathematical models of disease progress presented in Equations (2.1) and (2.2) demonstrate how man can affect the rest of the disease tetrahedron. The linear nature of disease progress for monocyclic epidemics means that a reduction in any one of the three variables on the right side of Equation (2.1) would result in an equal reduction in the total disease proportion, regardless of the variable chosen. The exponential nature of disease progress for polycyclic epidemics, however, dictates that a reduction in the rate of disease increase [r in Equation (2.2)] or the time of infection (t) would have a much greater affect on the total disease proportion than a change in the initial disease proportion would ($x_0$, a quantity mathematically related to, but not exactly equal to, the quantity of the initial inoculum).

As was discussed earlier, the rate of infection is dependent on a number of variables, some of which are meteorological conditions. In reality, meteorological conditions affect both the rate and period of infection. In all cases, a pathogen needs favorable environmental conditions in order to actively spread. With all of this in mind, it is easy to draw the conclusion that knowledge of the specific environmental conditions that maximize the rate of infection would allow for the most appropriate timing of pesticide applications.

In this thesis, the above concepts are applied to the forecasting of a specific disease, *Rhizoctonia* blight (brown patch), in turfgrass. Previous studies with similar objectives are described in the next subsection.

*2.2 Studies linking meteorological conditions to brown patch activity*

The idea that a link exists between weather conditions and turfgrass disease outbreaks is not new. Dickinson (1930) performed some of the earliest research attempting to link the occurrence of turfgrass disease with weather conditions. His studies focused on brown patch, and he found that outbreaks often occurred on days following afternoon irrigation when the daytime maximum air temperature was between 26 and 35ºC, and the overnight minimum air temperature was between 15 and 21ºC. He hypothesized that the period of lower temperature was required for sclerotial germination. A few years later, Dahl (1933) found that brown patch developed when the minimum air temperature was greater than 21ºC, contradicting Dickinson's finding that a period of low temperatures was necessary for germination. Kerr (1956) confirmed that either free moisture or high relative humidities (≥ 98%) were necessary for disease development, while Bloom and Couch (1960) found that soil moisture was not a factor in the development of this disease.

These studies were met with skepticism (L. Tredway 2005, personal communication) and were unable to create widespread interest in the use of weather-based epidemiological models for timing fungicide applications. It is likely that many factors contributed to the reluctance shown by turfgrass managers to incorporate the epidemiological models in their disease prevention systems. First, the results generated by the initial round of studies described above did not produce satisfactory results for the low tolerance for disease

necessary in the turfgrass industry. Collection of appropriate weather data was a concern, primarily due to the prohibitive cost of establishing a weather station on-site. Additionally, as a whole our ability to forecast the weather accurately was suspect. However, as our ability to forecast the weather has improved drastically from the early- and mid-twentieth century, studies investigating the environmental influences that lead to disease outbreaks have resumed [e.g. Nutter et al. (1983), Hall (1984), Schumann et al. (1994), Fidanza et al. (1996), and Gross et al. (1998)].

*2.2.1 Schumann epidemiological model*

Schumann et al. (1994; hereafter S94) conducted a four-year field program to analyze the link between brown patch activity in creeping bentgrass and local environmental conditions in Massachusetts, New Jersey, and Georgia. Preliminary greenhouse studies conducted by Rowley (1991) demonstrated that *R. solani* was capable of infecting turfgrass at 12ºC when the foliage remained wet for 8 to 12 consecutive hours. S94 found that relative humidities greater than 95% for at least 10 consecutive hours consistently preceded brown patch occurrence. When the above relative humidity criterion was met, any one of the following sets of conditions were found to be conducive to brown patch development:

(i) Minimum and mean air temperatures of 15 and 20ºC, and minimum and mean soil temperatures of 18 and 21ºC, for the 24 h period ending on the 10$^{th}$ consecutive hour of relative humidity exceeding 95%, and rainfall of at least 2.54 mm over the 36 h period ending on the 10$^{th}$ consecutive hour of relative humidities in excess of 95%;

(ii) rainfall of at least 15 mm for a period of 48 hours after the rainfall episode began, in addition to the air and soil temperature thresholds in (i); and

(iii) prolonged (at least 36 hours) high humidity (≥ 95%) and rainfall (> 15 mm) in combination with the soil temperature requirements listed in (i), even when the air temperature thresholds in (i) were not met.

*2.2.2 Fidanza epidemiological model*

Fidanza et al. (1996; hereafter F96) monitored environmental conditions and brown patch activity on perennial ryegrass at the University of Maryland from June 1991 through August 1993. Using two years of data they developed an environmental favorability index (E). Their study indicated that six variables could be related to brown patch occurrence: hours of relative humidity greater than 95%, mean relative humidity, leaf wetness duration and precipitation during the 48 h prior to sunrise (0600 LT), minimum air temperature, and minimum soil temperature. These six variables were combined to create a condition-based epidemiological model, quantified by an index ($E_6$), where integer point values are assigned to each of the six variables based on how favorable the variable is for disease development (e.g., minimum air temperature of at least 16ºC is worth one point, while minimum air temperature of less than 16ºC is worth –2 points). A value of $E_6$ of at least 6 is indicative of a high-risk for brown patch development. Because some of the input required for the $E_6$ index is not readily available to turfgrass managers (e.g. hours of leaf wetness duration, soil temperature), F96 showed that just two of the above variables, mean relative humidity and minimum air temperature, provided sufficient information to attain forecasts similar to those produced by the $E_6$ index. To do this, the authors subjected their data to multiple regression analysis, using stepwise multiple regression analysis to identify those meteorological parameters that explained most of the observed values of $E_6$. They found that minimum air

temperature and mean relative humidity provided the best-fit model, using a second-order regression. Thus, the following index ($E_2$) was developed:

$$E_2 = -21.5 + 0.15RH + 1.4T - 0.033T^2, \quad (2.3)$$

where RH is mean 24-h relative humidity, and T is minimum air temperature. Similar to $E_6$, the output of $E_2$ was interpreted in such a way that a value of at least 6 indicated a high-risk for brown patch development.

*2.3 Summary*

Although the authors of the studies detailed above met with success in the regions their respective studies were conducted, it is unclear whether or not the same weather conditions would result in the same disease response in other regions of the country. For example, S94 found that the epidemiological model developed using meteorological data from Massachusetts should be modified for use in Georgia in order to prevent false alarms, and Gross et al. (1998) showed that the epidemiological model developed by Fidanza et al. (F96) frequently over-predicted brown patch activity when tested in Indiana. Additionally, different turfgrass species may respond to the same pathogen in a different manner. In North Carolina, creeping bentgrass is grown for putting greens. The studies in S94 and F96, however, were performed on Colonial bentgrass and perennial ryegrass, respectively, and may therefore not be applicable to creeping bentgrass.

## 3. Methodology

### *3.1 Tests of currently available epidemiological models*

The weather-based epidemiological models developed in S94 and F96 were tested for their applicability in North Carolina. Daily observations of brown patch activity were conducted at the N.C. State Faculty Club Turfgrass Field Laboratory from 8 June-16 August 2003 at 0800 local time. Brown patch observations were conducted visually on creeping bentgrass maintained under golf course putting green conditions. Brown patch activity is typically evident by the presence of a black ring around the perimeter of the patch (often referred to as a "smoke ring"; Tredway et al. 2004). Therefore, a "yes" was recorded for disease activity if a smoke ring was evident at the time the observation was made; otherwise, a "no" was recorded.

The time scale at which diseased turf becomes symptomatic, and the disease begins to spread, is unknown. It is likely that the exact time scale varies based on the conditions. For example, actively spreading brown patch has been observed after an afternoon thunderstorm provides adequate moisture to a plot of turfgrass. In some cases, no sign of this smoke ring will be evident by 0800 local time, the time observations were made. This, of course, makes once-daily observations of disease activity problematic. However, the resources necessary to increase the temporal resolution of brown patch activity were unavailable, and further analysis will assume that the disease observations obtained in this study are accurate (with the exception of Section 4.2.4, where disease incidence observations are compared with disease activity observations).

The experimental area was established with 116.13-$m^2$ blocks of the cultivars 'SR1119', 'G-6', 'G-2', 'Crenshaw', 'L-93', 'Penncross', 'A-4', and 'A-1'. Mowing was

performed three times weekly to a height of 4 mm with clippings collected, and the site was irrigated to prevent drought stress. Fertilizer was applied as 24-5-11 (i.e. 24% Nitrogen, 5% Phosphorous, 11% Potassium, 60% carrier) on 9 April (2.44 kg N/1000 $m^2$), as 18-3-18 on 5 May (2.44 kg/1000 $m^2$), and as 18-4-0 on 15 May (2.44 kg/1000 $m^2$). Insect pests were suppressed with Dursban (477.49 ml/1000 $m^2$) on 16 May, 27 June, and 25 July and with Talstar (79.58 ml/1000 $m^2$) on 18 August. Canteen wetting agent (1.9 L/1000 $m^2$) was applied on 24 April, 12 May, 24 June, and 1 August to control localized dry spot. Disease observations were made around 0800 LT daily. Forecast days were from 0800-0800 LT. Disease observations were then compared with the output from the epidemiological models to evaluate their performance.

Beginning 7 July 2003, and continuing through the end of the 2003 study period, a hand-made grid mesh (Figure 3.1) was used to measure disease incidence in 16 predetermined sub-plots. The grid mesh was approximately 1 m by 1 m, with 289 intersects between 5.08 cm by 5.08 cm grid cells. Incidence was measured by counting the number of grid cells the disease was present in. These data may prove a better indicator of disease activity than the presence of a smoke ring at the observation time, as it may account for short activity cycles that occur at times other than the observation time (even though the disease incidence observations were made at the same time as the smoke-ring observations). In order to evaluate the disease incidence observations, the incidence reports from the 16 individual sub-plots was averaged. In Section 4, a dichotomous response was derived from the disease incidence observations, such that a “yes” was recorded if the average number of grid cells containing disease increased from the previous day, and a “no” was recorded otherwise.

An on-site weather observing station was established to record hourly precipitation, air temperature, relative humidity, soil temperature (at 0.1 m), soil moisture, incoming solar radiation, and wind direction and speed (at approximately 0.30 m). These data were used as inputs for the epidemiological models to assess disease risk.

As was stated in Section 2.2, one possible reason for the reluctance of turfgrass managers to incorporate weather-based decision aids into their fungicide application decisions is the prohibitive cost of establishing on-site weather stations, along with the regular maintenance such stations would require. In order to address this concern, weather observations collected from the Automated Surface Observing Station (ASOS) at the Raleigh-Durham International Airport (RDU), located approximately 17.7 kilometers from the Turf Field Lab, were also compiled and used as inputs into the epidemiological models. The output from the epidemiological models using ASOS data was then compared to output using the on-site data to determine whether off-site, regional data might be used as a proxy to on-site data in determining disease risk.

In addition to the on-site and RDU weather observations, output from the National Centers for Environmental Prediction's (NCEP) Eta model (Black 1994, Janjic 1994) was processed and used as an input for the decision aids (Recently, NCEP has renamed the Eta model the North American Mesoscale (NAM) model. In this thesis, Eta and NAM will be used interchangeably). The model output was derived from the Eta 215 grid (20-km grid spacing) and averaged for all grid points within 35 km of the Turf Field Lab (10 total grid points averaged). The resulting averages were used as an input to the brown patch decision aids. The Eta-based disease indices were also compared with disease observations at the Turf Field Lab. It is anticipated that if the disease indices produced with output from the Eta

model are comparable to those produced from on-site observations, turfgrass managers would have sufficient warning to make preventative fungicide applications before a disease outbreak occurred.

The meteorological observations collected from the Turf Field Lab and RDU, along with the Eta model output, were input into a spreadsheet application for analysis. Eta model output was only used as input into the epidemiological model developed in F96. Four separate outputs from the F96 epidemiological model were produced for each data source– two $E_2$ indices and two $E_6$ indices, one with an index using a (max + min)/2 average for mean relative humidity ($E_{2m}$ and $E_{6m}$), and one using a time average derived from all hourly observations for the day ($E_{2h}$ and $E_{6h}$). Only observed weather conditions (Turf Field Lab and RDU) were used as inputs into the epidemiological model developed in S94. Although this epidemiological model uses a moving 36-hour window in order to produce brown patch warnings, for verification purposes a 12 UTC-12 UTC day will be considered, allowing comparison to output from the Fidanza decision aid (F96). Therefore, if all of the criteria for a disease warning are met during any single hour of a 12 UTC-12 UTC day, a disease risk warning for that day is issued.

Several skill scores were calculated to quantify the performance of all of the epidemiological models tested in this study. The false alarm ratio (FAR) is the ratio of warnings without events to total warnings; the probability of detection (POD) is the ratio of warned events to total events; and the critical success index (CSI) is defined such that

$$CSI = \frac{1}{[1/(1-FAR)] + (1/POD) - 1} \qquad (3.1).$$

Additionally, correlation coefficients were calculated between the $E_{2h}$ index using meteorological data from the Turf Field Lab and the other $E_{2h}$ indices calculated during the course of the study. This was done to quantify the relationship between the indices, and determine whether or not the alternative sources of data could be used as a proxy for on-site meteorological observations.

*3.2 Development of a new epidemiological model*

The experimental setup for the summer of 2004 was very similar to the setup used the prior year. Disease observations were again made at the Turf Field Lab. Observations were only made of disease activity (this is, the presence of a smoke ring), and not of disease incidence. The period of observation began on 26 May 2004 and ended on 18 August 2004. While $E_2$ indices (F96) were calculated using meteorological data from the Turf Field Lab, the primary purpose of this portion of the study was the development of a new epidemiological model (per the results presented in Section 4). Therefore, no other epidemiological models were tested during this period.

Meteorological data collected at the Turf Field Lab for the summers of 2003 and 2004 were subjected to statistical analysis in order to determine which parameters were most associated with observations of brown patch activity. This was done in order to test the hypothesis that weather conditions need be favorable for a period longer than one day in order for infection to occur. The meteorological parameters measured and evaluated include air temperature, relative humidity, soil temperature, precipitation, wind speed, and incoming solar radiation.

Three methods were used in an attempt to develop a new epidemiological model. The common thread between each method is the underlying hypothesis that *R. solani* requires warm, moist conditions in order to infect turfgrass (Smiley et al. 1992). Specifically, it is thought that free moisture must be present in a warm setting for the spread of the brown patch disease. With this in mind, the meteorological parameters that were measured at the Turf Field Lab were combined into variables that focus on the likelihood of dew formation. These variables include minimum temperature, dewpoint depression, and wind speed. Because dew formation typically occurs at night, an emphasis will be placed on these variables from 2000-0800 local time, or approximately from dusk until dawn. These variables are evaluated using each of the three analysis methods discussed below.

*3.2.1 Autoregressive model*

The first method used in an attempt to quantify the link between brown patch activity and meteorological conditions was the autoregressive (AR) model (Box and Jenkins 1976). The AR model is a time-series model that categorizes a response variable by using both past information about the response variable and past and current information about other explanatory variables (SAS Institute 1999). The procedure was invoked using SAS software, and the simplified form of the model is

$$y_t = \sum_{i=1}^{N} (a_i y_{t-i}) + \sum_{j=1}^{M} (b_j x_{j,t}) + n_t, \quad (3.1)$$

where $y_t$ is the response variable at time t, $a_i$ and $b_j$ are coefficients determined by the procedure (using $\chi^2$ analysis to determine statistical significance), $x_{j,t}$ denotes different explanatory time series at time t, and $n_t$ is random noise assumed to have a mean of zero and

constant variance. The model is referred to as an AR(N) model. For this analysis, the response variable is the presence of disease, and the explanatory time series are meteorological parameters found to be statistically significant. This model assumes that a correlation exists between not only the response variable and explanatory variables at time t, but also the response variable on previous days and the presence of disease at the evaluation time.

### *3.2.2 Logistic regression*

The statistical tool described above assumes an autodependent response variable. The following tool, however, assumes that the variables are independent. It is possible that the continuation of a disease outbreak may be easier to maintain than the initialization of a new disease outbreak. If this is the case, the independence assumption used for this statistical tool would not be met, and the results obtained using this tool could not be considered valid. There are two reasons, however, that the independence assumption necessary for a logistic regression to be valid can be met. First, it is possible that *R. solani* has an incubation period on the order of a few hours, and that observed disease activity is in no way dependent on whether disease activity was observed on the previous day. Secondly, even if disease activity is autodependent, the primary concern of this study is to determine the initial time of a disease outbreak. Assuming this can be predicted accurately, fungicides can be applied and prolonged outbreaks would not occur. Because the details of the development of the disease are somewhat unknown, both models are used to explore multiple avenues to determine the conditions best suited for brown patch development.

Logistic regression is an analytical technique suited for binary and ordinal data. Several texts describe appropriate uses for the regression technique, including Cox and Snell (1989). The default logistic model employed by the SAS system is linear, and of the form

$$\text{logit}(p) \equiv \ln\left(\frac{p}{1-p}\right) = \alpha + \boldsymbol{\beta}'\mathbf{x}, \quad (3.2)$$

where logit(p) is the natural logarithm of the odds ratio, p is the probability that the response variable (usually denoted as y) is equal to a certain value, $\alpha$ is the intercept parameter, $\boldsymbol{\beta}'$ is the vector of slope parameters, and $\mathbf{x}$ is the vector of input variables. $\alpha$ and $\boldsymbol{\beta}'$ are determined using a maximum likelihood estimation. As with the AR model, a $\chi^2$ analysis is used to determine the statistical significance of explanatory variables employed in the model.

The inverse of the logit function is the sigmoid function,

$$p(t) = \frac{1}{1+e^{-t}}. \quad (3.3)$$

If logit(p) is substituted for t in Equation (3.3),

$$p = \frac{1}{1+e^{-\text{logit}(p)}}. \quad (3.4)$$

Using Equations 3.3 and 3.4, it can be seen that the predicted probability of disease occurrence, p, can be written as

$$p = \frac{1}{1+e^{-\alpha+\beta'x}}. \quad (3.5)$$

*3.2.3 Process-based evaluation*

A general understanding exists amongst plant epidemiologists that warm conditions with free moisture are necessary for the formation of brown patch. Therefore, it is not

unreasonable to expect that the warmer and more humid conditions become, the more favorable they would be for disease occurrence. That expectation is the motivation for using the following process in the attempt to develop a criterion-based epidemiological model, similar to the $E_6$ index developed by F96.

Point values were assigned based on several meteorological parameters in order to develop a criterion-based epidemiological model using the Turf Field Lab observations from both 2003 and 2004. The meteorological parameters that were evaluated include air temperature, dewpoint, wind speed, and hourly precipitation. These parameters were then combined into the following summary variables: minimum air temperature, maximum air temperature, daily precipitation, mean dewpoint depression (during evening hours, in order to capture the nighttime dew formation period), and wind speed (used as a modifier to the dewpoint depression criterion in order to better estimate the possibility of dew formation). A range of point values between –5 and 8 was possible, and skill scores using each of the possible integer values as the disease threshold were computed to determine the most effective value.

*3.3 NWP model sensitivity study*

In order to test the sensitivity of forecasting disease indices using weather-based epidemiological models, a meteorological model sensitivity study was undertaken. The fifth-generation Pennsylvania State University-National Center for Atmospheric Research (PSU/NCAR) Mesoscale Model (MM5; Grell et al. 1994, Dudhia et al. 2000) was employed for this study. The MM5 was initialized using the NCEP Eta model.

*3.3.1 NCEP Eta model*

The Eta model is initialized using the Eta Data Assimilation System (EDAS) as detailed in Rogers et al. (1995). The EDAS assumes that the previous short-term forecasts are reliable, and therefore may contain biases or errors due to flaws in the Eta forecast model. For the purposes of this study, however, a perfect depiction of the Earth's atmosphere by the model is not necessary as long as a reasonably accurate, physically consistent model atmosphere is produced.

The Eta model uses a step-mountain coordinate to represent terrain (Mesinger 1984). At the time this study was conducted, the Eta model was run on a 12-km grid with 60 vertical levels. For initializing the MM5, the Eta output was previously interpolated to a 40-km grid (Eta 212 gird), with the exception of relative humidity data. Relative humidity data are not available on the Eta 212 grid, and were instead obtained from the Eta 211 grid (80-km grid spacing). The Betts-Miller-Janjic (BMJ) convective precipitation scheme was used in the operational version of the model (Betts 1986, Betts and Miller 1986, Janjic 1994). To emulate the interactions between soil, vegetation, and the planetary boundary layer, the Eta model employs the four-level NOAH land-surface model (Ek et al. 2003).

*3.3.2 PSU/NCAR MM5 model*

*3.3.2.1 Model setup*

As was stated earlier, the MM5 model was chosen for conducting a meteorological model sensitivity study. Execution of the MM5 model involves the use of several preprocessing programs. The first, TERRAIN, generates elevation and vegetation information for the mesoscale grids. In conjunction with a land-surface model, TERRAIN

also generates fields such as soil types, vegetation fraction, and annual deep soil temperature (Dudhia et al. 2000). The next step in the preprocessing involves the program gridder. Gridder was developed at the University of Utah (and is not a part of the standard MM5 distribution). Gridder reads input model files and interpolates them onto the grid specified in TERRAIN. In the process, gridder also interpolates the data onto an isobaric coordinate grid if necessary. The final preprocessor, INTERPF, takes the pressure-level output from gridder and interpolates it onto the sigma coordinate system utilized in MM5.

*3.3.2.2 Model forecasts*

Model forecasts were run for two separate cases. The first was initialized at 1200 UTC 29 July 2004, and was run for 48 hours. The 1200 UTC 29 July 2004 analysis from the operational Eta model was used to initialize the MM5, and boundary conditions were updated using forecast output from the Eta model every six hours. The other model forecast run was initialized at 1200 UTC 6 August 2004. This run was also carried out for 48 hours, using the 1200 UTC Eta model analysis and forecast output (every 6 hours) for initialization and boundary conditions.

Very warm temperatures (high temperatures of approximately 31ºC and low temperatures ranging from 21 to 23ºC), high near-surface atmospheric moisture content (daily average dewpoints between 22 and 24ºC), and precipitation (approximately 18 mm fell during the period) marked the meteorological conditions during case one. In contrast, a cold-frontal passage occurred over the study area on 5 August 2004. Therefore, case two was characterized by much cooler (higher temperatures between 24 and 27ºC and low temperatures between 13 and 17ºC), drier (average dewpoints of approximately 13ºC and no

precipitation) conditions than case one. The diversity in meteorological conditions between cases one and two allowed for testing model sensitivity in varying conditions, and this diversity was the purpose for the selection of the test cases.

The purpose of this study is to test the sensitivity of near-surface temperature and moisture to the choice of LSM. Accordingly, the remainder of the model parameters, including physics options were held constant. The outer domain was a 90 by 90 grid with 27-km grid spacing, centered at 36 ºN, 85 ºW, while the inner-domain was a 118 by 118 grid with 9-km spacing (Figure 3.2). Both domains used 28 vertical sigma levels, and the model top was 100-hPa. All four runs employed an explicit moisture scheme that utilizes predictive equations for cloud water, rain water, snow, graupel, and ice number concentration (Reisner2; Reisner et al. 1998). The Grell cumulus parameterization (CP) scheme was also chosen for all of the model runs (Grell 1994). The Grell CP scheme depicts clouds as a single updraft and a single downdraft, and includes no direct entrainment or detrainment of environmental air into the side edges of the clouds. The MRF PBL scheme (Hong and Pan 1996) was chosen for all of the runs, primarily for its compatibility with the NOAH LSM.

For each case, one MM5 forecast was run using the NOAH LSM, while another was run using a 5-layer soil model. The NOAH LSM was first added to the MM5 modeling system by Chen and Dudhia (2001) as the Oregon State University LSM. It is a four-layer soil model (layers at 10, 30, 60, and 100 cm below the surface), and predicts numerous soil and surface parameters, including soil temperature and soil and canopy water. Use of the NOAH LSM requires the use of soil inputs not required by the 5-layer soil model built into the MM5, including soil texture, annual mean surface temperature, and seasonal vegetation fraction (which are provided by the TERRAIN pre-processor if requested), and initial soil

temperature and moisture (obtained from the Eta model). The 5-layer soil model has layers at depths of 1, 2, 4, 8, and 16 cm, and needs only an input of thermal inertia (as a function of land-use), in addition to other atmospheric parameters, to determine soil temperature. It uses seasonal values of soil moisture that are dependent on land-use, and do not change during the course of a simulation.

*3.3.2.3 Analysis of MM5 output*

The primary purpose in analyzing the MM5 output is to determine the sensitivity of predictions of near-surface air temperature, precipitation, dewpoint depression, and dewpoint, to changes in the LSM. In order to accomplish this, the MM5 output was converted into the General Meteorological Package (version 5.6; GEMPAK; desJardins et al. 1992) format. To compare the MM5 runs with each other, difference fields were calculated using GEMPAK for the parameters listed above. These fields were calculated for every six forecast hours, through 48 hours.

*3.4 Summary*

This thesis consisted of two major components: a field study, and a NWP model study. For the field study, a weather-observing station was erected at the NC State Turfgrass Field Laboratory; the same location at which once-daily observations of brown patch activity were made at 0800 local time. Additionally, weather data from the Raleigh-Durham International Airport and the operational runs of the NCEP Eta model were obtained. The weather data from all available sources were used as inputs in the epidemiological models developed in S94 and F96, and the predictive ability of each of the epidemiological models

was evaluated. Several statistical methods were also used in an effort to evaluate the data, in an effort to develop a new epidemiological model.

In conducting the NWP model study, output from the operational Eta model was used to initialize the PSU/NCAR MM5. Output from several experimental runs of the MM5 was generated and evaluated using several GEMPAK programs, primarily by the calculation of difference fields.

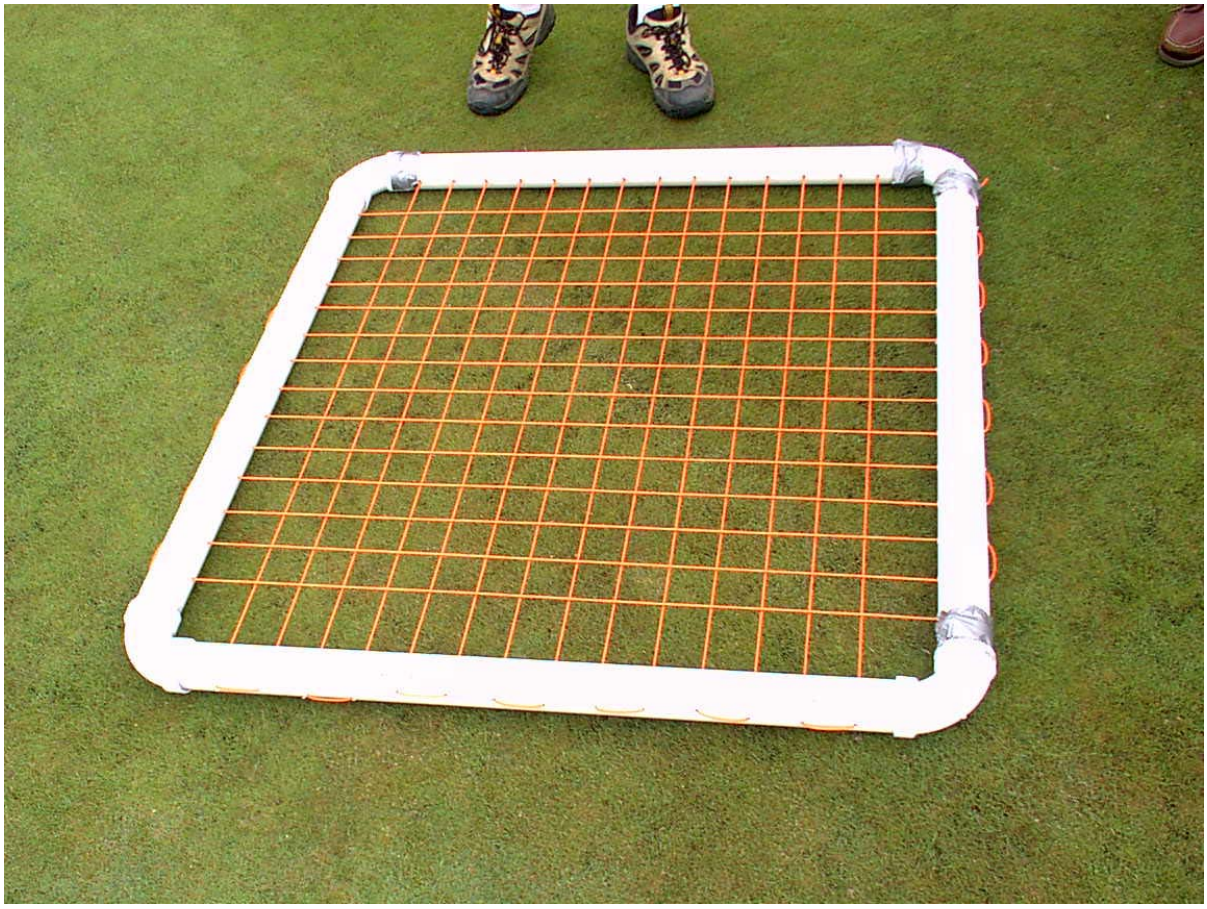

Figure 3.1. Picture of grid-mesh used in the collection of disease incidence data

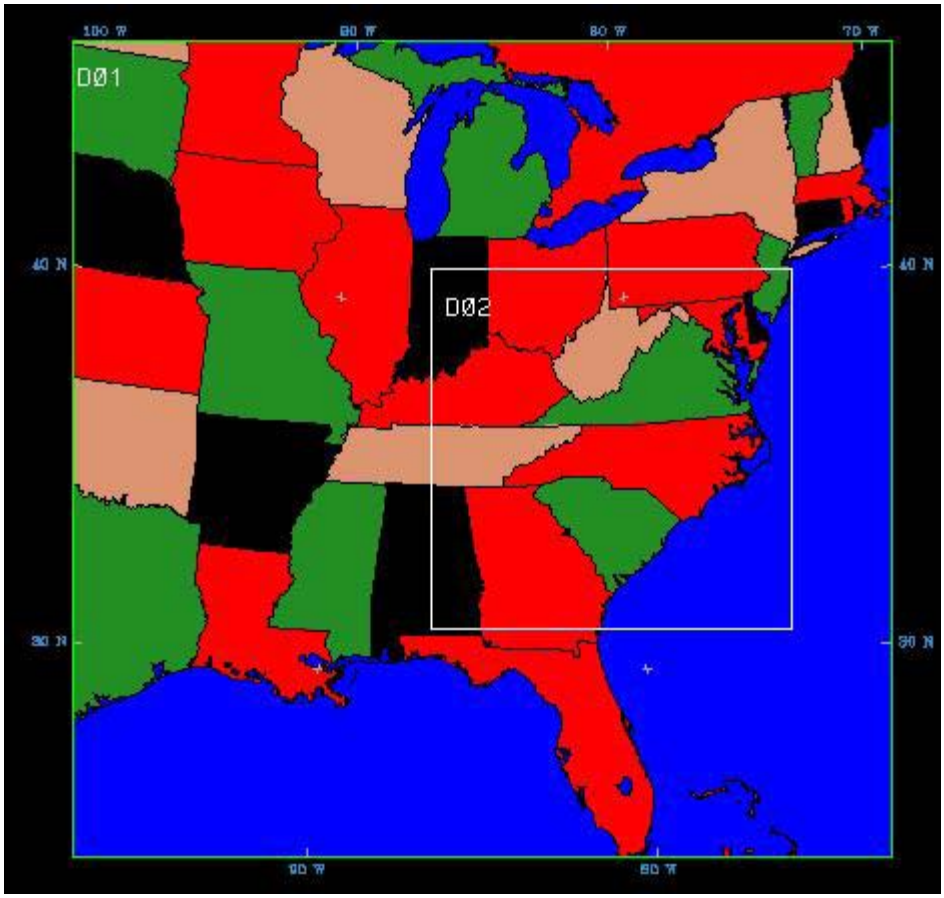

Figure 3.2. Model domain used in MM5 forecast of 29-31 July 2004. The outer domain has a grid-spacing of 27 km, and the inner domain a grid-spacing of 9 km

## 4. Test of Currently Available Epidemiological Models

### *4.1 Disease observations*

Brown patch activity was observed on 23 of the 70 days during the initial experimental period (summer of 2003): five days in June, 13 days in July, and five days in August. These 23 days can be grouped into seven episodes. An episode is defined as a period beginning on a day disease activity is observed and continuing until no disease activity is observed for two consecutive days. When two consecutive days pass with no observed disease activity, the episode is defined to have ended on the last day disease activity was observed. Table 4.1 lists each day that disease was observed, grouped by episode.

It is again important to note that some uncertainty exists in the disease observations. This uncertainty is spoken to in Section 3.1.

### *4.2 2003 results*

#### *4.2.1 Disease indices from on-site weather observations*

In this section, the brown patch indices generated by the Fidanza (F96) and Schumann (S94) epidemiological models, using on-site weather observations, are discussed. The $E_6$ indices ($E_{6h}$ and $E_{6m}$) generated at the Turf Field Lab were only different on nine days during the experimental period. Further, the two indices only differed in their prediction of brown patch development on 30 June, when $E_{6h}$ indicated conditions highly favorable for activity ($E_{6h} = 6$) while $E_{6m}$ did not ($E_{6m} = 5$). As shown in Figure 4.1, the $E_{6h}$ index matched observed conditions on 39 of the 70 days (56%) in the forecast period, while $E_{6m}$ did so on 40 days (57%).

Figure 4.2 summarizes the performance of the F96 epidemiological model using the $E_6$ indices. Dates listed in the upper-right quadrant are those dates that the index resulted in a false alarm, while dates in the lower-left quadrant are those dates that the index missed a disease event. Of the 23 days that brown patch activity was observed, both $E_{6h}$ and $E_{6m}$ correctly produced brown patch warnings on seven days, and missed 16 days. The $E_{6h}$ index produced 15 false alarms, while the $E_{6m}$ index produced 14 (the $E_{6h}$ index produced an additional false alarm on 30 June). Only the onset of episode two (15-19 June; Table 4.1) was captured by the $E_6$ indices.

More variability was evident between the $E_2$ indices ($E_{2h}$ and $E_{2m}$) than was evident between the two $E_6$ indices (Figure 4.3). The $E_{2h}$ index produced a total of 27 disease warnings. Only 11 of these warnings agreed with field observations, the other 16 resulting in false alarms (Figure 4.4a, Figure 4.4b). The $E_{2h}$ index missed 12 disease days. $E_{2h}$ proved more proficient than the $E_6$ indices at predicting the onset of disease episodes, producing disease warnings for the onset of episodes one, two, and five, while producing indices in the 5's for episodes four, six, and seven (Table 4.1). $E_{2m}$, on the other hand, indicated that a high-risk of brown patch activity existed on only eight days during the observation period. Brown patch was observed on only half of those days (Figure 4.3). The index missed 19 events and produced 4 false alarms (Figure 4.4b). The $E_{2m}$ index was able to capture the onset of only one disease episode (episode five).

The S94 epidemiological model produced 16 brown patch warnings during the experimental period. Of the 16, six corresponded with observed disease activity, and ten were false alarms (Figure 4.4c). Additionally, the index missed 17 disease events. The S94

index produced a warning for only one of the seven disease episodes observed during the test period (episode 2; Table 4.1).

*4.2.2 Disease indices from airport weather observations*

Using weather observations from RDU, the $E_6$ indices ($E_{6m}$ and $E_{6h}$) were exactly identical throughout the experimental period; therefore reference will be made only to $E_6$ in general. The $E_6$ index matched disease observations on 40 of the 70 days (57%) in the forecast period (Figure 4.5). $E_6$ produced 17 disease warnings, but brown patch activity only occurred on 5 of those days. The index also produced 12 false alarms and 18 missed events (Figure 4.6a). When analyzed on an episode-by-episode basis (Table 4.1), $E_6$ was unable to capture the onset of any of the seven disease episodes.

As was the case with the Turf Field Lab data, large variability existed between the two $E_2$ indices based on RDU meteorological data (Figure 4.5). The $E_{2h}$ index produced 30 brown patch warnings, of which 11 verified, and 19 were false alarms (Figure 4.6b). The $E_{2m}$ index produced 14 brown patch warnings; seven of these verified, and seven were false alarms. The $E_{2h}$ index matched field observations of brown patch on 39 of 70 days (56%), while the $E_{2m}$ index did so on 46 of 70 days (66%; Figure 4.5, Figure 4.6c). $E_{2h}$ correctly predicted the onset of three of the seven brown patch episodes (episodes two, five, and seven), while $E_{2m}$ correctly predicted only one (episode five; Table 4.1). Comparing the $E_{2h}$ indices produced using the RDU data to the Turf Field Lab-derived $E_{2h}$ indices shows a strong correlation between the two ($r = 0.944$). This likely implies that using weather observations (at least temperature and relative humidity observations) from off-site sources

will provide an adequate approximation of the $E_{2h}$ values on-site, given the distance between the sources is not too great.

The S94 output matched observed disease conditions on 42 days of the 70-day experimental period (60%; Figure 4.5), with brown patch observed on seven of these days. For the experimental period, the Schumann epidemiological model produced 19 disease warnings, 12 of which were false alarms, and 16 missed forecasts (Figure 4.6d). The index was able to correctly indicate the onset of disease episode two (Table 4.1).

*4.2.3 Disease indices from operational Eta forecasts*

Eta forecasts were used to generate only the $E_{2h}$ indices based on one- (F24) and two-day (F48) forecasts (Figure 4.7). This index was chosen over the others primarily because results to this point indicate it is the most accurate. Eta model one-day forecasts were available for 63 days during the experiment (9 July, 12 July, 16 July, 19 July, 23 July, 25 July, and 15 August were not available). A summary of the performance of the one-day Eta model forecasts of $E_{2h}$ is provided in Figure 4.8a. The one-day forecasts of $E_{2h}$ produced 22 brown patch warnings. On days that the Eta model one-day forecast produced a warning, disease was observed six times (Figure 4.8a), leaving 17 events unpredicted (four on days that indices were unavailable), with 16 false alarms. When evaluated for its usefulness in predicting the onset of disease episodes (Table 4.1), the Eta model one-day forecasts only predicted the onset of episode seven, though a warning was very nearly issued for the onset of episode two ($E_{2h}$ = 5.94; no forecast was available for 23 July, the onset of episode five).

Eta model two-day forecasts were unavailable for 8 June, 10 July, 13 July, 17 July, 20 July, 22 July, and 16 August. A time-series of the generated indices is provided in Figure

4.7. This $E_{2h}$ index produced 17 disease warnings, of which six verified with observations (Figure 4.8b). Seventeen brown patch infection events were missed by this index (though two of these infection events fell on days an index was unavailable), and 11 false alarms were issued. Interestingly, the one- and two-day $E_{2h}$ forecasts nearly predicted the same two disease episodes (Table 4.1), with the two-day forecast producing a warning for episode seven, while very nearly issuing a warning for episode two ($E_{2h}$ = 5.95).

Surprisingly, both the Eta 24- and 48-h forecast values of $E_{2h}$ correlate very well with those values calculated using on-site weather data (r = 0.872 and 0.873, respectively). The implication of this is that it should be possible to use forecasted weather conditions to predict $E_{2h}$ values with enough accuracy to be useful at least two days in advance, vastly increasing the utility of such an index.

*4.2.4 Disease incidence observations*

There were a total of 17 days on which disease activity was observed between 7 July and 16 August 2003. In contrast, there were 21 days during which incidence of brown patch increase from one day to the next during the same period. Interestingly, different conclusions were reached concerning disease activity on 20 of the 41 days during the period (that is, no visual evidence of disease activity was noted, but disease incidence increased, or vice versa). While it is unclear which method provides the best estimate of total disease activity due to the small area the disease incidence observations were taken over, it is apparent that work needs to be done to determine why such a large discrepancy exists between the two methods.

When comparing TFL-derived $E_{2h}$ indices to disease incidence observations, the index matched observed conditions on 24 days. Of those 24 days, disease was observed on

11. Use of the $E_{2h}$ index would have resulted in seven false alarm and 10 missed events. The skill scores associated with these observations are listed in Table 4.2.

*4.3 2004 results*

The primary purpose of data collection during the summer of 2004 was to create a larger dataset for the development of a new epidemiological model. However, $E_{2h}$ values were generated using weather observations collected at the Turf Field Lab to further evaluate the necessity of a new epidemiological model.

Little disease activity was observed during the summer of 2004 observational period, which spanned from 26 May 2004 through 18 August 2004. In total, disease activity was observed on only six days. It is unclear why such anomalously low disease activity was observed.

Figure 4.9 shows a time-series of the $E_{2h}$ values generated from meteorological data collected at the Turf Field Lab. In summary, use of the $E_{2h}$ index in operational disease forecasting during the summer of 2004 would have resulted in 66 days on which the index matched observed conditions. However, disease only occurred on two of these days. Additional, the index resulted in 15 false alarms, and four missed events.

*4.4 Summary*

The primary objective of this study was to evaluate the currently available epidemiological models for fungal infection of turfgrass (specifically, the infection of creeping bentgrass by brown patch) for use in North Carolina, developed in S94 and F96. A secondary objective was to determine whether off-site, regional weather observations or

weather model forecast output might serve as a suitable proxy for on-site observations for use in brown patch epidemiological models.

As shown in Table 4.2, high FARs and low PODs and CSIs characterized the study period. This is not desired of an operational system. An attempt was therefore made to use a lower threshold for $E_2$ and $E_6$ indices to increase the POD, but this caused the already high FARs to increase even more, lowering the utility of the indices.

Interestingly, the $E_{2h}$ index performed best when compared to observations of disease incidence, even when compared to the performance of the index against observations of disease activity during the period that disease incidence was observed (Table 4.2). This again speaks to the uncertainty in disease observation methodology. It is likely that some integrated measure of disease activity is necessary to obtain the most accurate analysis of the relationship between weather conditions and disease.

While it is apparent that the epidemiological models tested in this study will need some modification, it appears likely from the results of this study that both regional weather observations and forecasted weather conditions can serve as an adequate proxy for on-site weather observations. Calculation of correlation coefficients between the Turf Field Lab-$E_{2h}$ index and the RDU-$E_{2h}$ index, Eta 24-h-$E_{2h}$ index, and Eta 48-h-$E_{2h}$ index results in values of 0.944, 0.872, and 0.873, respectively. The indices correlate well with one another, implying that observations of relative humidity and minimum temperature are also well correlated. For example, the correlation coefficient for hourly temperature readings between the Turf Field Lab and RDU is about 0.906, with a mean absolute difference between hourly temperature readings of less than 1.3ºC. While epidemiological models in this study did not perform well enough to be used operationally, there is hope that, should an accurate

epidemiological model be developed, the use of on-site weather stations for its calculation will not be necessary. If this proves to be the case, it is much more likely that turfgrass managers will use the epidemiological models, and by doing so reducing their fungicide usage.

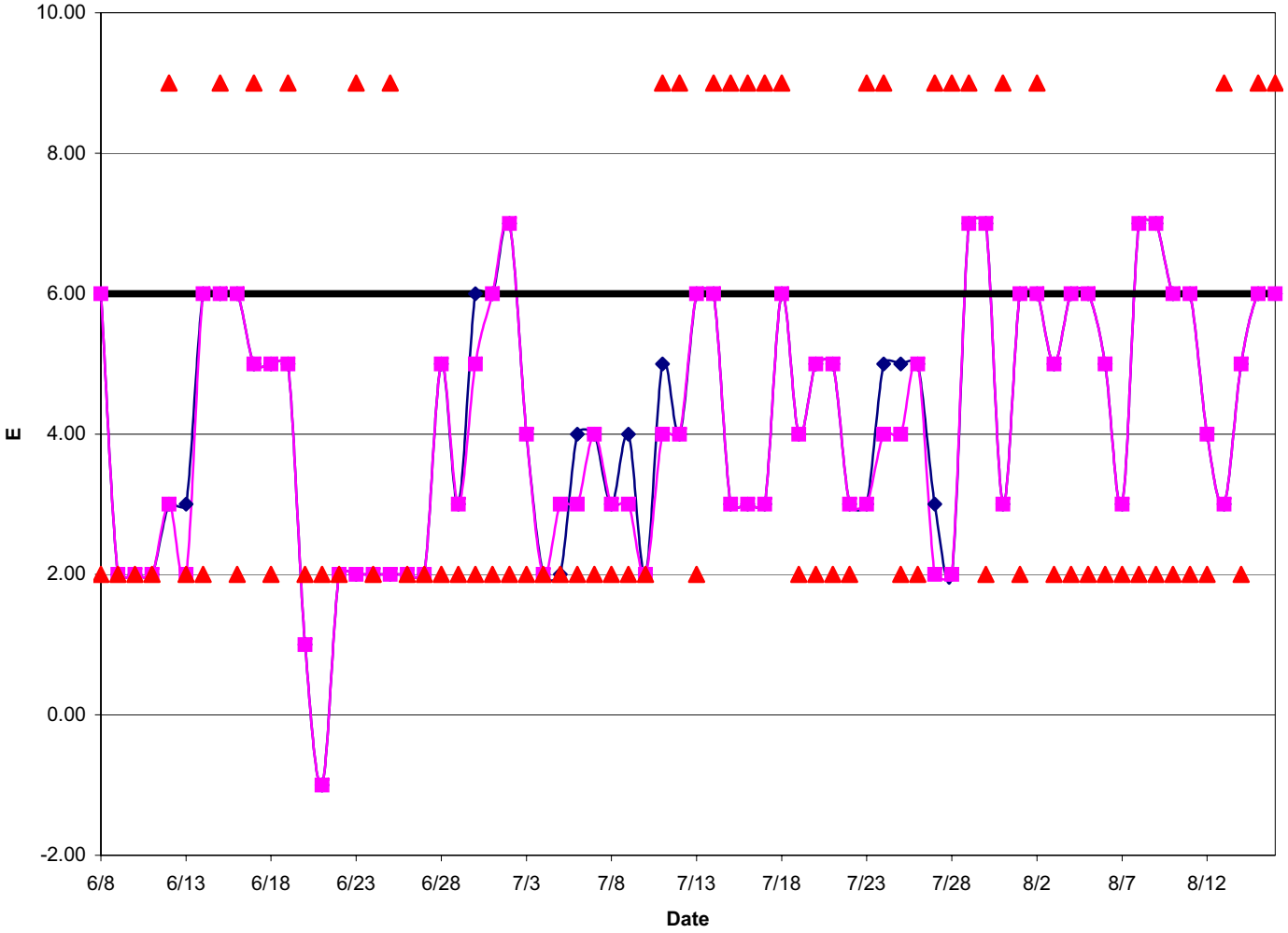


Figure 4.1. Turf Field Lab-derived $E_{6m}$ and $E_{6h}$ indices, with observations of disease activity overlaid. The series of squares represents $E_{6m}$, and the series of diamonds represents $E_{6h}$. Where the series of triangles lies below the solid E = 6 line, disease was not observed. Triangles above the line represent days disease was observed.

**a)**

$E_{6h}$

| Index Yes/Observations Yes (7) | | | Index Yes/Observations No (15) | | |
|---|---|---|---|---|---|
| 15-Jun | 14-Jul | 2-Aug | 8-Jun | 1-Jul | 1-Aug |
| | 18-Jul | 15-Aug | 14-Jun | 2-Jul | 4-Aug |
| | 29-Jul | 16-Aug | 16-Jun | 13-Jul | 5-Aug |
| | | | 30-Jun | 30-Jul | 8-Aug |
| | | | | | 9-Aug |
| | | | | | 10-Aug |
| | | | | | 11-Aug |
| | | | | 3-Jul | |
| | | | 9-Jun | 4-Jul | |
| | | | 10-Jun | 5-Jul | |
| | | | 11-Jun | 6-Jul | |
| | 11-Jul | | 13-Jun | 7-Jul | |
| | 12-Jul | | 18-Jun | 8-Jul | |
| | 15-Jul | | 20-Jun | 9-Jul | |
| | 16-Jul | | 21-Jun | 10-Jul | |
| | 17-Jul | | 22-Jun | 19-Jul | |
| 12-Jun | 23-Jul | | 24-Jun | 20-Jul | 3-Aug |
| 17-Jun | 24-Jul | | 26-Jun | 21-Jul | 6-Aug |
| 19-Jun | 27-Jul | | 27-Jun | 22-Jul | 7-Aug |
| 23-Jun | 28-Jul | | 28-Jun | 25-Jul | 12-Aug |
| 25-Jun | 31-Jul | 13-Aug | 29-Jun | 26-Jul | 14-Aug |
| Index No/Observations Yes (16) | | | Index No/Observations No (32) | | |

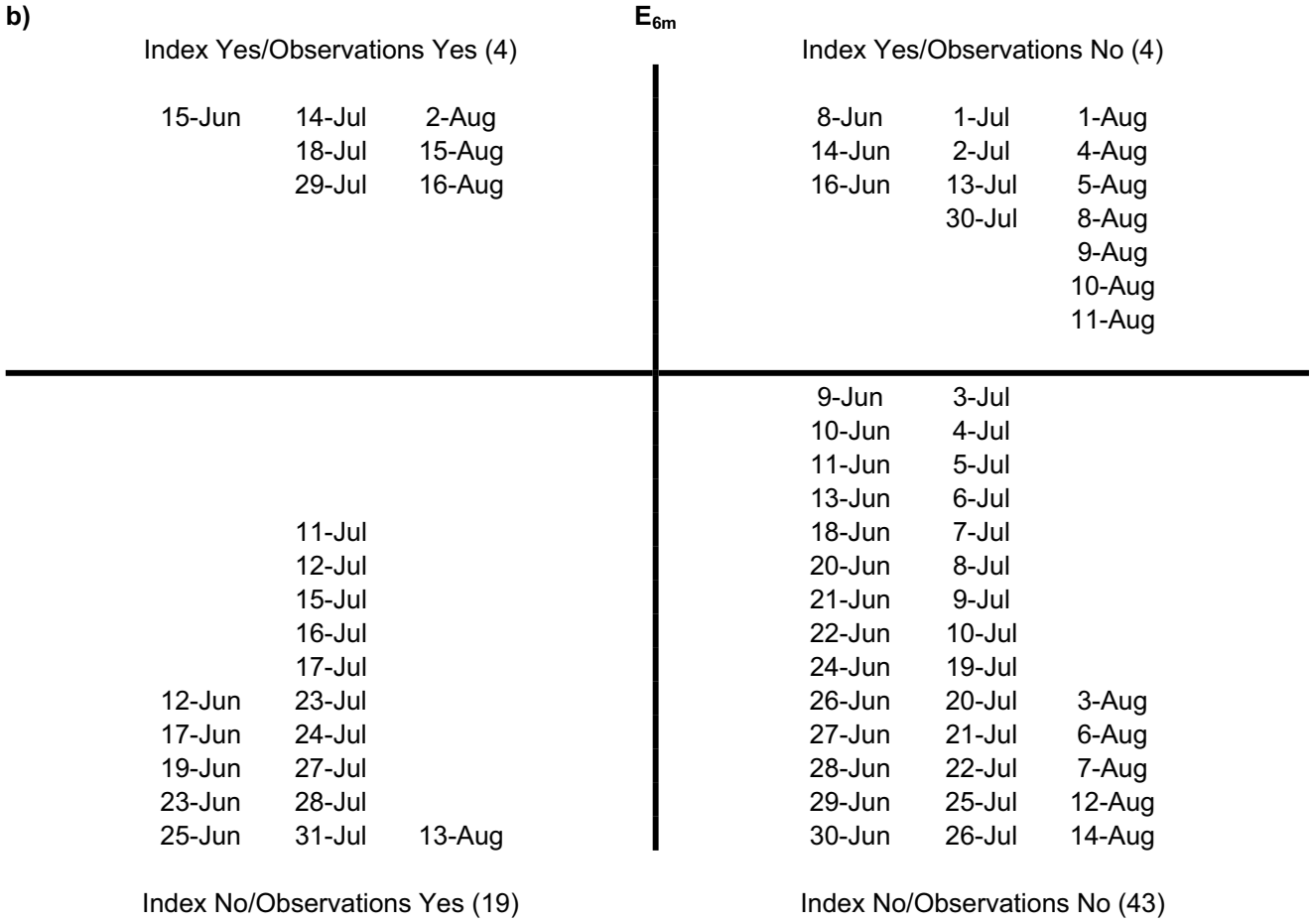


Figure 4.2. 4-quadrant plots illustrating the performance of the Turf Field Lab derived a) $E_{6h}$ and b) $E_{6m}$ indices. Dates listed in the upper-left and lower-right quadrants are days that the index matched observed conditions. Dates listed in the upper-right quadrant represent false alarms, and dates listed in the lower-left quadrant represent missed events.

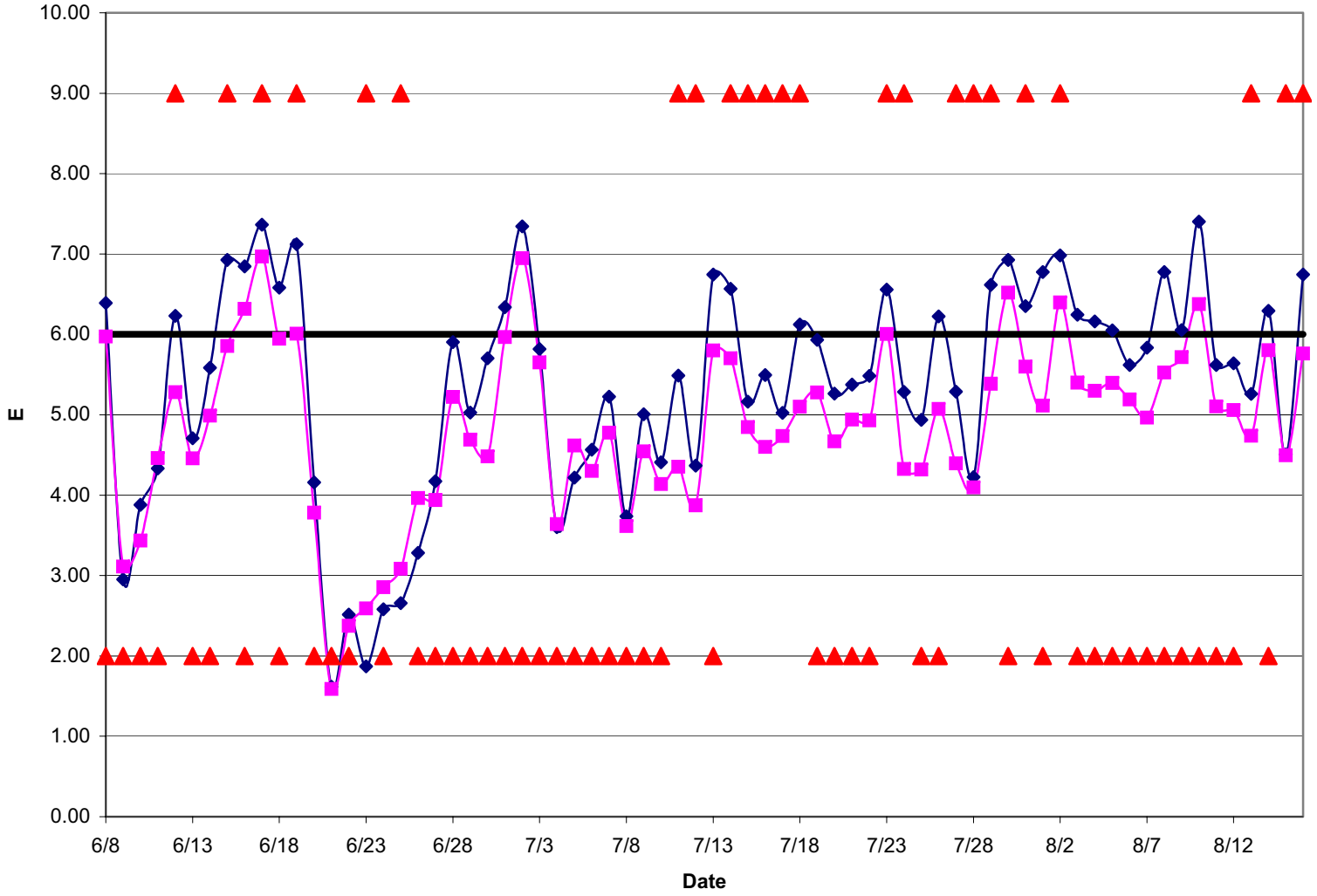


Figure 4.3. Turf Field Lab-derived $E_{2m}$ and $E_{2h}$ indices, with observations of disease activity overlaid. The series of squares represents Turf Field Lab-derived $E_{2m}$, and the series of diamonds represents $E_{2h}$. Where the series of triangles lies below the solid E = 6 line, disease was not observed. Triangles above the line represent days disease was observed.

**a)**

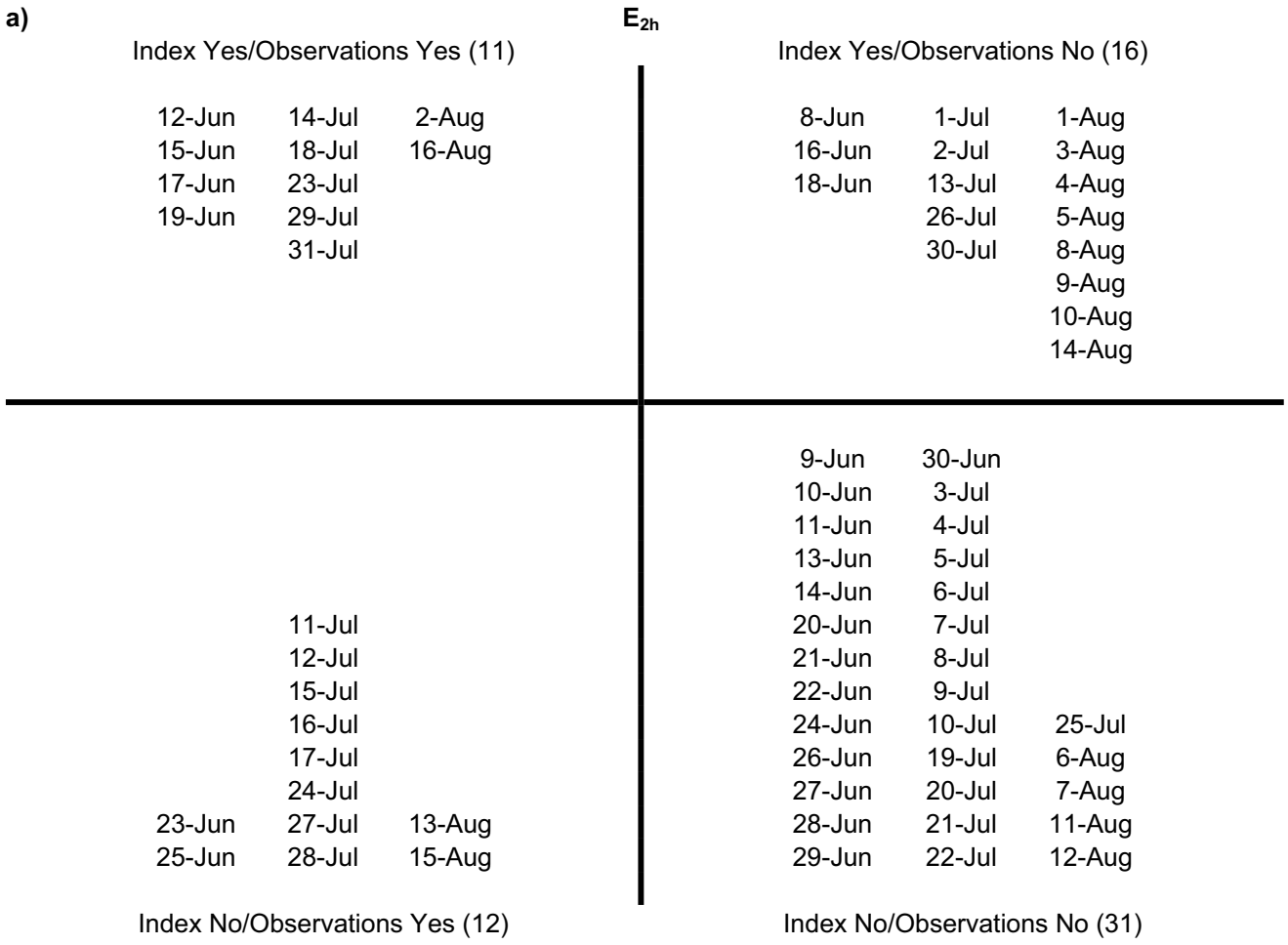
$E_{2h}$
Index Yes/Observations Yes (11)
12-Jun 14-Jul 2-Aug
15-Jun 18-Jul 16-Aug
17-Jun 23-Jul
19-Jun 29-Jul
31-Jul
Index Yes/Observations No (16)
8-Jun 1-Jul 1-Aug
16-Jun 2-Jul 3-Aug
18-Jun 13-Jul 4-Aug
26-Jul 5-Aug
30-Jul 8-Aug
9-Aug
10-Aug
14-Aug
Index No/Observations Yes (12)
11-Jul
12-Jul
15-Jul
16-Jul
17-Jul
24-Jul
23-Jun 27-Jul 13-Aug
25-Jun 28-Jul 15-Aug
Index No/Observations No (31)
9-Jun 30-Jun
10-Jun 3-Jul
11-Jun 4-Jul
13-Jun 5-Jul
14-Jun 6-Jul
20-Jun 7-Jul
21-Jun 8-Jul
22-Jun 9-Jul
24-Jun 10-Jul 25-Jul
26-Jun 19-Jul 6-Aug
27-Jun 20-Jul 7-Aug
28-Jun 21-Jul 11-Aug
29-Jun 22-Jul 12-Aug

**b)**

$E_{2m}$

| Index Yes/Observations Yes (4) | | | Index Yes/Observations No (4) | | | |
|---|---|---|---|---|---|---|
| 17-Jun | 23-Jul | 2-Aug | 16-Jun | 2-Jul | 10-Aug | |
| 19-Jun | | | | 30-Jul | | |
| | | | 8-Jun | 28-Jun | 19-Jul | |
| | 11-Jul | | 9-Jun | 29-Jun | 20-Jul | |
| | 12-Jul | | 10-Jun | 30-Jun | 21-Jul | |
| | 14-Jul | | 11-Jun | 1-Jul | 22-Jul | |
| | 15-Jul | | 13-Jun | 3-Jul | 25-Jul | |
| | 16-Jul | | 14-Jun | 4-Jul | 26-Jul | |
| | 17-Jul | | 18-Jun | 5-Jul | 1-Aug | |
| | 18-Jul | | 20-Jun | 6-Jul | 3-Aug | |
| | 24-Jul | | 21-Jun | 7-Jul | 4-Aug | |
| 12-Jun | 27-Jul | | 22-Jun | 8-Jul | 5-Aug | 9-Aug |
| 15-Jun | 28-Jul | 13-Aug | 24-Jun | 9-Jul | 6-Aug | 11-Aug |
| 23-Jun | 29-Jul | 15-Aug | 26-Jun | 10-Jul | 7-Aug | 12-Aug |
| 25-Jun | 31-Jul | 16-Aug | 27-Jun | 13-Jul | 8-Aug | 14-Aug |
| Index No/Observations Yes (19) | | | Index No/Observations No (43) | | | |

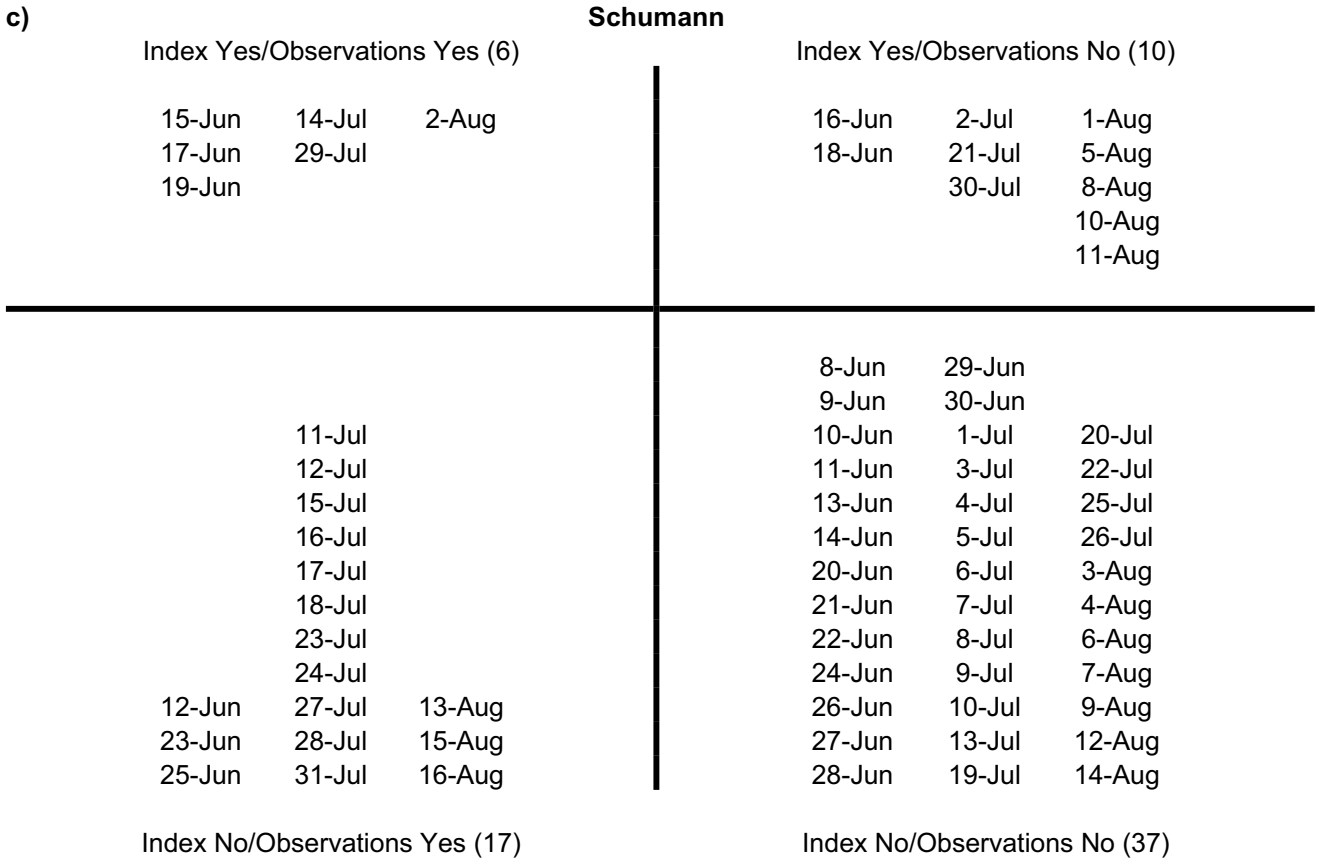


Figure 4.4. 4-quadrant plots illustrating the performance of the Turf Field Lab-derived a) $E_{2h}$, b) $E_{2m}$, and c) Schumann indices. Dates listed in the upper-left and lower-right quadrants are days that the index match observed conditions. Dates listed in the upper-right quadrant represent false alarms, and dates listed in the lower-left quadrant represent missed events.

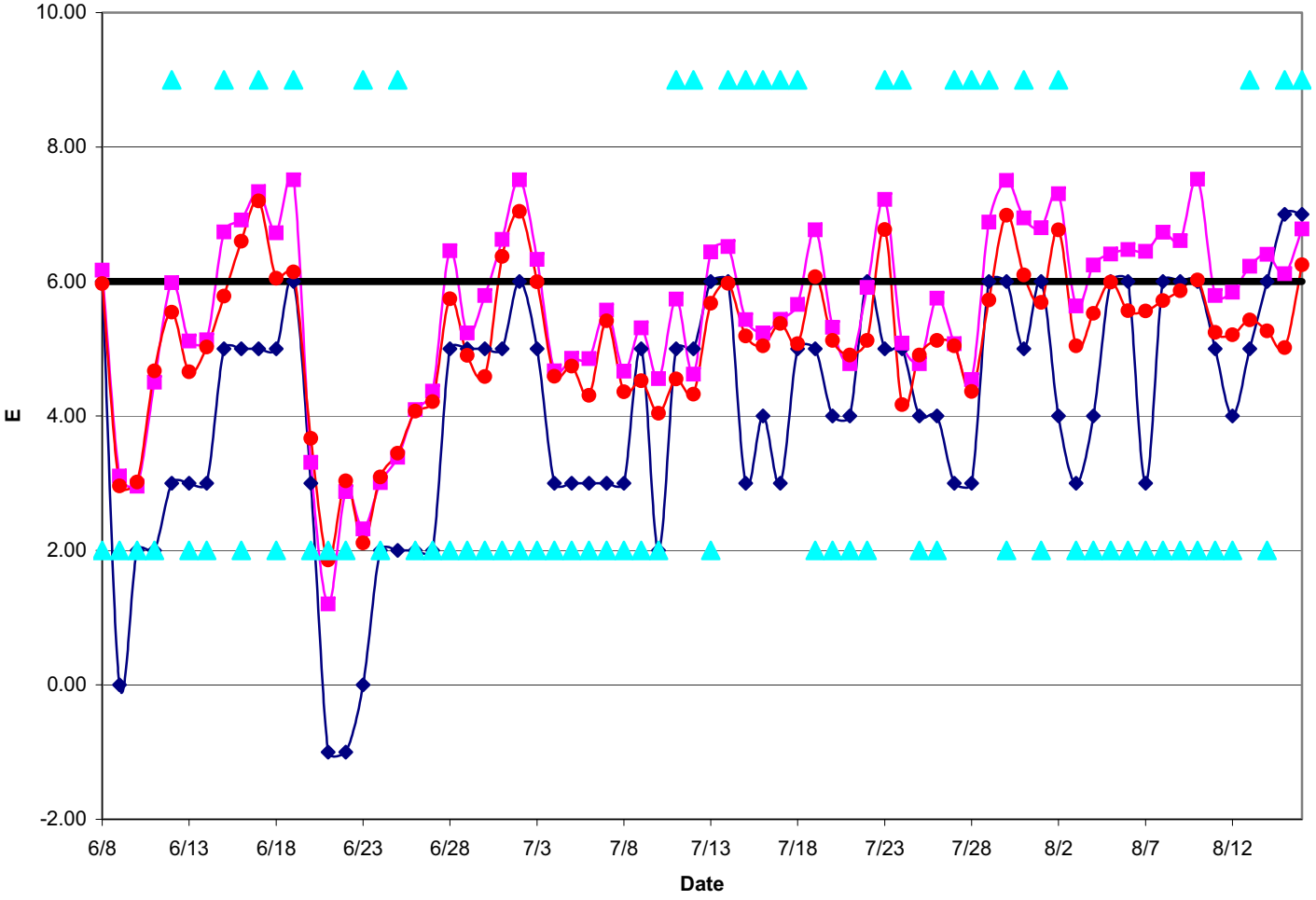


Figure 4.5. RDU-derived $E_6$, $E_{2m}$, and $E_{2h}$ indices, with observations of disease activity overlaid. The series of diamonds represents RDU-derived $E_6$, the series of circles represents $E_{2m}$, and the series of squares represents $E_{2h}$. Where the series of triangles lies below the solid E = 6 line, disease was not observed. Triangles above the line represent days disease was observed.

**a)**

**$E_6$**

| Index Yes/Observations Yes (5) | | |
|---|---|---|
| 19-Jun | 14-Jul | 15-Aug |
| | 29-Jul | 16-Aug |

| Index Yes/Observations No (12) | | |
|---|---|---|
| 8-Jun | 2-Jul | 1-Aug |
| | 13-Jul | 5-Aug |
| | 22-Jul | 6-Aug |
| | 30-Jul | 8-Aug |
| | | 9-Aug |
| | | 10-Aug |
| | | 14-Aug |

| Index No/Observations Yes (18) | | |
|---|---|---|
| | 11-Jul | |
| | 12-Jul | |
| | 15-Jul | |
| | 16-Jul | |
| | 17-Jul | |
| | 18-Jul | |
| 12-Jun | 23-Jul | |
| 15-Jun | 24-Jul | |
| 17-Jun | 27-Jul | |
| 23-Jun | 28-Jul | 2-Aug |
| 25-Jun | 31-Jul | 13-Aug |

| Index No/Observations No (35) | | |
|---|---|---|
| 9-Jun | 28-Jun | |
| 10-Jun | 29-Jun | |
| 11-Jun | 30-Jun | |
| 13-Jun | 1-Jul | |
| 14-Jun | 3-Jul | 20-Jul |
| 16-Jun | 4-Jul | 21-Jul |
| 18-Jun | 5-Jul | 25-Jul |
| 20-Jun | 6-Jul | 26-Jul |
| 21-Jun | 7-Jul | 3-Aug |
| 22-Jun | 8-Jul | 4-Aug |
| 24-Jun | 9-Jul | 7-Aug |
| 26-Jun | 10-Jul | 11-Aug |
| 27-Jun | 19-Jul | 12-Aug |

**b)**

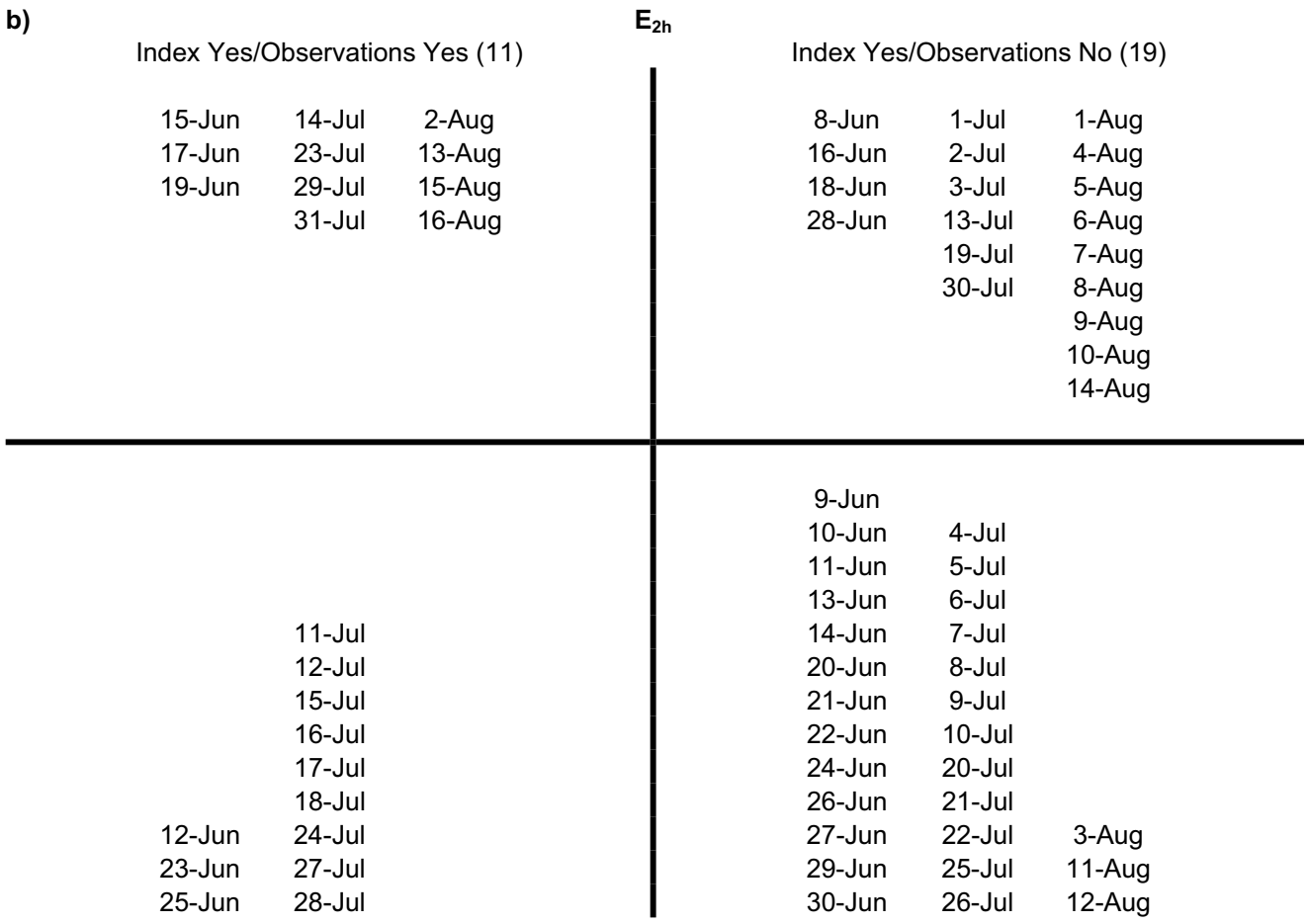
$E_{2h}$
Index Yes/Observations Yes (11)
15-Jun 14-Jul 2-Aug
17-Jun 23-Jul 13-Aug
19-Jun 29-Jul 15-Aug
31-Jul 16-Aug
Index Yes/Observations No (19)
8-Jun 1-Jul 1-Aug
16-Jun 2-Jul 4-Aug
18-Jun 3-Jul 5-Aug
28-Jun 13-Jul 6-Aug
19-Jul 7-Aug
30-Jul 8-Aug
9-Aug
10-Aug
14-Aug
11-Jul
12-Jul
15-Jul
16-Jul
17-Jul
18-Jul
12-Jun 24-Jul
23-Jun 27-Jul
25-Jun 28-Jul
Index No/Observations Yes (12)
9-Jun
10-Jun 4-Jul
11-Jun 5-Jul
13-Jun 6-Jul
14-Jun 7-Jul
20-Jun 8-Jul
21-Jun 9-Jul
22-Jun 10-Jul
24-Jun 20-Jul
26-Jun 21-Jul
27-Jun 22-Jul 3-Aug
29-Jun 25-Jul 11-Aug
30-Jun 26-Jul 12-Aug
Index No/Observations No (28)

**c)**

$E_{2m}$

| Index Yes/Observations Yes (6) | | | Index Yes/Observations No (7) | | |
|---|---|---|---|---|---|
| 17-Jun | 23-Jul | 2-Aug | 16-Jun | 1-Jul | 10-Aug |
| 19-Jun | 31-Jul | 16-Aug | 18-Jun | 2-Jul | |
| | | | | 19-Jul | |
| | | | | 30-Jul | |
| | | | | | 22-Jul |
| | | | 8-Jun | 29-Jun | 25-Jul |
| | | | 9-Jun | 30-Jun | 26-Jul |
| | 11-Jul | | 10-Jun | 3-Jul | 1-Aug |
| | 12-Jul | | 11-Jun | 4-Jul | 3-Aug |
| | 14-Jul | | 13-Jun | 5-Jul | 4-Aug |
| | 15-Jul | | 14-Jun | 6-Jul | 5-Aug |
| | 16-Jul | | 20-Jun | 7-Jul | 6-Aug |
| | 17-Jul | | 21-Jun | 8-Jul | 7-Aug |
| | 18-Jul | | 22-Jun | 9-Jul | 8-Aug |
| 12-Jun | 24-Jul | | 24-Jun | 10-Jul | 9-Aug |
| 15-Jun | 27-Jul | | 26-Jun | 13-Jul | 11-Aug |
| 23-Jun | 28-Jul | 13-Aug | 27-Jun | 20-Jul | 12-Aug |
| 25-Jun | 29-Jul | 15-Aug | 28-Jun | 21-Jul | 14-Aug |

Index No/Observations Yes (17) | Index No/Observations No (40)

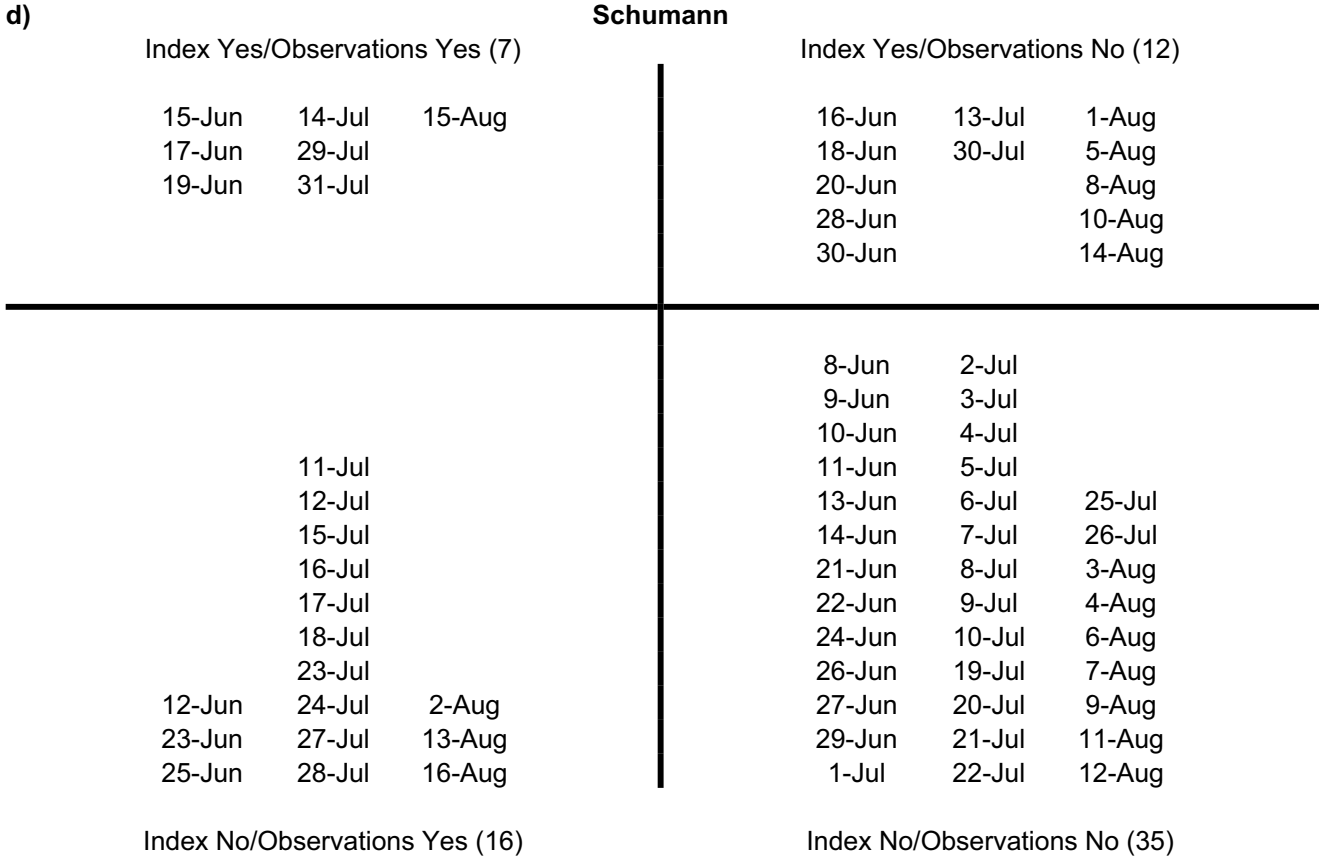


Figure 4.6. 4-quadrant plots illustrating the performance of RDU-derived a) $E_6$, b) $E_{2h}$, c) $E_{2m}$, and d) Schumann indices. Dates in the upper-left and lower-right quadrants are days that the index match observed conditions. Dates listed in the upper-right quadrant represent false alarms, and dates listed in the lower-left quadrant represent missed events.

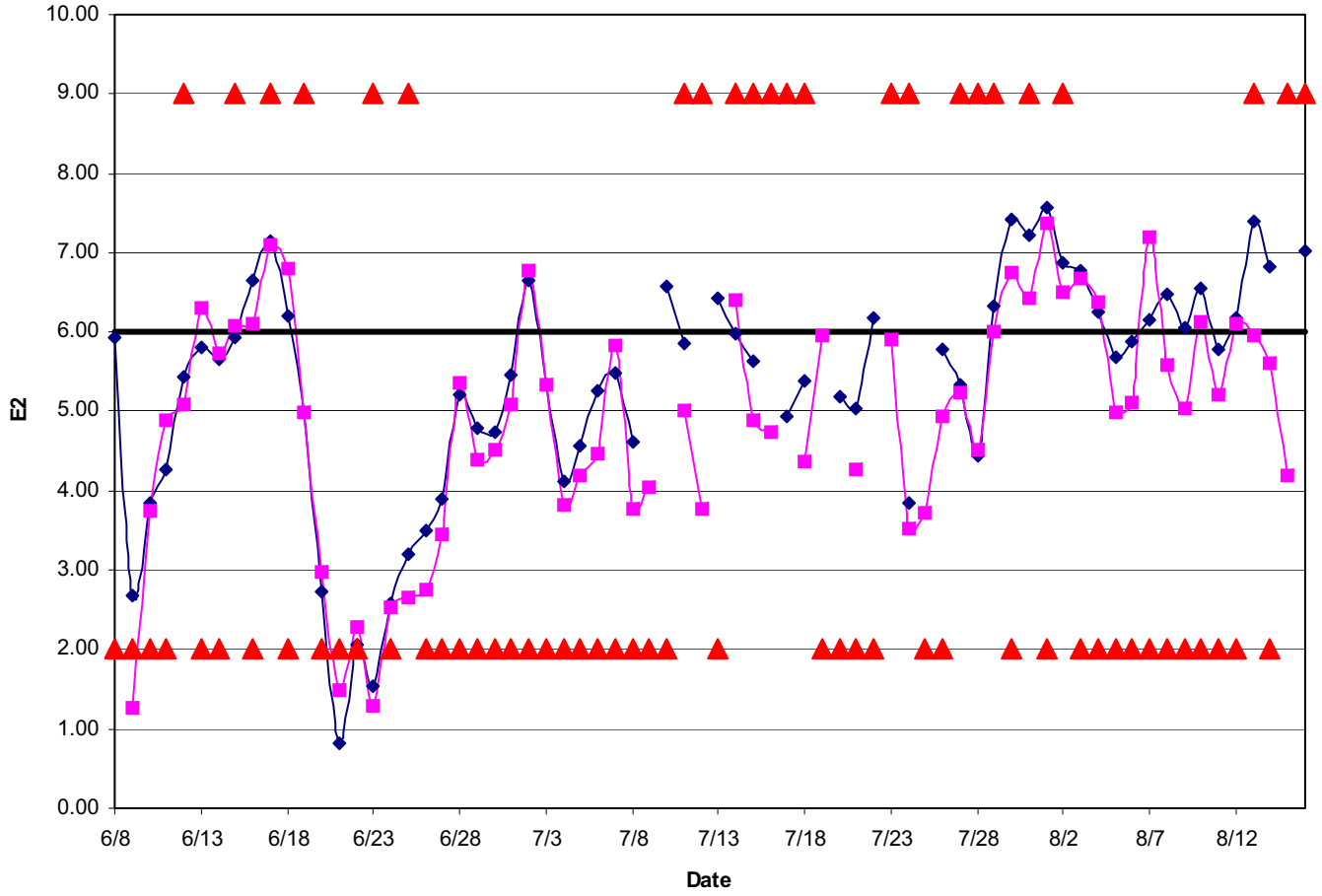


Figure 4.7. Eta-derived 24- and 48-hour forecasts of $E_{2h}$, with disease observations overlaid. The series of diamonds represents Eta-derived 24-h forecasts of $E_{2h}$, and the series of squares represents 48-h forecasts of $E_{2h}$. Where the series of triangles lies below the solid E = 6 line, disease was not observed. Triangles above the line represent days disease was observed.

**a)** **24 h-$E_{2h}$**

Index Yes/Observations Yes (6)

| | | |
|---|---|---|
| 17-Jun | 29-Jul | 2-Aug |
| | 31-Jul | 13-Aug |
| | | 16-Aug |

Index Yes/Observations No (16)

| | | |
|---|---|---|
| 16-Jun | 2-Jul | 1-Aug |
| 18-Jun | 10-Jul | 3-Aug |
| | 13-Jul | 4-Aug |
| | 22-Jul | 7-Aug |
| | 30-Jul | 8-Aug |
| | | 9-Aug |
| | | 10-Aug |
| | | 12-Aug |
| | | 14-Aug |

---

Index No/Observations Yes (13)

| | | |
|---|---|---|
| | 11-Jul | |
| | 14-Jul | |
| | 15-Jul | |
| 12-Jun | 17-Jul | |
| 15-Jun | 18-Jul | |
| 19-Jun | 24-Jul | |
| 23-Jun | 27-Jul | |
| 25-Jun | 28-Jul | |

Index No/Observations No (28)

| | | |
|---|---|---|
| 8-Jun | | |
| 9-Jun | 29-Jun | |
| 10-Jun | 30-Jun | |
| 11-Jun | 1-Jul | |
| 13-Jun | 3-Jul | |
| 14-Jun | 4-Jul | |
| 20-Jun | 5-Jul | |
| 21-Jun | 6-Jul | |
| 22-Jun | 7-Jul | |
| 24-Jun | 8-Jul | |
| 26-Jun | 20-Jul | 5-Aug |
| 27-Jun | 21-Jul | 6-Aug |
| 28-Jun | 26-Jul | 11-Aug |

**b)** **48 h-$E_{2h}$**

| Index Yes/Observations Yes (4) | | | Index Yes/Observations No (4) | | |
|---|---|---|---|---|---|
| 15-Jun | 14-Jul | 2-Aug | 13-Jun | 2-Jul | 1-Aug |
| 17-Jun | 29-Jul | | 16-Jun | 30-Jul | 3-Aug |
| | 31-Jul | | 18-Jun | | 4-Aug |
| | | | | | 7-Aug |
| | | | | | 10-Aug |
| | | | | | 12-Aug |
| | | | 9-Jun | | |
| | | | 10-Jun | | |
| | | | 11-Jun | 1-Jul | |
| | | | 14-Jun | 3-Jul | |
| | | | 20-Jun | 4-Jul | |
| | 11-Jul | | 21-Jun | 5-Jul | |
| | 12-Jul | | 22-Jun | 6-Jul | |
| | 15-Jul | | 24-Jun | 7-Jul | 5-Aug |
| | 16-Jul | | 26-Jun | 8-Jul | 6-Aug |
| 12-Jun | 18-Jul | | 27-Jun | 9-Jul | 8-Aug |
| 19-Jun | 23-Jul | | 28-Jun | 19-Jul | 9-Aug |
| 23-Jun | 27-Jul | 13-Aug | 29-Jun | 21-Jul | 11-Aug |
| 25-Jun | 28-Jul | 15-Aug | 30-Jun | 25-Jul | 14-Aug |
| Index No/Observations Yes (19) | | | Index No/Observations No (43) | | |

Figure 4.8. 4-quadrant plots illustrating the performance of the Eta-derived a) 24-h and b) 48-h $E_{2h}$ forecasted indices. Dates listed in the upper-left and lower-right quadrants are days that the index match observed conditions. Dates listed in the upper-right quadrant represent false alarms, and dates listed in the lower-left quadrant represent missed events.

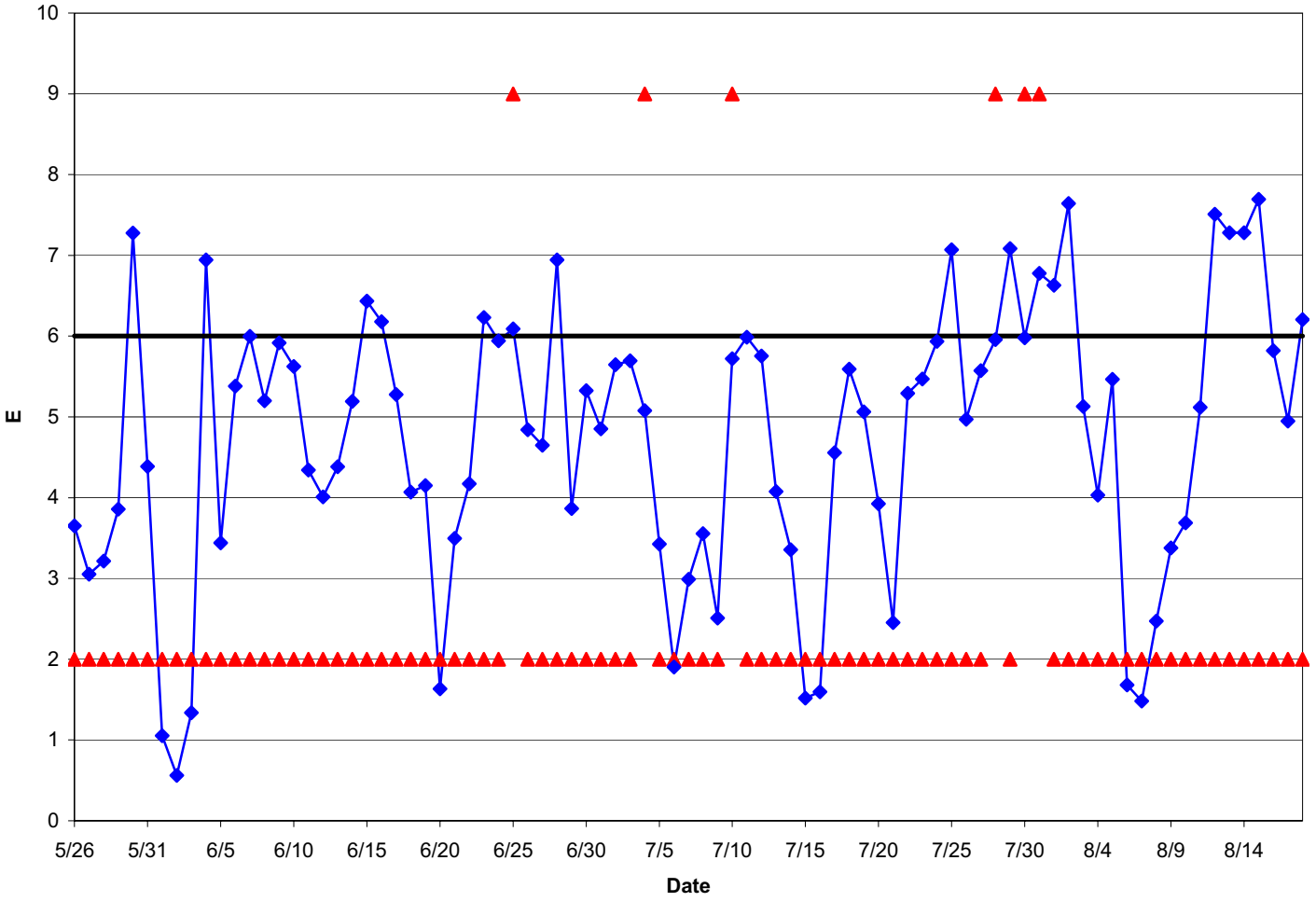


Figure 4.9. Turf Field Lab-derived E2h indices using data from the summer of 2004, with observations of disease activity overlaid. Where the series of triangles lies below the solid E = 6 line, disease was not observed. Triangles above the line represent days disease was observed.

| | | Turf | | | | | RDU | | Eta | | Disease |
|---|---|---|---|---|---|---|---|---|---|---|---|
| | Date | $E_{6m}$ | $E_{6h}$ | $E_{2m}$ | $E_{2h}$ | $E_6$ | $E_{2m}$ | $E_{2h}$ | 24-h $E_{2h}$ | 48-h $E_{2h}$ | obs |
| Episode 1 | 12-Jun | 3 | 3 | 5.3 | 6.2 | 3 | 5.5 | 5.9 | 5.4 | 5.1 | yes |
| Episode 2 | **15-Jun** | **6** | **6** | **5.8** | **6.9** | **5** | **5.8** | **6.7** | **5.9** | **6.3** | **yes** |
| | 16-Jun | 6 | 6 | 6.3 | 6.8 | 5 | 6.6 | 6.9 | 6.7 | 5.7 | no |
| | **17-Jun** | **5** | **5** | **7.0** | **7.4** | **5** | **7.2** | **7.3** | **7.2** | **6.1** | **yes** |
| | 18-Jun | 5 | 5 | 5.9 | 6.6 | 5 | 6.0 | 6.7 | 6.2 | 6.1 | no |
| | **19-Jun** | **5** | **5** | **6.0** | **7.1** | **6** | **6.1** | **7.5** | **5.0** | **7.1** | **yes** |
| Episode 3 | 23-Jun | 2 | 2 | 2.6 | 1.9 | 0 | 2.1 | 2.3 | 1.5 | 1.3 | yes |
| | **24-Jun** | **2** | **2** | **2.8** | **2.6** | **2** | **3.1** | **3.0** | **2.6** | **2.5** | **no** |
| | 25-Jun | 2 | 2 | 3.1 | 2.7 | 2 | 3.4 | 3.4 | 3.2 | 2.6 | yes |
| Episode 4 | **11-Jul** | **4** | **5** | **4.4** | **5.5** | **5** | **4.6** | **5.7** | **5.9** | **5.0** | **yes** |
| | 12-Jul | 4 | 4 | 3.9 | 4.4 | 5 | 4.3 | 4.6 | 0 | 3.8 | yes |
| | **13-Jul** | **6** | **6** | **5.8** | **6.8** | **6** | **5.7** | **6.4** | **6.4** | **0** | **no** |
| | 14-Jul | 6 | 6 | 5.7 | 6.6 | 6 | 5.9 | 6.5 | 5.9 | 6.4 | yes |
| | **15-Jul** | **3** | **3** | **4.8** | **5.2** | **3** | **5.2** | **5.4** | **5.6** | **4.9** | **yes** |
| | 16-Jul | 3 | 3 | 4.6 | 5.5 | 4 | 5.0 | 5.2 | 0 | 4.7 | yes |
| | **17-Jul** | **3** | **3** | **4.7** | **5.0** | **3** | **5.4** | **5.4** | **4.9** | **0** | **yes** |
| | 18-Jul | 6 | 6 | 5.1 | 6.1 | 5 | 5.1 | 5.7 | 5.4 | 4.4 | yes |
| Episode 5 | **23-Jul** | **3** | **3** | **6.0** | **6.7** | **5** | **6.8** | **7.2** | **0** | **5.9** | **yes** |
| | 24-Jul | 4 | 5 | 4.3 | 5.3 | 5 | 4.2 | 5.1 | 3.8 | 3.5 | yes |
| Episode 6 | **27-Jul** | **2** | **3** | **4.4** | **5.2** | **3** | **5.0** | **5.1** | **5.3** | **5.2** | **yes** |
| | 28-Jul | 2 | 2 | 4.1 | 4.2 | 3 | 4.4 | 4.5 | 4.4 | 4.5 | yes |
| | **29-Jul** | **7** | **7** | **5.4** | **6.6** | **6** | **5.7** | **6.9** | **6.3** | **6.0** | **yes** |
| | 30-Jul | 7 | 7 | 6.5 | 6.9 | 6 | 7.0 | 7.5 | 7.4 | 6.8 | no |
| | **31-Jul** | **3** | **3** | **5.6** | **6.4** | **5** | **6.1** | **6.9** | **7.2** | **6.4** | **yes** |
| | 1-Aug | 6 | 6 | 5.1 | 6.8 | 6 | 5.7 | 6.8 | 7.6 | 7.4 | no |
| | **2-Aug** | **6** | **6** | **6.4** | **7.0** | **4** | **6.8** | **7.3** | **6.9** | **6.5** | **yes** |
| Episode 7 | 13-Aug | 3 | 3 | 4.7 | 5.3 | 5 | 5.4 | 6.2 | 7.4 | 5.9 | yes |
| | **14-Aug** | **5** | **5** | **5.8** | **6.3** | **6** | **5.3** | **6.4** | **6.8** | **4.2** | **no** |
| | 15-Aug | 6 | 6 | 4.5 | 4.5 | 7 | 5.0 | 6.1 | 0 | 5.6 | yes |
| | **16-Aug** | **6** | **6** | **5.8** | **6.7** | **7** | **6.2** | **6.8** | **7.0** | **0** | **yes** |

Table 4.1. Brown patch disease events grouped by disease episode, with decision aid indices from the Turf Field Lab, RDU, and the Eta model, and visual disease observations from the Turf Field Lab.

| Index | FAR | POD | CSI |
|---|---|---|---|
| Field Lab $E_{6m}$ | 0.67 | 0.30 | 0.19 |
| **Field Lab $E_{6h}$** | **0.68** | **0.30** | **0.18** |
| Field Lab $E_{2m}$ | 0.50 | 0.17 | 0.15 |
| **Field Lab $E_{2h}$** | **0.59** | **0.48** | **0.28** |
| Field Lab Schumann | 0.62 | 0.26 | 0.18 |
| **RDU $E_6$** | **0.71** | **0.22** | **0.14** |
| RDU $E_{2m}$ | 0.54 | 0.26 | 0.20 |
| **RDU $E_{2h}$** | **0.63** | **0.48** | **0.26** |
| RDU Schumann | 0.63 | 0.30 | 0.20 |
| **Eta 24-h $E_{2h}$** | **0.73** | **0.26** | **0.15** |
| Eta 48-h $E_{2h}$ | 0.65 | 0.26 | 0.18 |
| **Field Lab $E_{2h}$ vs Incidence** | **0.39** | **0.52** | **0.39** |
| Field Lab $E_{2h}$ vs Activity (during incidence period) | 0.61 | 0.41 | 0.25 |
| **2004 Field Lab $E_{2h}$** | **0.88** | **0.33** | **0.10** |

Table 4.2. Skill scores (FAR, POD, and CSI) for all generated disease indices.

## 5. Development of a New Epidemiological Model

The results presented in Section 4 demonstrate the necessity of developing a new epidemiological model for the prediction of brown patch for use in North Carolina. This section details several attempts at producing such an epidemiological model. For details on the techniques used in the following subsections, see Section 3.2.

### *5.1 Autoregressive model*

An autoregressive (AR) model was used in an attempt to model and predict brown patch occurrence. For a general description of the technique, refer to Section 3.2.1. Disease and meteorological observations from both 2003 and 2004 were used in developing the model. Output from the SAS procedure is useful in determining the level of autoregression appropriate for the data being evaluated. The output suggests a second-order autoregressive [AR(2)] model is most appropriate (Table 5.1) In other words, the SAS procedure found that disease activity on any given day was most correlated with disease activity two time-lags (in this case, two days) prior.

A correlation analysis performed in SAS (Table 5.2) shows that the best correlated meteorological parameters with disease occurrence were minimum air temperature, maximum and average dewpoint depression, and maximum and average hourly wind speed (all of these values were for the period from 2200 to 0800 local time the night before the disease observation). The probabilities listed in Table 5.2 are computed using a t-distribution.

The meteorological parameters listed above were input into SAS in order to generate an AR model. Several combinations of these variables were attempted, and the coefficients attained from the AR output, along with the results of a significance test for those coefficients, are listed in Table 5.3. As can be seen in Table 5.3, no combination of the above parameters as inputs led to the development of a model that showed statistically significant results (at the $p \leq 0.05$ level).

*5.2 Logistic regression*

Using SAS software, logistic regression was applied to the brown patch activity observations and meteorological data in order to develop an epidemiological model to describe brown patch growth. An initial attempt at creation of a model included all of the variables that correlated to disease occurrence in a statistically significant way in Section 5.1. That attempt led to the discovery that, using a logistic regression, the only meteorological parameter among those tested that made a statistically significant difference in the epidemiological model was the minimum air temperature between 2200 and 0800 local time, inclusive. The epidemiological model developed using logistic regression was:

$$\hat{p} = \frac{1}{1 + e^{8.14-0.31T_{min}}}, \quad (5.1)$$

where $\hat{p}$ is the predicted probability of brown patch occurrence, and $T_{min}$ is the minimum air temperature between 2200 and 0800 local time in Celsius.

Figure 5.1 shows a time series of all predicted probabilities using Equation 5.1. Equation 5.1 led to a range of probabilities between 0.020 (when $T_{min}$ was 13.54ºC) and 0.44 (when $T_{min}$ was 25.13ºC). For days that disease was observed, the predicted probabilities

ranged between 0.108 and 0.348, compared to a range of 0.020 and 0.44 for days disease was not observed. Table 5.4 shows a breakdown of the number of times disease was observed versus a range of probabilities. While there is a general trend for the ratio of days with brown patch activity versus days without disease activity to increase as the probability range increases, it is apparent from Table 5.4 that the epidemiological model in Equation 5.1 is not sufficient to explain the disease activity alone (assuming the disease observations are accurate).

*5.3 Process-based evaluation*

As described in Section 3.2.3, meteorological variables were assigned points in an attempt to develop a criterion-based epidemiological model, following a similar methodology to F96. The points were assigned in such a manner that the warmest, most humid day with calm winds would receive the most points, and a day with opposite conditions (cold, dry, and windy) would receive few or no points. For daily minimum and maximum air temperature, values in the top 15% were assigned two points; values in the top 30% were assigned one point; values in the top 50% were assigned no points; and values in the bottom 50% were assigned –1 point (non-cumulative). For dewpoint depression, values less than or equal to 2ºC were assigned two points, values between 2ºC and 4ºC were assigned one point, values between 4ºC and 6ºC were assigned no points, and values greater than 6ºC were assigned –1 point. In order to factor the affects of wind speed on dew formation, one point was added if the average nighttime wind speed was less than 1.03 $ms^{-1}$ (two knots), and one point was subtracted if the wind speed was greater than 3.60 $ms^{-1}$ (seven knots). If more than a trace (0.254 mm) of precipitation fell during the day, one point is added, unless during any one

hour of that day more than 12.7 mm (0.5 in) fell. Because brown patch spreads by physically extending hyphae from one plant to another, it is possible that intense rain rates may act to break that physical connection, retarding disease spread (Tredway et al. 2004). In the case of heavy precipitation, two points were removed from the overall score. While the above methodology makes the epidemiological model somewhat relative to the two summers during the study period, it should be just as effective as arbitrarily selecting values of the meteorological variables to serve as delineation points. Table 5.5 shows a breakdown of how points were assigned using the breakdowns described above.

Figure 5.2 is a time series of the point totals for all of the days in the study period. The first 11 days of the summer 2003 study period were not included, as the wind sensor was not functioning properly during that period. In a qualitative sense, there appears to be some promise in using this methodology. Several peaks in the time-series correspond with disease activity outbreaks (e.g., late July/early August 2004), and several valleys correspond to periods during which no disease activity was observed (e.g., the period around 8 August 2003). Table 5.6 shows the same skill scores used in Section 4.4 using all of the possible point values (between –3 and 7) as the threshold for disease. The most accurate results were obtained using a threshold of four points, which resulted in a CSI of 0.212. It can be seen, however, that the CSI scores are most often negatively affected by the FAR, which remains high regardless of how high or low the disease forecasting threshold is set. This implies that we may lack an understanding of factors that tend to inhibit *R. solani* from infecting turfgrass.

In an attempt to determine what factors may be responsible for the high FARs, box-and-whisker plots comparing the distributions of 14 different meteorological variables on

those days that the point total was greater than or equal to four. Four was chosen as the analysis threshold in an attempt to strike a balance between the high PODs expected with using a threshold so low that disease activity is predicted by chance rather than by skill, and not so high that the threshold would be overly restrictive. The variables analyzed included daily maximum, minimum, and mean air temperature and dewpoint, total daily precipitation, the highest daily single-hour precipitation reading, and nightly maximum, minimum, and mean dewpoint depression and wind speed. Two box-and-whisker plots were made for each variable; one plot is for those days that disease activity was observed, the other for days no disease activity was observed. The plots are shown in Figure 5.3. Most of the distributions overlap each other, and there does not appear to be any apparent difference in the variables on days with disease versus days without, with the exception of the daily maximum dewpoint (Figure 5.3d).

T-tests were conducted using SAS software to test the null hypothesis that no difference exists between the means of the variables for days disease was observed versus days disease was not observed. T-tests are appropriate for smaller samples, and assume that the population distributions are normal and independent. While a few of the variables have a somewhat skewed distribution, the t-test is a fairly robust test, and a relaxation of some of the assumptions involved should be acceptable.

The formula for the test statistic, t, is

$$t = \frac{\left(\overline{X}_1 - \overline{X}_2\right)}{s\sqrt{\frac{1}{n_1} + \frac{1}{n_2}}}, \quad (5.2)$$

where $\overline{X}_1$ and $\overline{X}_2$ are the sample means of the two groups, $n_1$ and $n_2$ and samples sizes, and s is the square root of the pooled variance, where $s^2$ (the pooled variance) is

$$s^2 = \frac{(n_1 - 1)s_1^{\,2} + (n_2 - 1)s_2^{\,2}}{n_1 + n_2 + 2}, \quad (5.3)$$

where $s_1^2$ and $s_2^2$ are the sample variances of each group (SAS Institute 1999). Equations (5.2) and (5.3) assume that the variances of the two populations (in this case the populations are days with disease activity observed and days with disease activity unobserved) are equal. When they are unequal, the t statistic is approximated by

$$t = \frac{\overline{X}_1 - \overline{X}_2}{\sqrt{w_1 + w_2}}, \quad (5.4)$$

where $w_x = [(s_x^2)/n_x]$. SAS performs a test to determine whether or not the population variances are equal. In this case, $n_1$ (the sample of days with no disease activity observed) is 26, and $n_2$ is 11. The results of the t-test are listed in Table 5.7. Because the risk of a Type I error (that is, determining a difference in means is statistically significant when it is not) increases when multiple t-tests are performed, a Bonferroni factor must be applied to ensure the experiment-wide significance level 0.05. The corrected p-value using a Bonferroni factor is 0.05 divided by the total number of variables. In this case, 0.05/14 = 0.0036. Reviewing Table 5.7, it is quickly apparent that none of the p-values are beneath that level, and therefore, the null hypothesis that no difference exists between the means of these distributions holds.

*5.4 Summary*

After determining that the epidemiological models developed by S94 and F96 performed inadequately in North Carolina on creeping bentgrass, a study was undertaken to develop a new epidemiological model tailored to the disease and meteorological observations obtained over the summers of 2003 and 2004. Three methods were used to this end: attempting to fit the data to an autoregressive (AR) model, a logistic model, and attempting to use a basic understanding that warm conditions with free moisture availability are most conducive to disease development to develop a criterion-based epidemiological model.

Correlation analysis determined that five meteorological variables most explained the variance in the disease observations: minimum air temperature, maximum and average dewpoint depression, and maximum and average hourly wind speed (all of these values were for the period from 2200 to 0800 local time the night before the disease observation); these variables were used in the AR and logistic regression analyses. For the method based on a process-based evaluation of the meteorological conditions most favorable for brown patch infection, point values were arbitrarily assigned to different meteorological parameters based on specific criterion. None of the methods were able to produce an epidemiological model that performed better than the $E_2$ model developed in F96, and therefore, none would be useful in an operational setting. Several factors may have contributed to the limited success of this method, including:

- Uncertainty concerning the pathology of the disease. The period of time from the infection of the plant until symptoms become apparent is unknown, an in fact may vary based on meteorological conditions. It is possible that looking at 24-hour summaries of meteorological conditions is inappropriate.

- Insufficient knowledge of the meteorological conditions that are *unfavorable* for disease development. High false alarm ratios indicate that an overprediction of brown patch activity is the primary reason CSI scores remain low.

a)

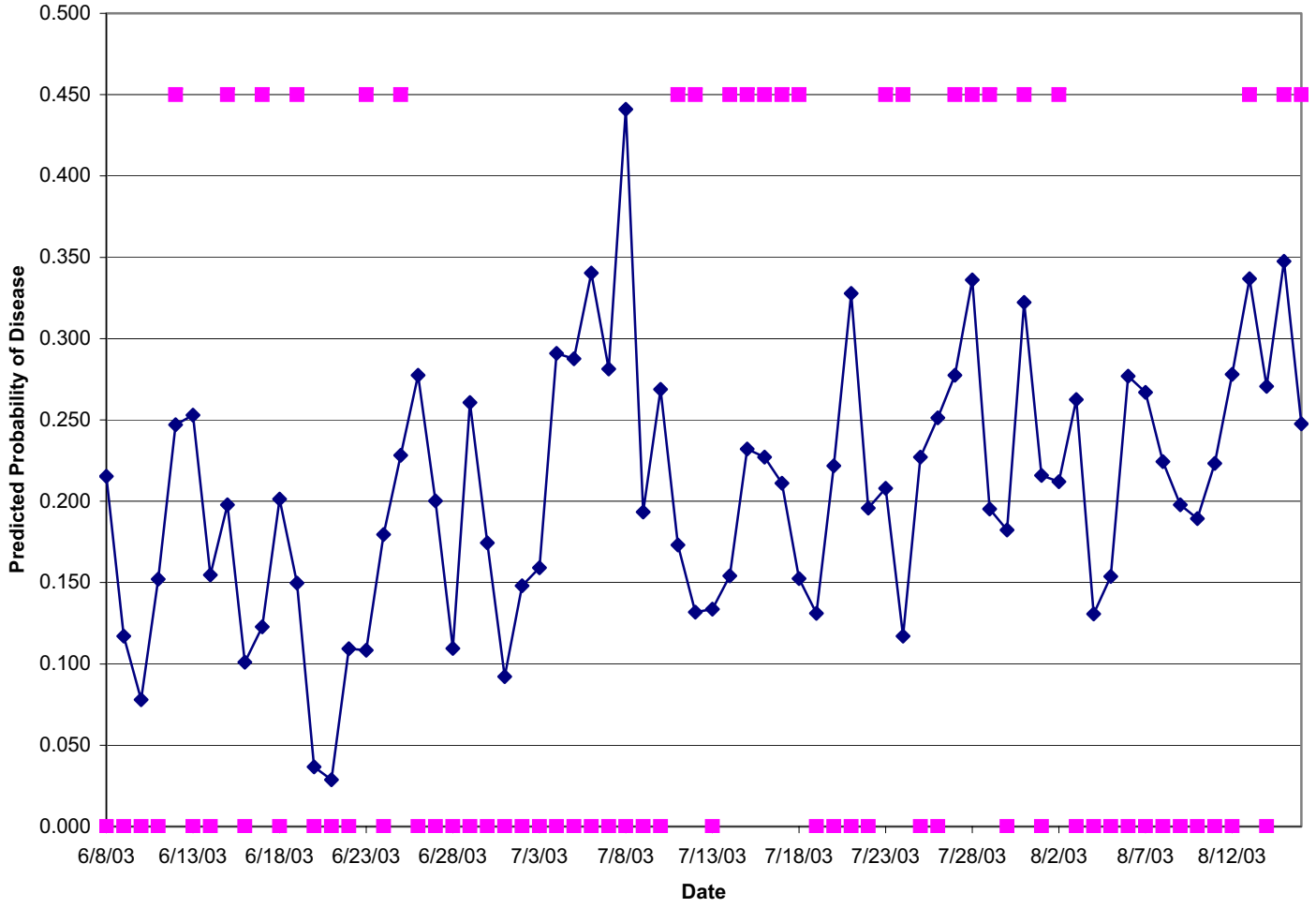
0.500
0.450
0.400
0.350
0.300
0.250
0.200
0.150
0.100
0.050
0.000
Predicted Probability of Disease
6/8/03
6/13/03
6/18/03
6/23/03
6/28/03
7/3/03
7/8/03
7/13/03
7/18/03
7/23/03
7/28/03
8/2/03
8/7/03
8/12/03
Date

b)

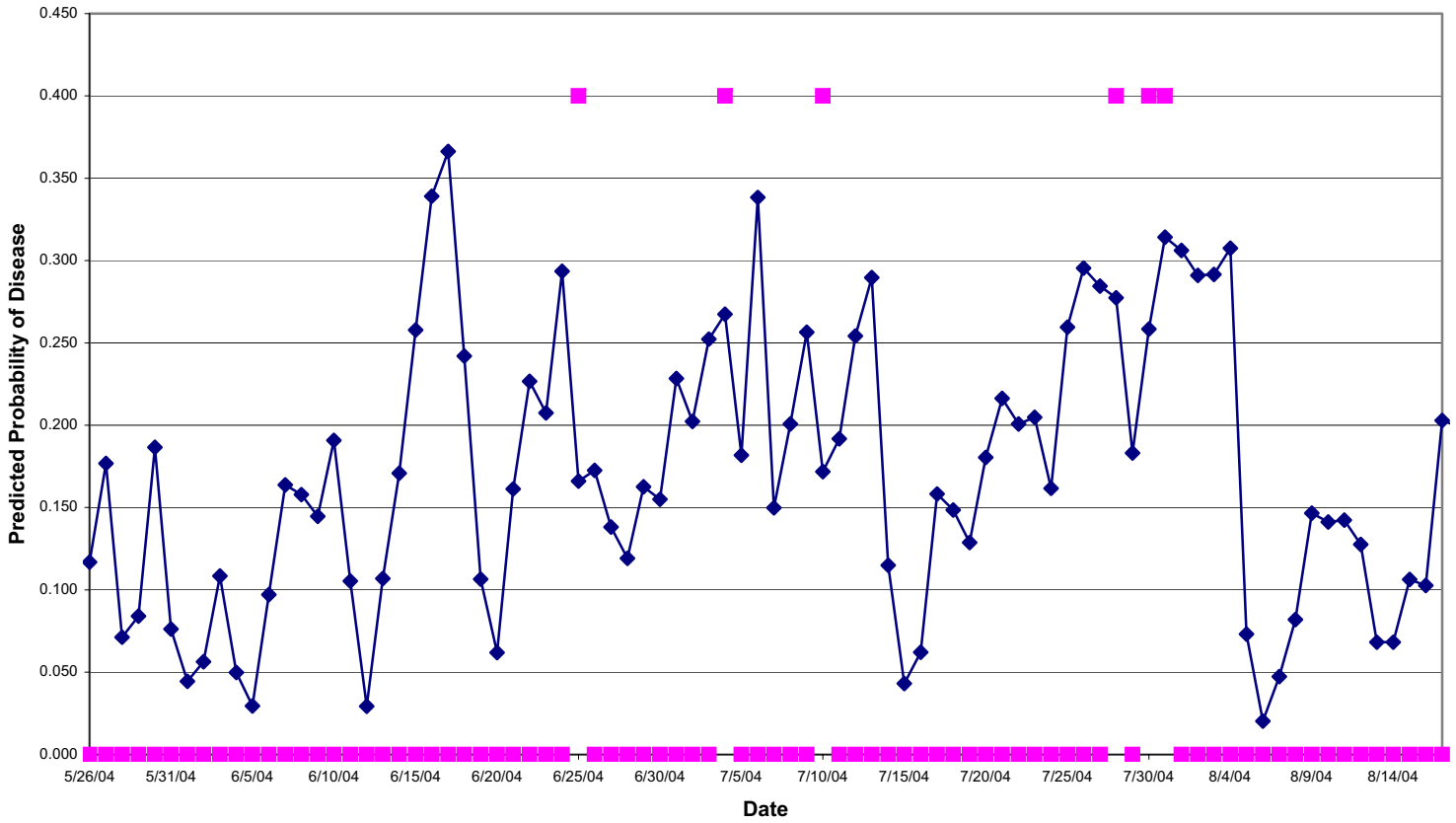


Figure 5.1. Time series of predicted disease probabilities for the summers of a) 2003 and b) 2004. For both a) and b), where the series of square lies below the predicted probability series denotes days disease activity was not observed.

a)

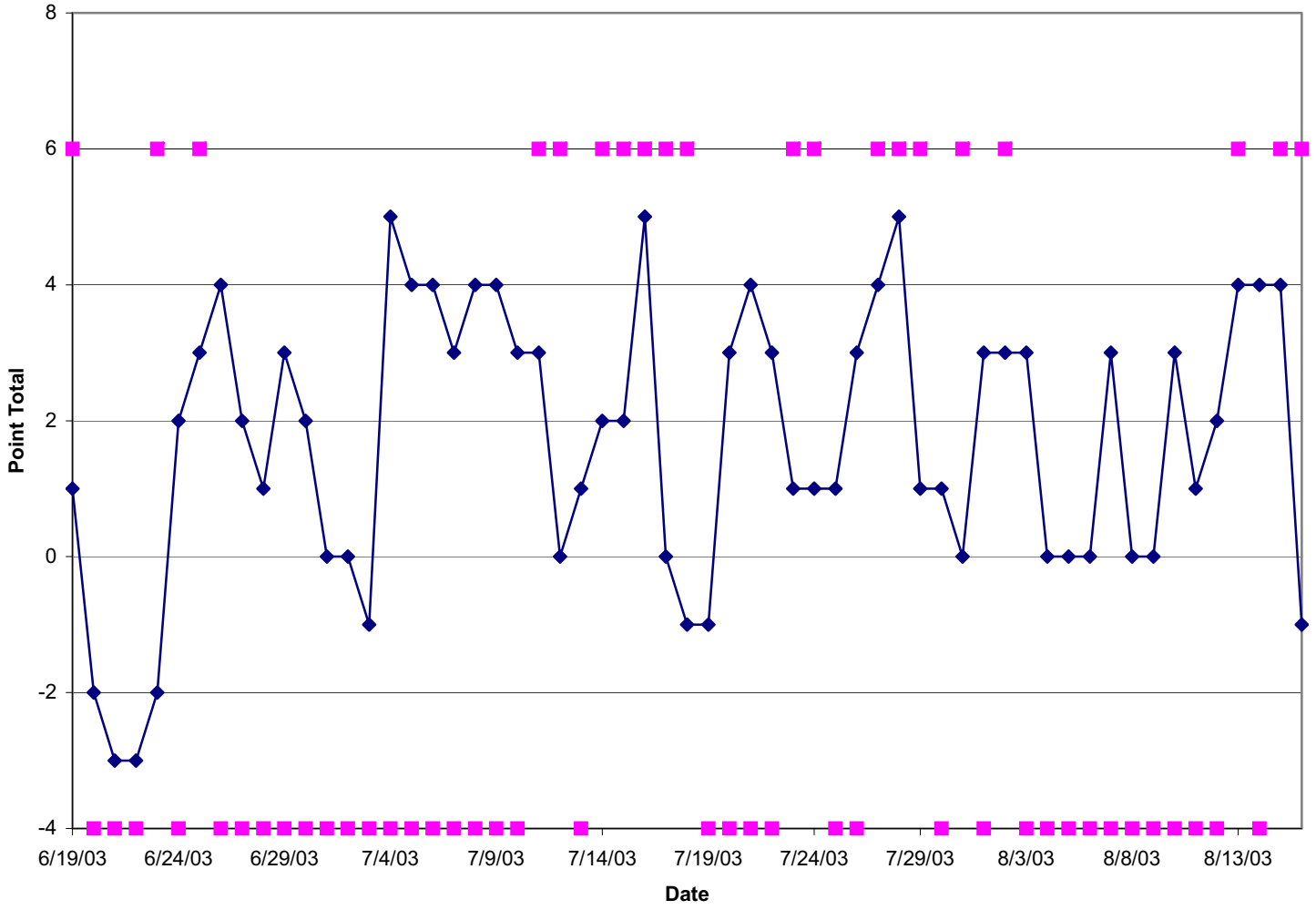
8
6
4
2
0
-2
-4
Point Total
6/19/03
6/24/03
6/29/03
7/4/03
7/9/03
7/14/03
7/19/03
7/24/03
7/29/03
8/3/03
8/8/03
8/13/03
Date

b)

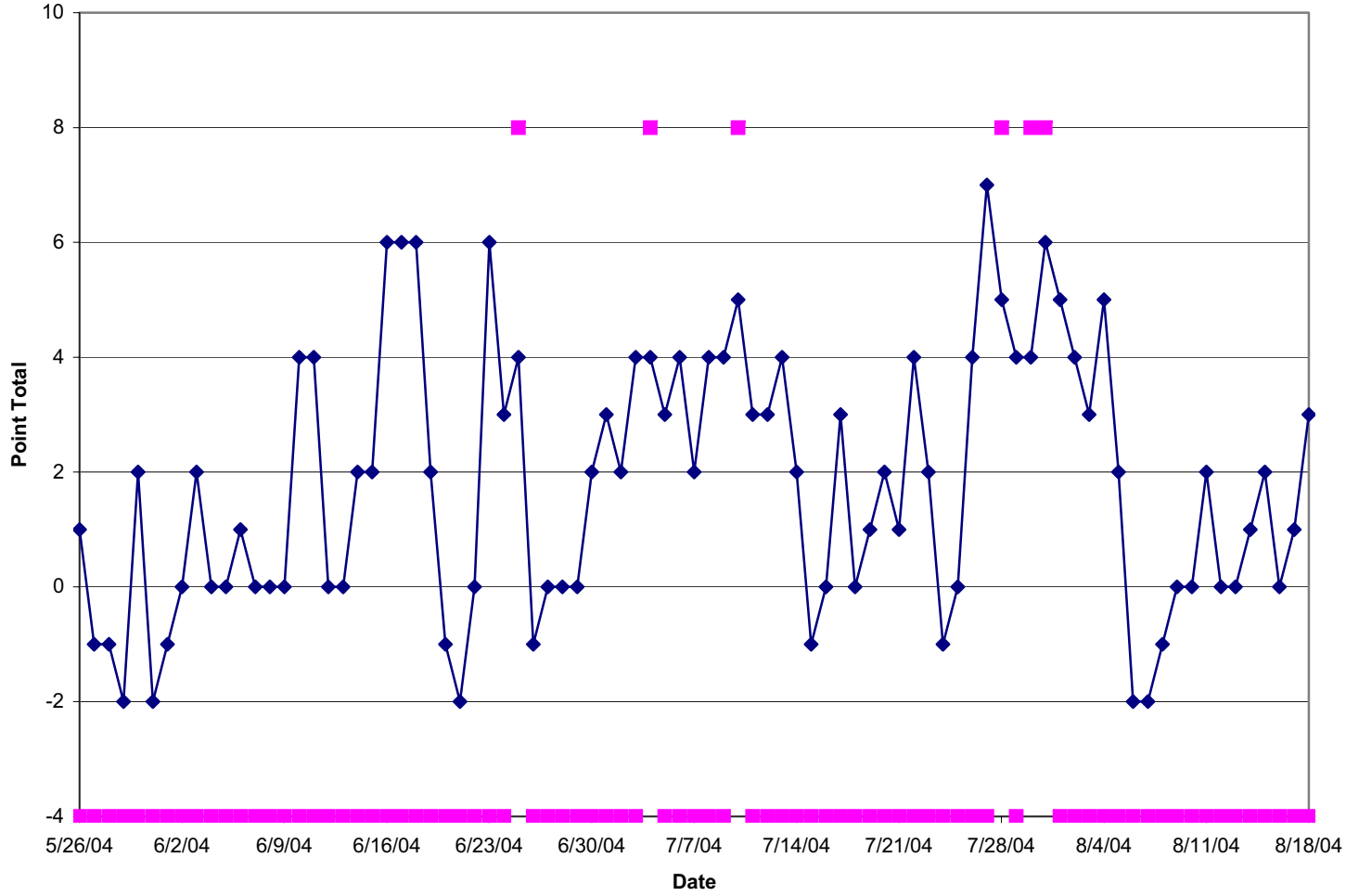


Figure 5.2. Time-series plots of point totals derived from the process-based evaluation for the summers of a) 2003 and b) 2004. Where the series of squares lies below the time series, disease activity was not observed.

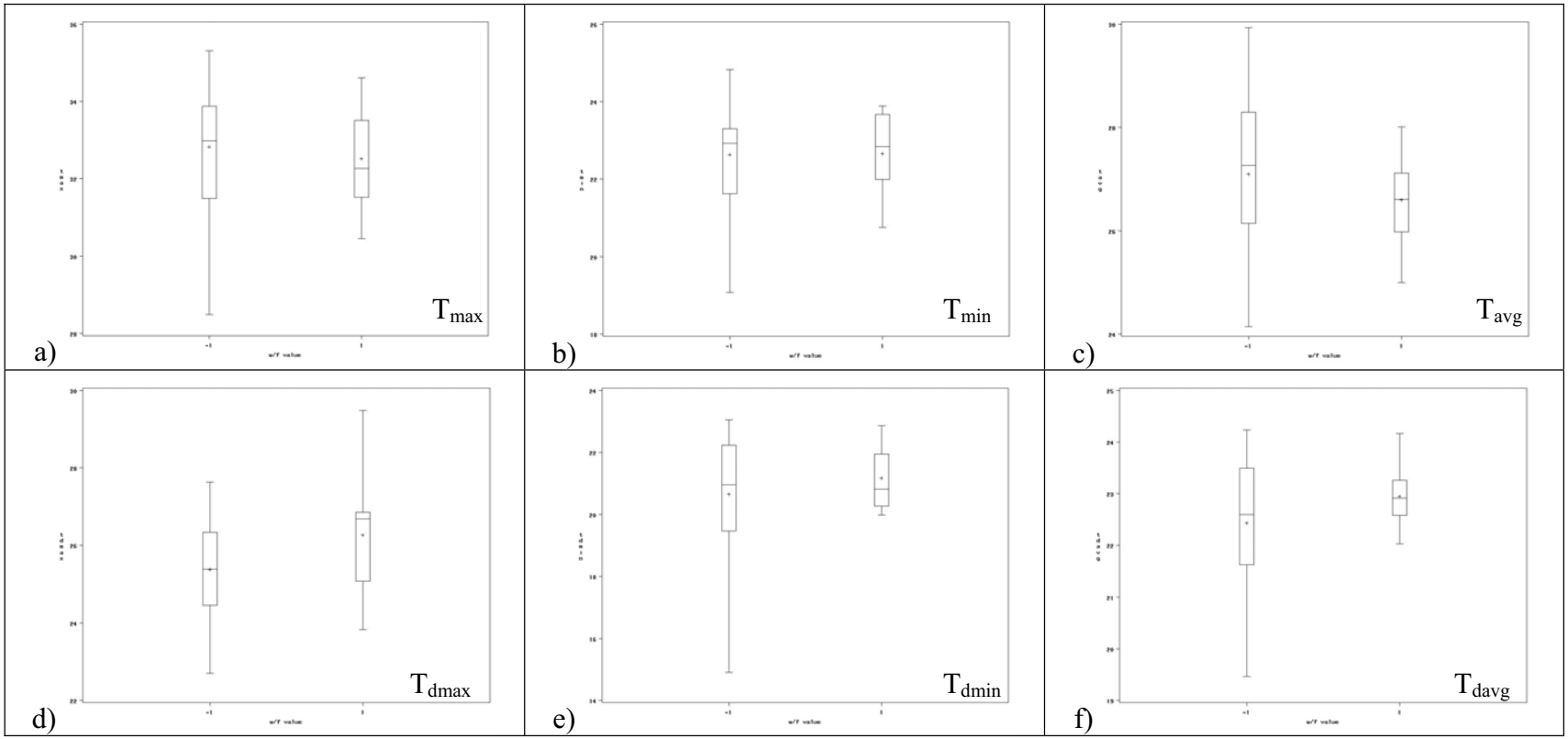
a)
$T_{max}$
b)
$T_{min}$
c)
$T_{avg}$
d)
$T_{dmax}$
e)
$T_{dmin}$
f)
$T_{davg}$

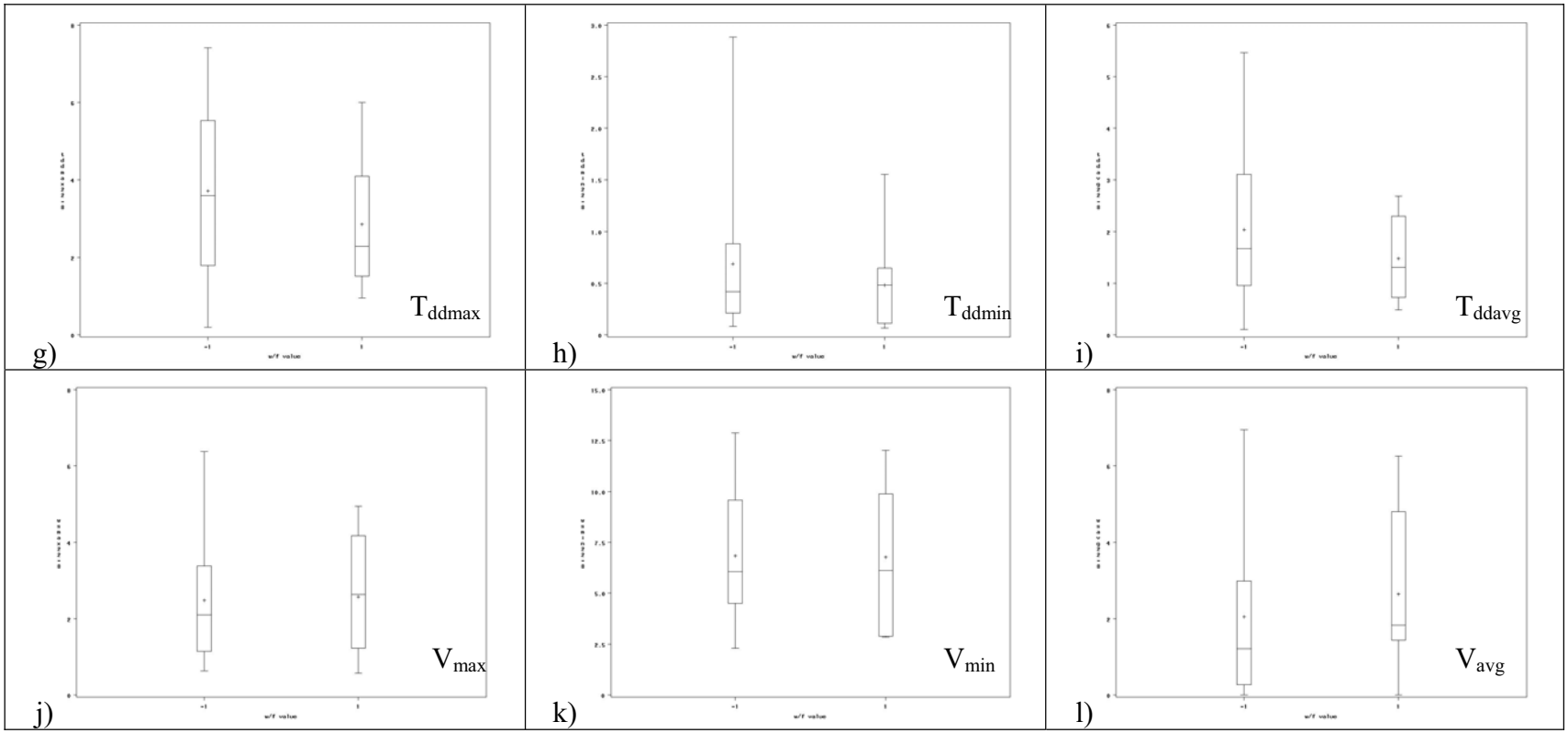
g)
$T_{ddmax}$
h)
$T_{ddmin}$
i)
$T_{ddavg}$
j)
$V_{max}$
k)
$V_{min}$
l)
$V_{avg}$

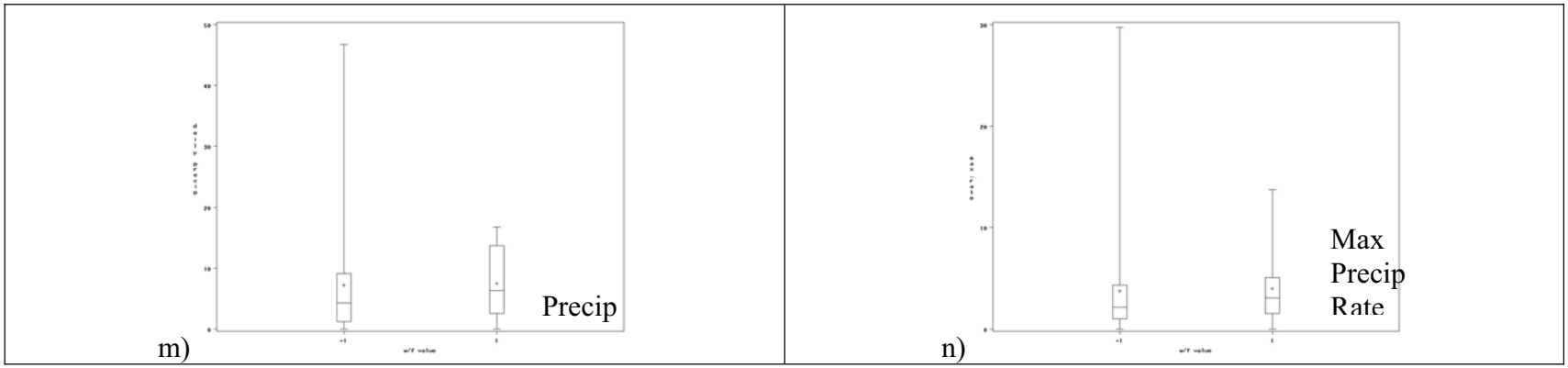


Figure 5.3. Whisker-and-box plots comparing the distribution of meteorological variables on days with observed disease activity to days without observed activity (with point totals of at least 4). The variables compared are a) daily $T_{max}$, b) daily $T_{min}$, c) daily $T_{avg}$, d) daily $T_{dmax}$, e) daily $T_{dmin}$, f) daily $T_{davg}$, g) nightly (between 2200 and 0800 LT) $T_{ddmax}$, h) nightly $T_{ddmin}$, i) nightly $T_{ddavg}$, j) nightly $V_{max}$, k) nightly $V_{min}$, l) nightly $V_{avg}$, m) daily precipitation, and n) daily maximum single-hour precipitation.

| Lag | Covariance | Correlation | Standard Error |
|---|---|---|---|
| 0 | 0.15209 | 1.00000 | 0.00000 |
| **1** | **0.02929** | **0.19255** | **0.08032** |
| 2 | 0.04196 | 0.27590 | 0.08325 |
| **3** | **0.02239** | **0.14716** | **0.08895** |
| 4 | 0.02216 | 0.14568 | 0.09050 |
| **5** | **0.01023** | **0.06729** | **0.09201** |
| 6 | 0.02291 | 0.15064 | 0.09233 |
| **7** | **-0.00312** | **-0.20520** | **0.09390** |
| 8 | -0.00214 | -0.01407 | 0.09393 |
| **9** | **-0.00237** | **-0.01555** | **0.09394** |
| 10 | -0.00138 | -0.00910 | 0.09366 |
| **11** | **0.00484** | **0.03183** | **0.09396** |
| 12 | -0.00063 | -0.00414 | 0.09403 |
| **13** | **0.01850** | **0.12164** | **0.09403** |
| 14 | -0.00753 | -0.04952 | 0.09504 |
| **15** | **0.01160** | **0.07625** | **0.09521** |
| 16 | 0.01258 | 0.08270 | 0.09560 |
| **17** | **0.01235** | **0.08122** | **0.09606** |
| 18 | 0.00688 | 0.04525 | 0.09651 |
| **19** | **0.00786** | **0.05170** | **0.09664** |
| 20 | 0.00239 | 0.01573 | 0.09682 |
| **21** | **0.00217** | **0.01425** | **0.09684** |
| 22 | 0.00315 | 0.02070 | 0.09685 |
| **23** | **0.00292** | **0.01921** | **0.09688** |
| 24 | -0.00376 | -0.02469 | 0.09690 |

Table 5.1. Results of the autocorrelation analysis performed in SAS on disease observations from the summers of 2003 and 2004. The lag column is t minus lag, where t is the current day.

| Parameter | R | Probability(r) |
|---|---|---|
| $T_{max}$ | 0.10773 | 0.1821 |
| **$T_{min}$** | **0.20449** | **0.0107** |
| $T_{avg}$ | 0.1089 | 0.1083 |
| **$T_{ddmax}$** | **-0.18441** | **0.0216** |
| $T_{ddmin}$ | -0.07466 | 0.3559 |
| **$T_{ddavg}$** | **-0.1622** | **0.0437** |
| Total Precip | 0.02554 | 0.7525 |
| **$V_{max}$** | **0.17425** | **0.0367** |
| $V_{min}$ | 0.06466 | 0.4413 |
| **$V_{avg}$** | **0.19455** | **0.0195** |

Table 5.2. Correlation coefficients between select variables and disease observations (all values between 2200 and 0800 LT). Probabilities show significance when less than 0.05.

| Variable | Coefficient/Probability | | | | | |
|---|---|---|---|---|---|---|
| Disease Lag 1 | 0.18/0.039 | 0.18/0.033 | 0.18/0.038 | 0.18/0.037 | 0.18/0.039 | 0.19/0.028 |
| **Disease Lag 2** | **0.17/0.045** | **0.17/0.04** | **0.17/0.044** | **0.17/0.044** | **0.17/0.041** | **0.18/0.036** |
| $T_{min}$ | 0.024/0.17 | 0.021/0.21 | 0.025/0.13 | 0.024/0.17 | 0.024/0.15 | XX |
| **$T_{ddmax}$** | **-0.011/0.74** | **-0.010/0.75** | **-0.011/0.73** | **-0.015/0.33** | **XX** | **-0.016/0.62** |
| $T_{ddavg}$ | -0.0070/0.90 | -0.013/0.81 | -0.0052/0.92 | XX | -0.023/0.35 | -0.0061/0.91 |
| **$V_{max}$** | **0.0077/0.87** | **0.033/0.15** | **XX** | **0.0064/0.89** | **0.0089/0.85** | **0.028/0.54** |
| $V_{avg}$ | 0.019/0.53 | XX | 0.024/0.12 | 0.020/0.51 | 0.019/0.54 | 0.0080/0.79 |

| Variable | Coefficient/Probability | | | | | |
|---|---|---|---|---|---|---|
| Disease lag 1 | 0.18/0.039 | 0.18/0.031 | 0.13/0.12 | 0.13/0.11 | 0.17/0.039 | 0.18/0.031 |
| **Disease lag 2** | **0.17/0.040** | **0.17/0.042** | **0.23/0.0048** | **0.23/0.0053** | **0.18/0.034** | **0.18/0.032** |
| $T_{min}$ | 0.025/0.11 | 0.021/0.21 | 0.027/0.088 | 0.23/0.12 | 0.027/0.090 | 0.024/0.14 |
| **$T_{ddmax}$** | **XX** | **-0.017/0.23** | **XX** | **-0.021/0.13** | **XX** | **XX** |
| $T_{ddavg}$ | -0.022/0.36 | XX | -0.030/0.19 | XX | XX | XX |
| **$V_{max}$** | **XX** | **0.033/0.16** | **XX** | **XX** | **XX** | **0.032/0.17** |
| $V_{avg}$ | 0.024/0.11 | XX | XX | XX | 0.025/0.094 | XX |

Table 5.3. Autocorrelative coefficients and correlation coefficients for several time series input variables, for tests of several input time series combinations, along with the probability of statistical significance.

| Probability range | Days with Disease | Days w/o Disease | Total |
|---|---|---|---|
| 0.000-0.049 | 0/0% | 9/100% | 9 |
| **0.050-0.099** | **0/0%** | **13/100%** | **13** |
| 0.100-0.149 | 5/16% | 26/84% | 31 |
| **0.150-0.199** | **7/20%** | **28/80%** | **35** |
| 0.200-0.249 | 8/31% | 18/69% | 26 |
| **0.250-0.299** | **4/14%** | **24/86%** | **28** |
| 0.300-0.349 | 5/45% | 6/55% | 11 |
| **0.350-0.399** | **0/0%** | **1/100%** | **1** |
| 0.400+ | 0/0% | 1/100% | 1 |
| **Total** | **29** | **126** | **155** |

Table 5.4. Correlation between the predicted probabilities of disease from the logistic regression and disease observations. The percentages are of the percent of days with (or without) disease against the total number of days the probability fell within a given range.

| Variable | Criterion | Points |
|---|---|---|
| $T_{max}$ | ≥ 33.08ºC | 2 |
| | ≥ 31.89ºC & < 33.08ºC | 1 |
| | ≥ 30.75ºC & < 31.89ºC | 0 |
| | < 30.75ºC | -1 |
| $T_{min}$ | ≥ 22.74ºC | 2 |
| | ≥ 21.89ºC & < 22.74ºC | 1 |
| | ≥ 21.03ºC & < 21.89ºC | 0 |
| | < 21.03ºC | -1 |
| Nighttime $T_{ddavg}$ | ≤ 2ºC | 2 |
| | > 2ºC & ≤ 4ºC | 1 |
| | > 4ºC & ≤ 6ºC | 0 |
| | > 6ºC | -1 |
| Nighttime $V_{avg}$ | ≤ 1.03 ms-1 | 1 |
| | > 1.03 ms-1 & ≤ 3.60 ms-1 | 0 |
| | > 3.60 ms-1 | -1 |
| Daily precip | ≥ 0.254 mm | 1 |
| Hourly precip | any one hour ≥ 12.7 mm | -2 |

Table 5.5. Variables used to calculate the index for the criterion-based epidemiological model, and the point values assigned to those variables.

| Threshold | FAR | POD | CSI |
|---|---|---|---|
| -3 | 0.82 | 1.000 | 0.181 |
| -2 | 0.82 | 1.000 | 0.183 |
| -1 | 0.815 | 0.962 | 0.184 |
| 0 | 0.813 | 0.885 | 0.183 |
| 1 | 0.785 | 0.769 | 0.202 |
| 2 | 0.795 | 0.615 | 0.182 |
| 3 | 0.759 | 0.538 | 0.200 |
| 4 | 0.702 | 0.423 | 0.212 |
| 5 | 0.615 | 0.192 | 0.147 |
| 6 | 0.833 | 0.038 | 0.032 |
| 7 | 1.000 | 0 | N/A |
| $E_2 \geq 6$ | 0.421 | 0.384 | 0.300 |

Table 5.6. Skill scores for using several point values as the threshold above which disease activity is forecast, along with the experiment-total skill scores for the $E_2$ epidemiological model.

| Variables | p-vaule |
|---|---|
| $T_{max}$ | 0.59 |
| $T_{min}$ | 0.95 |
| $T_{avg}$ | 0.30 |
| $T_{dmax}$ | 0.089 |
| $T_{dmin}$ | 0.28* |
| $T_{davg}$ | 0.083* |
| Nightly $T_{ddmax}$ | 0.24 |
| Nightly $T_{ddmin}$ | 0.39 |
| Nightly $T_{ddavg}$ | 0.23 |
| Nightly $V_{max}$ | 0.93 |
| Nightly $V_{min}$ | 0.91 |
| Nightly $V_{avg}$ | 0.89 |
| Daily precip | 0.96 |
| Daily max hourly precip | 0.46 |

Table 5.7. Results from t-tests conducted to test the null hypothesis that no difference exists between the above variables on days that disease activity was observed and disease activity was not observed, and the total points assigned using the criterion-based epidemiological model was at least four. * indicates unequal sample variances.

## 6. NWP Model Sensitivity Study

In an effort to determine the sensitivity of those parameters that are likely most important to disease forecasting to changes in model physics (specifically to changes in the land-surface parameterization), a sensitivity study was undertaken using the MM5 model. In the course of this study, two land-surface models were used: a 5-layer soil model, and the NOAH LSM. The land-surface schemes used here have very different methods of handling such meteorological parameters as soil temperature and moisture, and it is expected that these differences will have a non-negligible impact on the forecast of near-surface meteorological parameters. Two cases were studied; the first beginning at 1200 UTC 29 July 2004 and ending at 1200 UTC 31 July 2004, and the second beginning at 1200 UTC 6 August 2004, ending at 1200 UTC 8 August 2004 (see Section 3.3.2.2 for an explanation of why these cases were chosen). The results of this sensitivity study are presented below, and are organized first by case, and by analysis parameter within each case.

### *6.1 Case I: 29-31 July 2004*

Figure 6.1 is the MM5 inner-nest (9-km grid spacing) analysis of conditions at 1200 UTC on 29 July 2005. A trough of low pressure extends from southwest to northeast across the model domain, across eastern Tennessee, western and northern North Carolina, and southern Virginia. A high pressure system is centered to the east of the domain. The model was initialized at 0800 local time, so in general dewpoint depressions are fairly low, and dewpoint temperatures are nearly equal to the air temperatures.

#### *6.1.1 Air temperature*

The a frames in Figures 6.2-6.9 are plots of 2-meter air temperature in Kelvin, contoured every 2 K, valid from 6 through 48 hours after the initialization time, every six hours, for the forecast run using the NOAH LSM. The b frames are the same plot for the forecast run using the 5-layer soil model, and the c frames are difference fields, subtracting the values in the b frames from the a frames (all of the a and b frames have mean sea level pressure overlaid, contoured every 2 hPa). While, as a whole, the differences between the two model runs are not that great, non-negligible differences do exist. Looking at the difference fields from every forecast hour, it can be seen that while most of the difference between the two model runs is in the ± 1 K range, differences greater than ± 5 K exist at some times. Generally speaking, the most widespread areas of temperature difference between the model runs exist in the northwestern quadrant of the model domain. Without reviewing any other parameters in connection with the differing temperature fields, it appears that some of the variability may be diurnal in nature. Careful examination of the temperature and difference fields reveals that over large portions of the domain (especially over the Appalachian Mountains and points north and west), the model run utilizing the NOAH-LSM cools more quickly and over a larger area in response to diurnal variation than does the model run utilizing the 5-layer soil model.

One possible explanation for the differences between each run is that each model utilizes different prognostic equations for soil temperature. The 5-layer soil model uses a constant temperature at a layer beginning at 31 cm below the surface and extending 32 cm in depth. To forecast soil temperature, the model uses the following equation:

$$\frac{\partial T_s}{\partial t} = -\frac{1}{\rho_s c_s}\frac{\partial F}{\partial z}. \quad (6.1)$$

In Equation (6.1), $T_s$ is the soil temperature in Kelvin, $\rho_s$ is its density in $kgm^{-3}$, $c_s$ is its heat capacity in $Jkg^{-1}K^{-1}$, and F is the heat flux in $Wm^{-2}$, which is linearly proportional to the temperature gradient using the relation:

$$F = -K\rho_s c_s \frac{\partial T_s}{\partial z}, \quad (6.2)$$

where K is the thermal diffusivity of the soil in $m^2s^{-1}$. This model uses a constant value for K of 5 * 10-7 $m^2s^{-1}$ (Dudhia 1996). In contrast, the NOAH-LSM uses the equation:

$$\Delta z_i C_i \frac{\partial T_i}{\partial t} = \left( K_t \frac{\partial T}{\partial z} \right)_{z_i+1} - \left( K_t \frac{\partial T}{\partial z} \right)_{z_i} \quad (6.3)$$

for the temperature in the $i^{th}$ soil layer, where C is the volumetric heat capacity in $Jm^{-3}K^{-1}$ (Chen and Dudhia 2001). In the NOAH LSM, both C and K vary with the soil moisture content (a parameter held constant in the 5-layer soil model). These difference likely account for some of the variability between the two separate model runs. Other factors that may also have an effect on the model's temperature output will be discussed in conjunction with analysis of other parameters. A cursory review of meteorological conditions during the previous week (using surface analysis maps available online at http://weather.unisys.com) shows that the northwest quadrant of the inner domain used in this study (where the most widespread variation between the model runs was noted) experience several episodes of heavy precipitation. It is likely, then, that the soil moisture values were higher than their climatological averages. If the NOAH LSM were able to account for this, it would explain many of the variations between the model runs noted above.

*6.1.2 Precipitation*

Figures 6.2-6.9 d and e frames are 6-hourly precipitation totals ending at the time each forecast is valid, and corresponding to the model run of the a and b frame above it. Frame f of these figures is a difference field for the precipitation forecasts from each model run. While most of the differences between the precipitation forecasts between the model runs are slight (slightly more than a trace difference per 6 hours), some significant differences do exist. Some of these differences exceed 25 mm per 6 hours, likely due to localized convection (such as in Figure 6.5f).

The differences in these forecasts could stem from multiple sources. First, in many cases, differences in model precipitation fields correspond with differences in near-surface air temperature fields (that is, greater precipitation rates in the NOAH LSM than in the 5-layer soil model run are associated with lower temperatures, and vice versa). In other cases, it is likely that differences in soil moisture content resulted in differences in atmospheric moisture availability, in turn affecting the manner in which precipitation developed in the model. The NOAH LSM allows for the soil moisture content to vary in time using prognostic equations. In contrast, the 5-layer soil model uses a value for soil moisture that is a function of land use, and is held constant throughout the model run. This possibility will be examined in section 6.1.3. Due to the non-linear nature of atmospheric process, and in turn atmospheric models, it is difficult to determine whether differences in the fields just discussed caused differences the precipitation field, or if differences in the precipitation field contributed to the differences in the other fields. More likely than not, a solution somewhere between the two extremes is the reality.

*6.1.3 Dewpoint depression, and dewpoint*

Dewpoint depressions from each model run are plotted in the g and h frames of Figures 6.2-6.9, with the differences plotted in frame i. Throughout the simulation, dewpoint depressions in the northwest quadrant of the domain are much lower [more than 5 K lower in parts of West Virginia, Kentucky, and Ohio (as in Figure 6.7i)] when the 5-layer soil model was utilized in the model, as opposed to when the NOAH LSM was utilized. The differences were greatest during daytime hours, during periods when daytime temperatures typically far exceed dewpoints, and the natural spread between air temperature and dewpoint is at its largest.

An investigation of dewpoint depression would be incomplete without an analysis of the dewpoints themselves, and plots of these values are displayed in Figures 6.2-6.9 j and k, with difference fields between the runs plotted in the l frames. If the entire variability between dewpoint depression fields from the two model runs were due to differences in the dewpoint fields, one would expect these fields to look nearly identical, but with the signs of the difference fields reversed. Indeed, in some areas, differences in dewpoint seem to explain a large portion of the variability. In the northwest quadrant of the domain, for example, areas of large variation between the dewpoint depression fields are well correlated with large differences in the dewpoint fields. However, in the central portion of the domain (including central and eastern portion of North Carolina and Virginia), areas where a greater than 2 K difference in forecasted dewpoint depressions are collocated with differences in the dewpoint fields of less than 1 K (see figures 6.3 and 6.4 i and l), indicating that in these areas, the difference in dewpoints between the model runs does not explain the entire difference observed in the dewpoint depression fields.

Another possible source for the variability between dewpoint depressions fields is the difference in air temperature fields noted in Section 6.1.1. Obviously, given identical dewpoint temperatures at any single location, a change in the air temperature would result in a corresponding change in the dewpoint depression. Examination of model output indicates that this process is in fact responsible for some of the variability in the dewpoint depression fields. Figures 6.3c (air temperature difference field) and 6.3i (dewpoint depression difference field) show that bulls-eyes of negative difference in air temperature (indicating a warmer model atmosphere in the model run utilizing the 5-layer soil model) in eastern Tennessee and throughout most of North Carolina correspond almost exactly (in size and in the amount of difference observed) with bulls-eyes of negative difference in dewpoint depression (indicating that a larger dewpoint depression exists in the 5-layer soil model run than in the NOAH LSM model run). The higher temperatures in the northwest quadrant of the 5-layer soil model run (when compared to the NOAH LSM run) also correspond with higher dewpoint depressions in the same region. Other examples of this can be seen when comparing the temperature and dewpoint depression fields throughout the remainder of the model runs.

As stated earlier, the meteorological parameters in a model atmosphere (as in the Earth's atmosphere) interact in a non-linear manner, and as such, a definitive discussion on the causal relationship of the differences between the model runs is difficult. Nonetheless, it is apparent that some of the differences noted in the other meteorological parameters are related to differences noted in the dewpoint depression fields.

*6.2 Case II: 6-8 August 2004*

At model initialization time, a cold front had just finished making its way across the model domain, leaving cooler, drier conditions behind. (Figure 6.10). Only the first 24 hours of model output was plotted for this case, and those plots are shown in Figures 6.11-6.15. The trends in the temperature fields (frames a, b, and c in each figure) follow much the same pattern as the temperature fields in Case I (Figures 6.2-6.9 a-c). The northwest quadrant of the domain is marked by lower temperatures in the northwest frame, especially in the evening and nighttime hours. Differences in precipitation are almost non-existent, due to the frontal passage that occurred just before model initialization, resulting in a downslope westerly flow, and overall absence of precipitation through most of the domain (frames d, e, and f).

In the northwest portion of the domain, the dewpoint depression fields are similar to their counterparts for Case I (Figures 6.2-6.9 g-i). Higher dewpoint depressions and lower dewpoints are collocated with higher temperatures in the model forecast run utilizing the 5-layer soil model. Unlike in Case I, a large area where dewpoint depressions are lower in the model forecast utilizing the 5-layer soil model develops in the southwest quadrant of the model domain during the forecast run. Most of this variability seems to be explained by the dewpoint fields, with dewpoints running lower in the NOAH LSM model run than in the 5-layer soil model run. With drier air overhead, the NOAH LSM will allow soil moisture to decrease, also lowering the availability of moisture from the surface to the atmosphere. The 5-layer soil model, however, uses a constant soil moisture value. These constant values may be greater than those that the NOAH LSM predicts, resulting in a greater evapotranspiration potential, and a moister model atmosphere.

*6.3 Summary*

The purpose of this model sensitivity study was to determine if model forecasts of those meteorological parameters that are likely to influence the formation of turfgrass disease (including air temperature, precipitation, and dewpoint depression) were highly influenced by selection of the method in which land-surface processes are parameterized. In order to test this hypothesis, two case studies were performed. The first, spanning from 1200 UTC 29 July 2004 until 1200 UTC 31 July 2004, represented a typical hot, humid summer period in North Carolina. The second, spanning from 1200 UTC 6 August 2004 until 1200 UTC 8 August 2004, was initialized shortly after a cold front had made its way into the Atlantic, leaving behind cooler, drier conditions. It was believed that using these two cases would give an adequate look at the differences changing the land-surface parameterization scheme would have over a range of meteorological conditions. For each case, two model forecasts were performed, one using the NOAH LSM, the other using a less-advanced 5-layer soil model.

An examination of the model forecast output (Figures 6.2-6.9 and 6.11-6.15) shows that non-negligible differences between the model runs in each case did in fact occur. Parameter feedback in meteorological models is non-linear, and it is thus difficult to discuss the exact causal feedbacks that occurred in each model run. However, two key differences between the two land-surface schemes utilized exist that likely led to most of the variation seen between the model runs. First, the NOAH LSM and 5-layer soil model use different prognostic equations for soil temperature, and the NOAH LSM uses an overall deeper soil layer than does the 5-layer soil model. Secondly, the NOAH LSM uses prognostic equations in its determination of soil moisture, while the 5-layer soil model uses a constant soil

moisture content throughout the duration of the model run, dependent only on land-use and season. In combination, these differences can be used to explain much of the variation observed between model runs in each case.

In comparing the results from this section with those from Section 4, it can be seen that, in a relative sense, it is likely that alterations of land-surface parameterizations (and perhaps other physics options as well) are likely to affect forecasts of epidemiological model output than is altering the source of weather data. One method of quantifying this uncertainty would be to create an ensemble epidemiological model forecast, using differing LSM's in each ensemble member. Quantifying the uncertainty in the forecasts would allow end-users of the system to better assess the data they obtain, which would assist them in deciding whether or not to use the output from the epidemiological model on any given day.

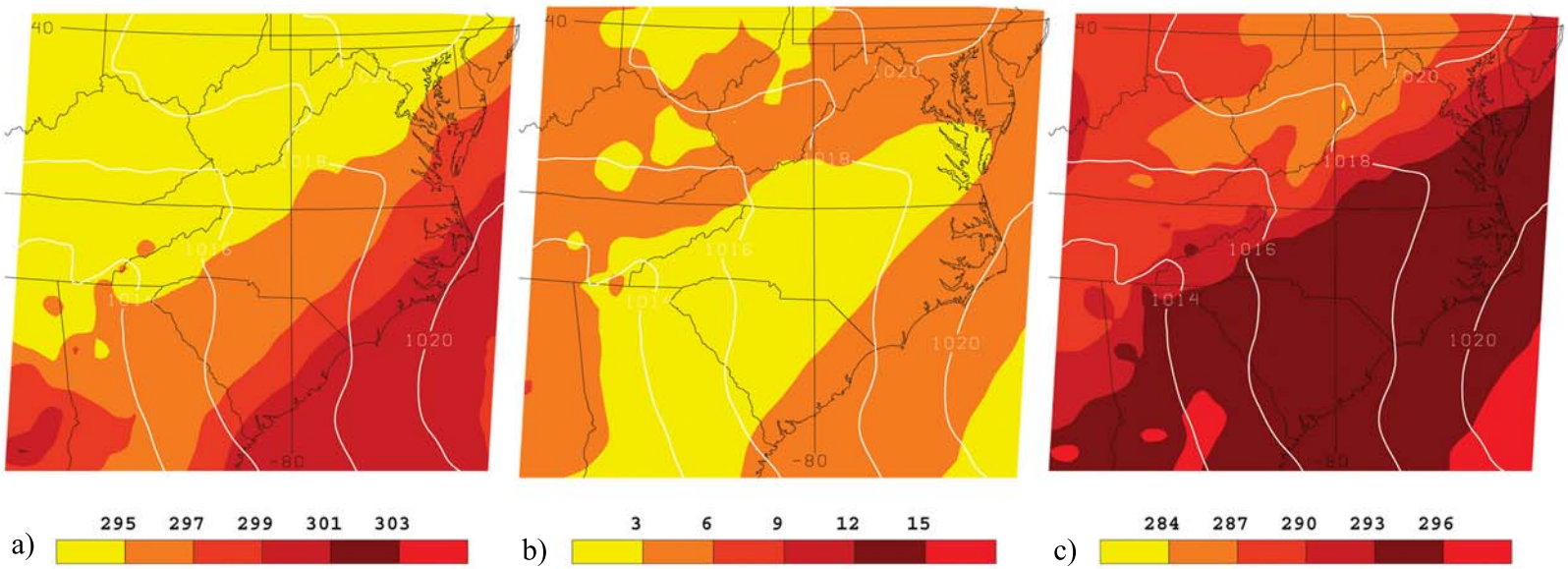


Figure 6.1. MM5 analysis of a) air temperature, b) dewpoint depression, and c) dewpoint temperature valid at 1200 UTC 29 July 2004. All values plotted in Kelvin. Isobars are plotted in white every 2 hPa in all panels.

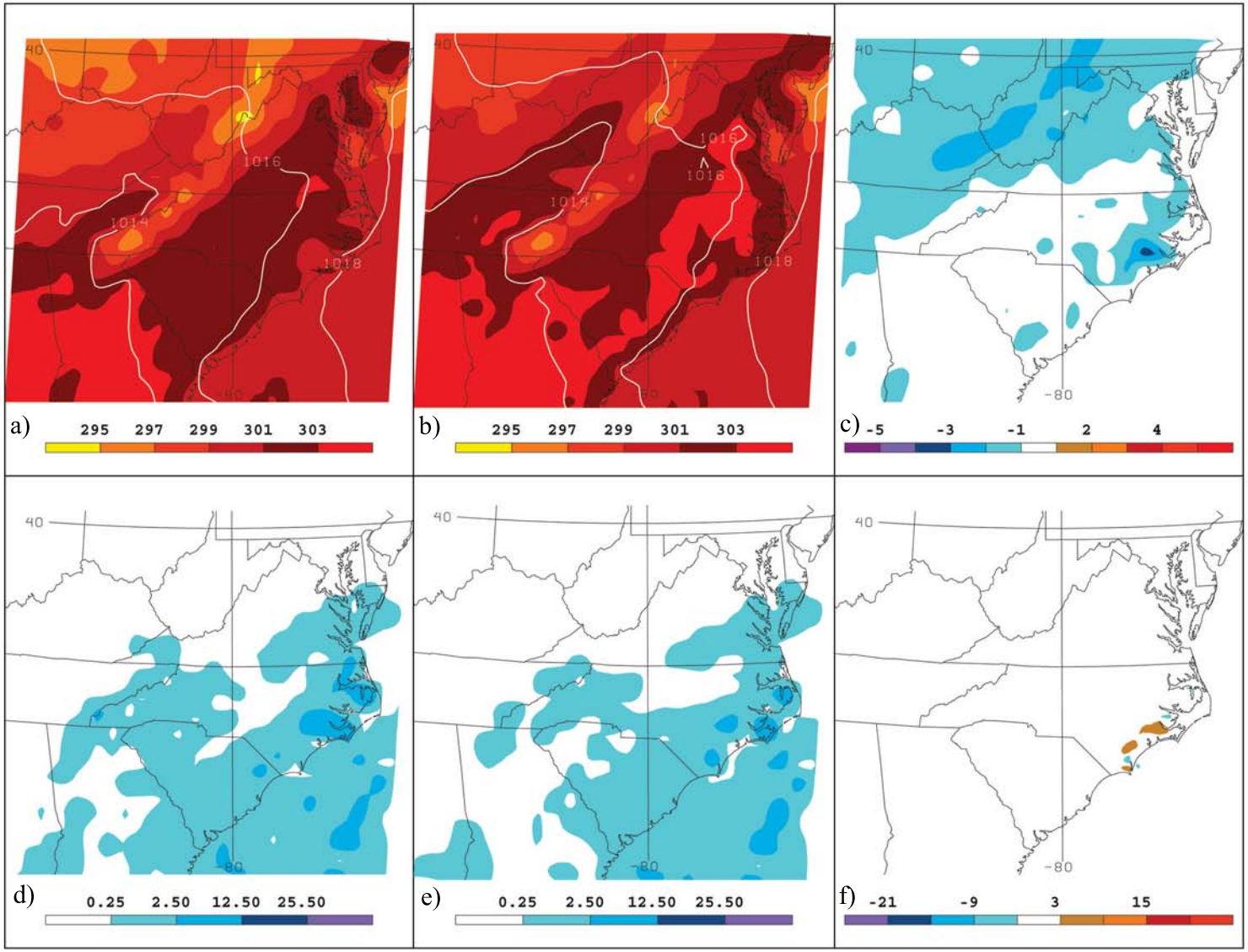
a)
295 297 299 301 303
b)
295 297 299 301 303
c)
-5 -3 -1 2 4
d)
0.25 2.50 12.50 25.50
e)
0.25 2.50 12.50 25.50
f)
-21 -9 3 15
40
-80
1014
1016
1018

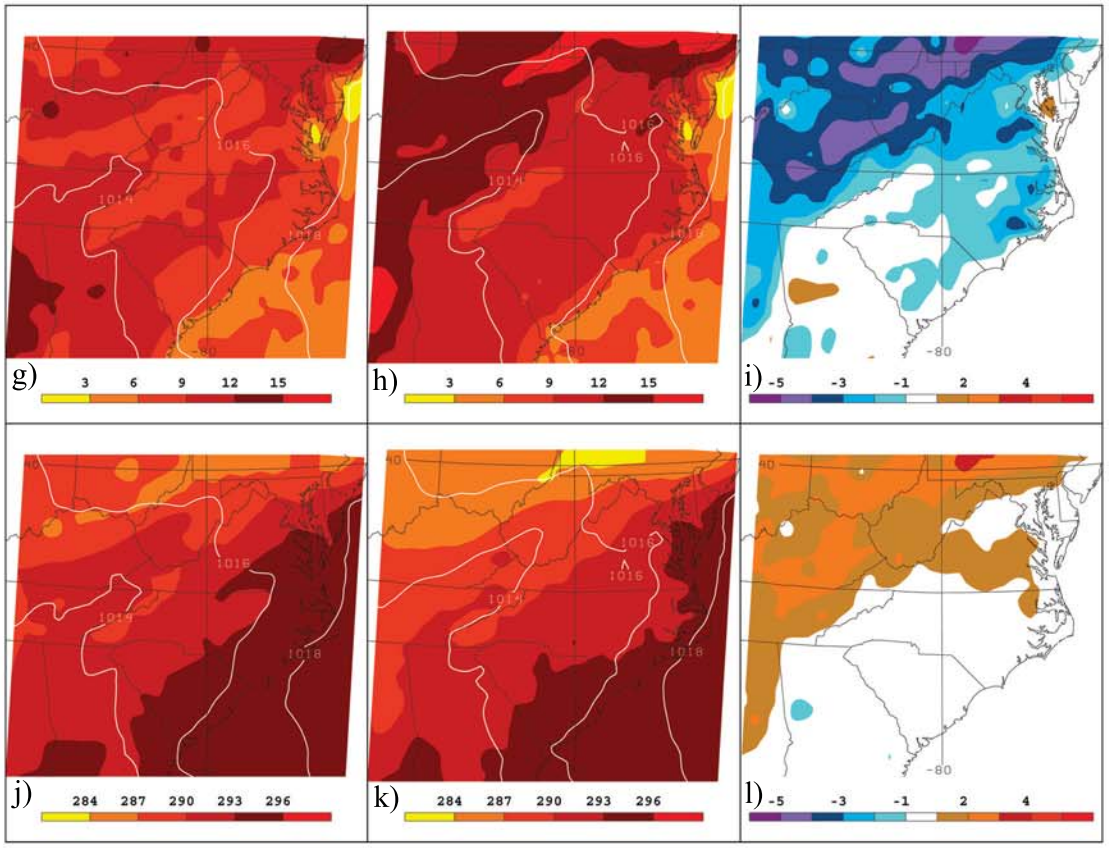


Figure 6.2. Six-hour MM5 forecasts of a) and b): air temperature; c): a minus b; d) and e): 6-hour total precipitation; f): d minus e; g) and h): dewpoint depression; i): g minus h; j) and k): dewpoint temperature; and l): j minus k, valid at 1800 UTC 29 July 2005. a), d), g), and j) are NOAH LSM images, while b), e), h), and k) are 5-layer soil model images. All temperatures plotted in Kelvin. Precipitation plotted in millimeters. Isobars contoured every 2hPa where contoured.

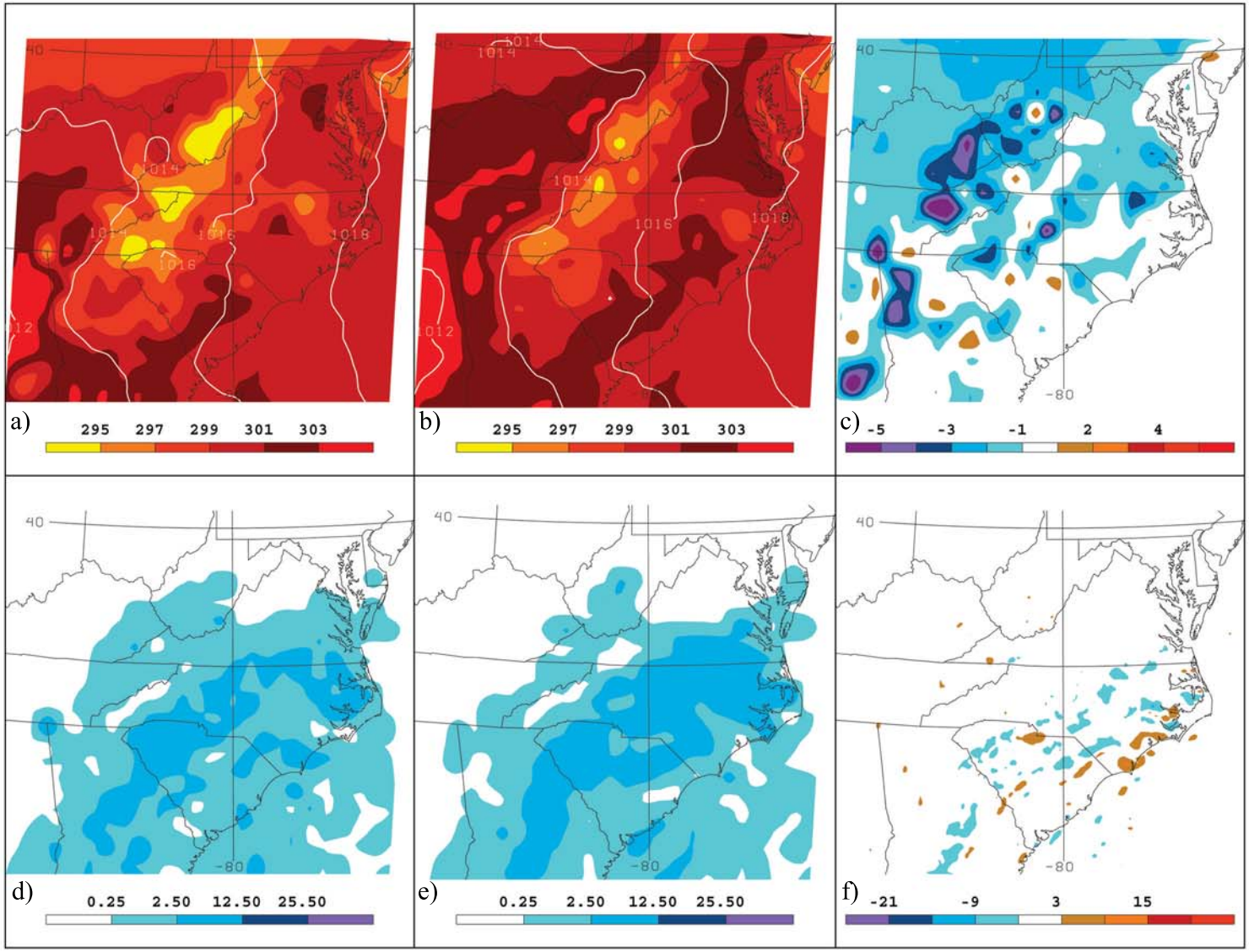
a)
295 297 299 301 303
b)
295 297 299 301 303
c)
-5 -3 -1 2 4
d)
0.25 2.50 12.50 25.50
e)
0.25 2.50 12.50 25.50
f)
-21 -9 3 15

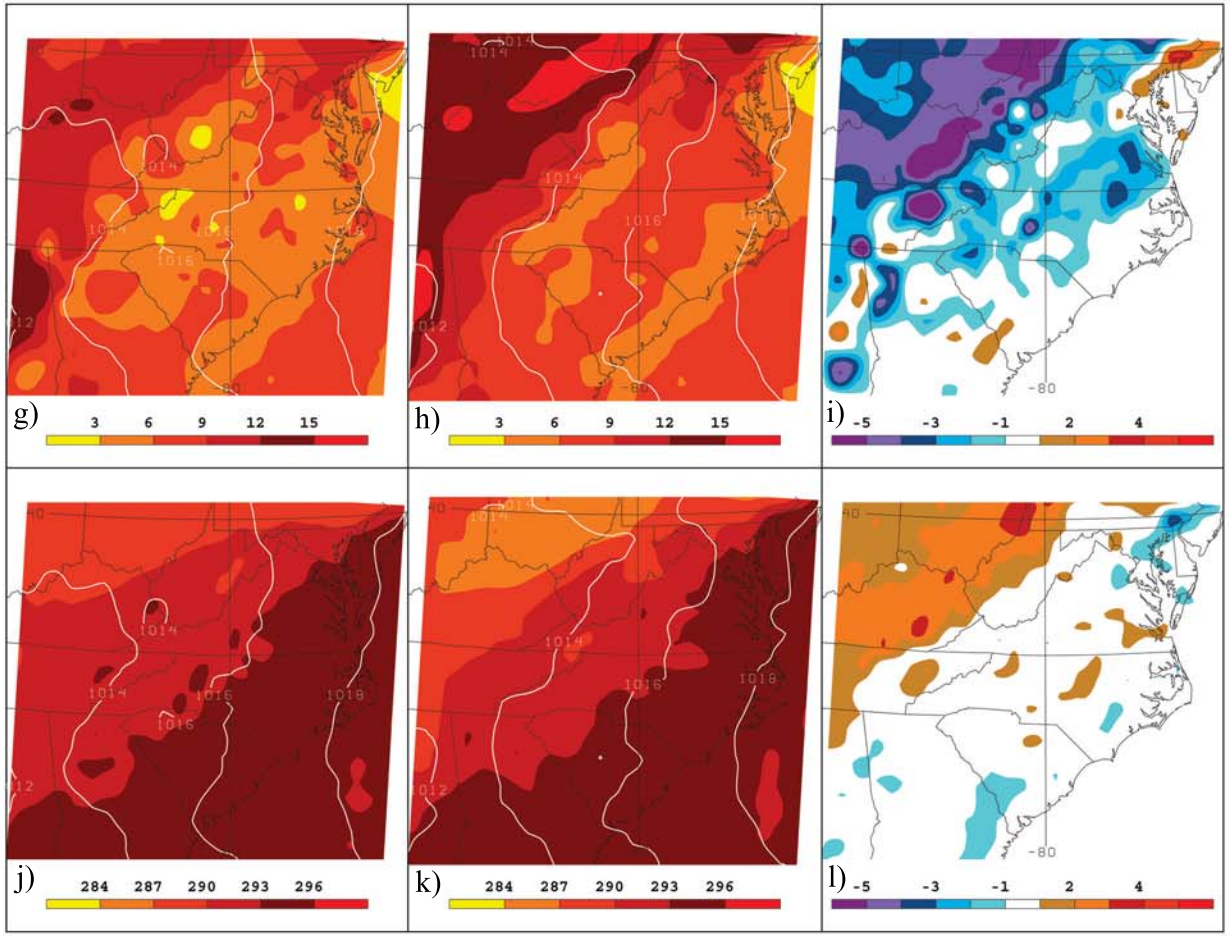


Figure 6.3. 12-hour forecast of a) and b): air temperature; c): a minus b; d) and e): 6-hour precipitation; f): d minus e; g) and h): dewpoint depression; i): g minus h; j) and k): dewpoint temperature; and l): j minus k, valid at 0000 UTC 30 July 2004. a), d), g), and j) are NOAH LSM images, while b), e), h), and k) are 5-layer soil model images. All temperatures plotted in Kelvin. Precipitation plotted in millimeters. Isobars contoured every 2 hPa where contoured.

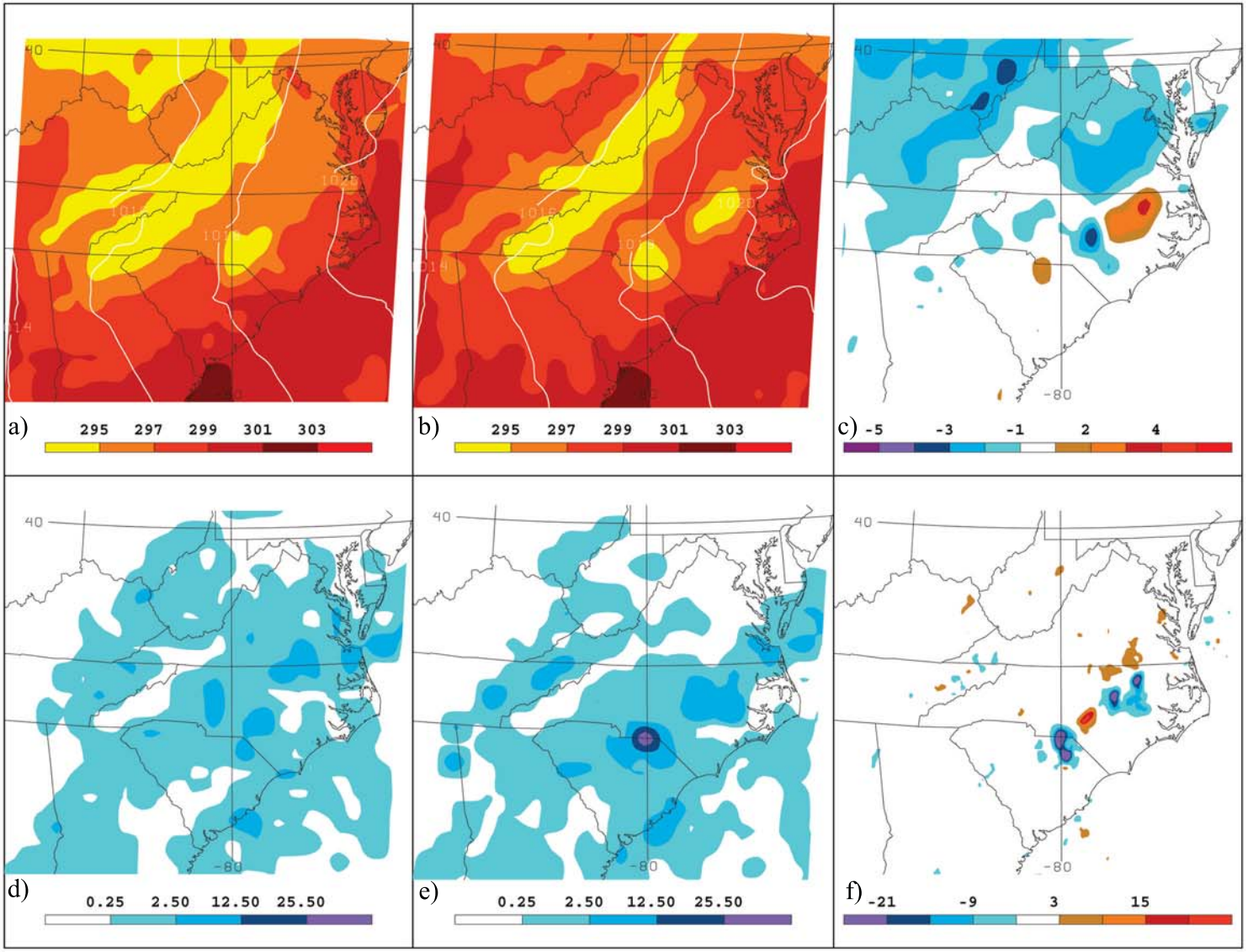
a)
295 297 299 301 303
b)
295 297 299 301 303
c)
-5 -3 -1 2 4
d)
0.25 2.50 12.50 25.50
e)
0.25 2.50 12.50 25.50
f)
-21 -9 3 15
40
-80

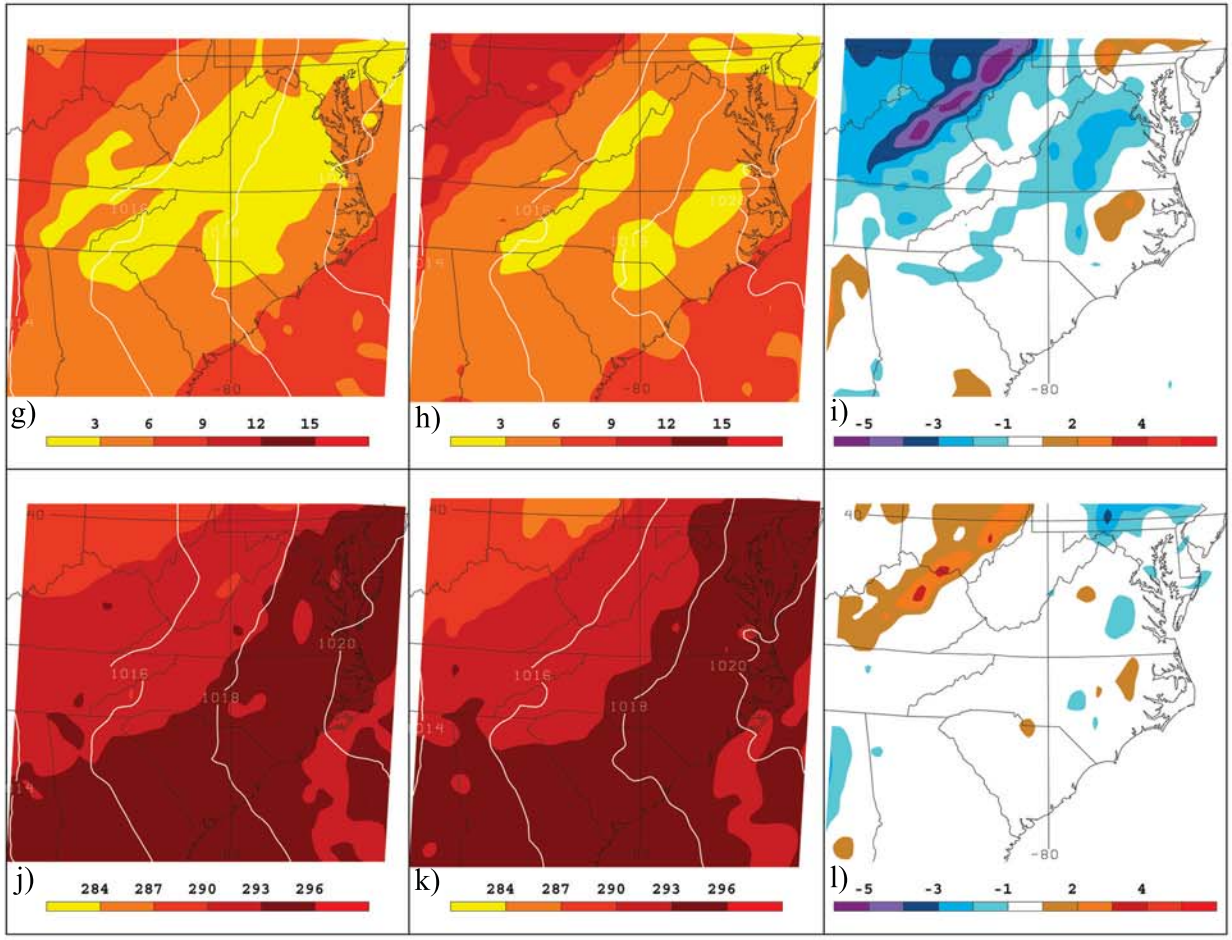


Figure 6.4. 18-hour forecast of a) and b): air temperature; c): a minus b; d) and e): 6-hour precipitation; f): d minus e; g) and h): dewpoint depression; i): g minus h; j) and k): dewpoint temperature; and l): j minus k, valid at 0600 UTC 30 July 2004. a), d), g), and j) are NOAH LSM images, while b), e), h), and k) are 5-layer soil model images. All temperatures plotted in Kelvin. Precipitation plotted in millimeters. Isobars contoured every 2 hPa where contoured.

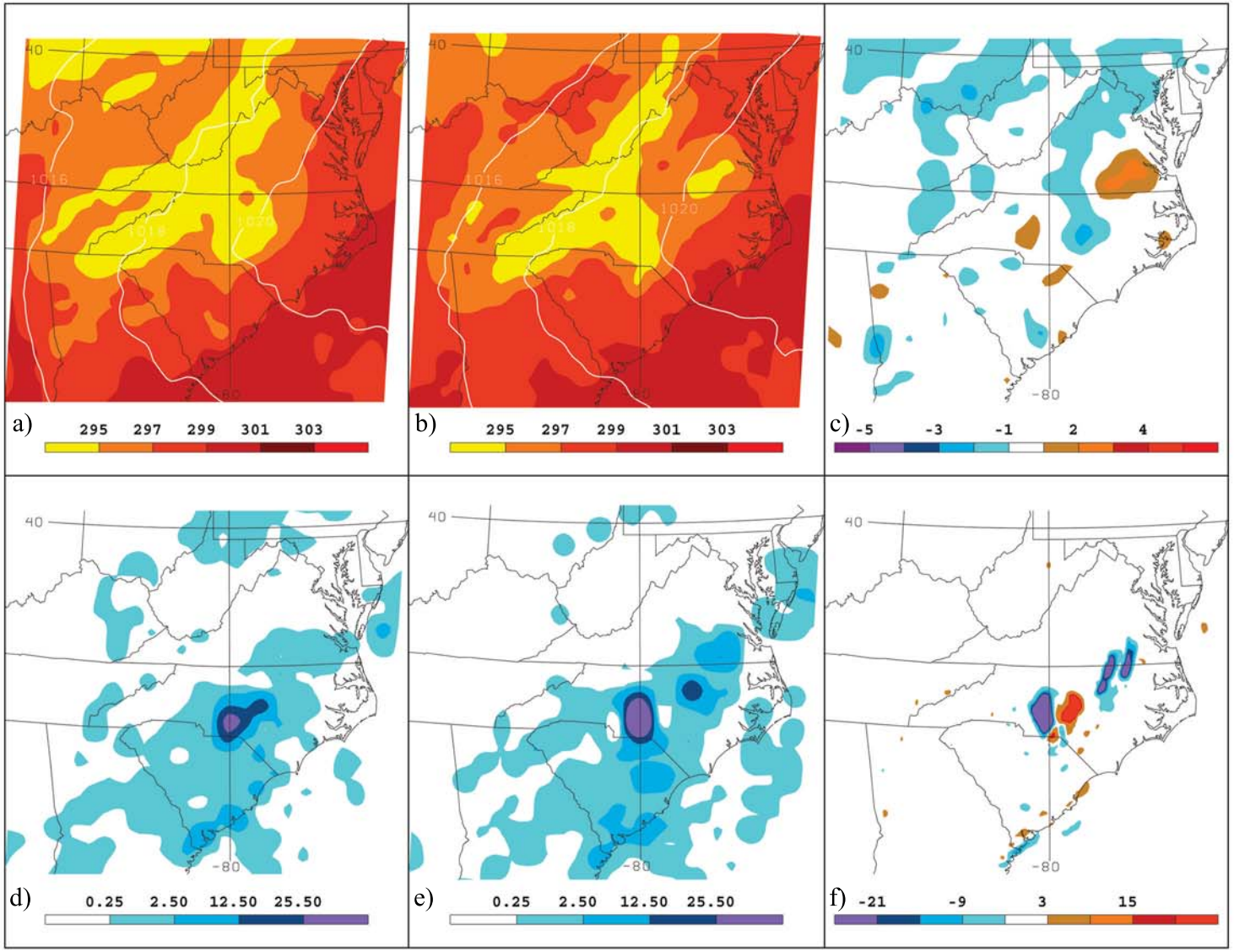
a)
295 297 299 301 303
b)
295 297 299 301 303
c)
-5 -3 -1 2 4
d)
0.25 2.50 12.50 25.50
e)
0.25 2.50 12.50 25.50
f)
-21 -9 3 15

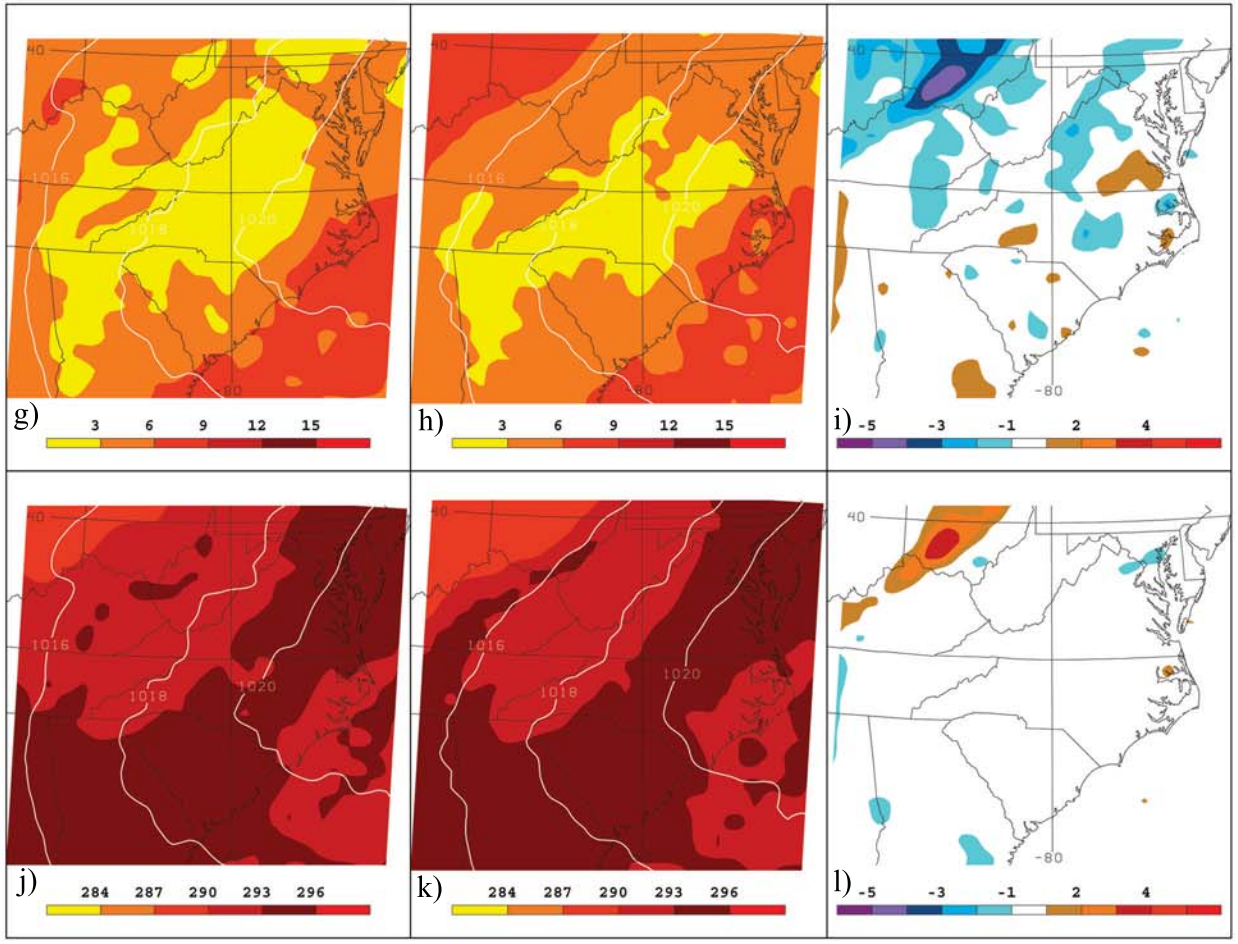


Figure 6.5. 24-hour forecast of a) and b): air temperature; c): a minus b; d) and e): 6-hour precipitation; f): d minus e; g) and h): dewpoint depression; i): g minus h; j) and k): dewpoint temperature; and l): j minus k, valid at 1200 UTC 30 July 2004. a), d), g), and j) are NOAH LSM images, while b), e), h), and k) are 5-layer soil model images. All temperatures plotted in Kelvin. Precipitation plotted in millimeters. Isobars contoured every 2 hPa where contoured.

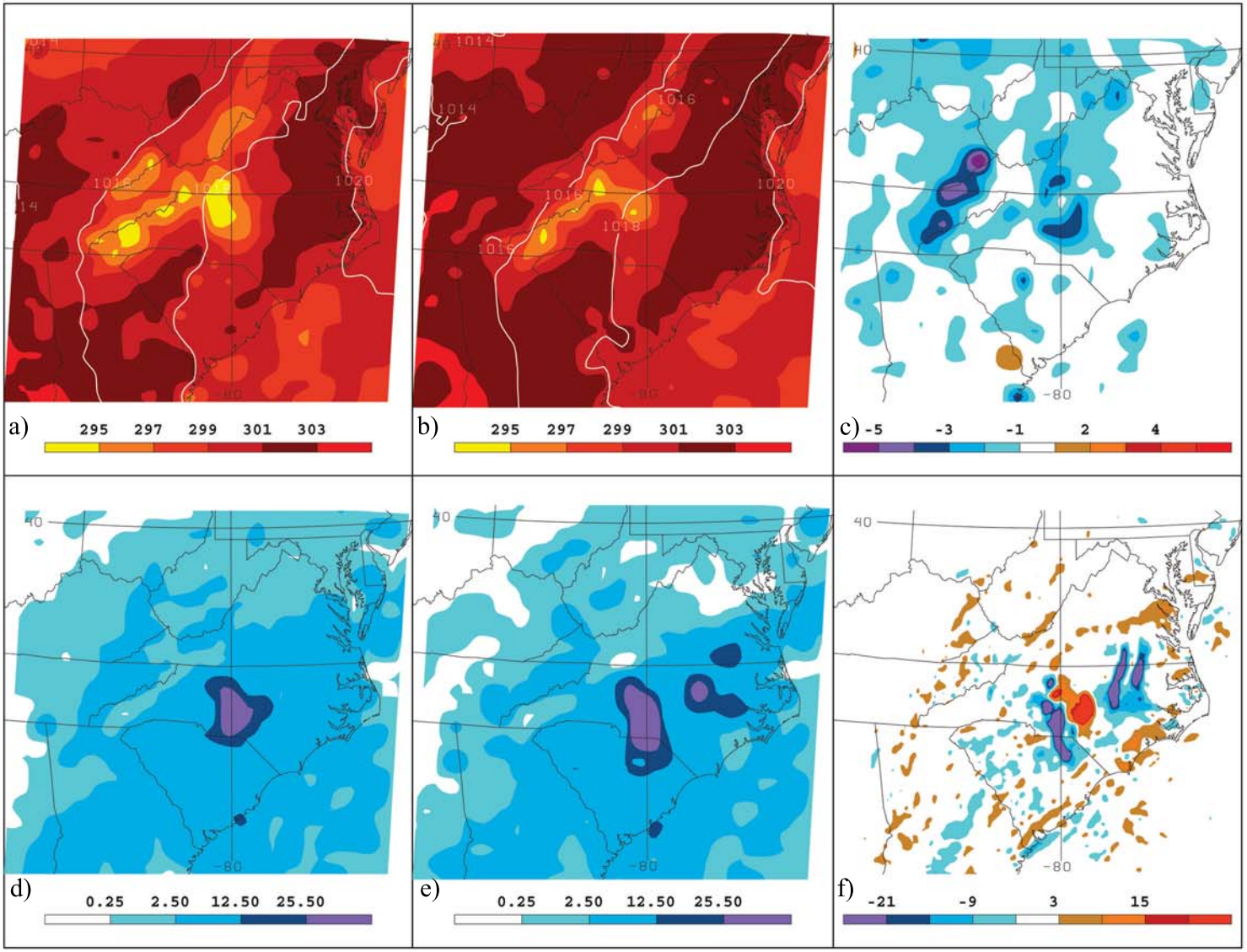
a)
295 297 299 301 303
b)
295 297 299 301 303
c)
-5 -3 -1 2 4
d)
0.25 2.50 12.50 25.50
e)
0.25 2.50 12.50 25.50
f)
-21 -9 3 15

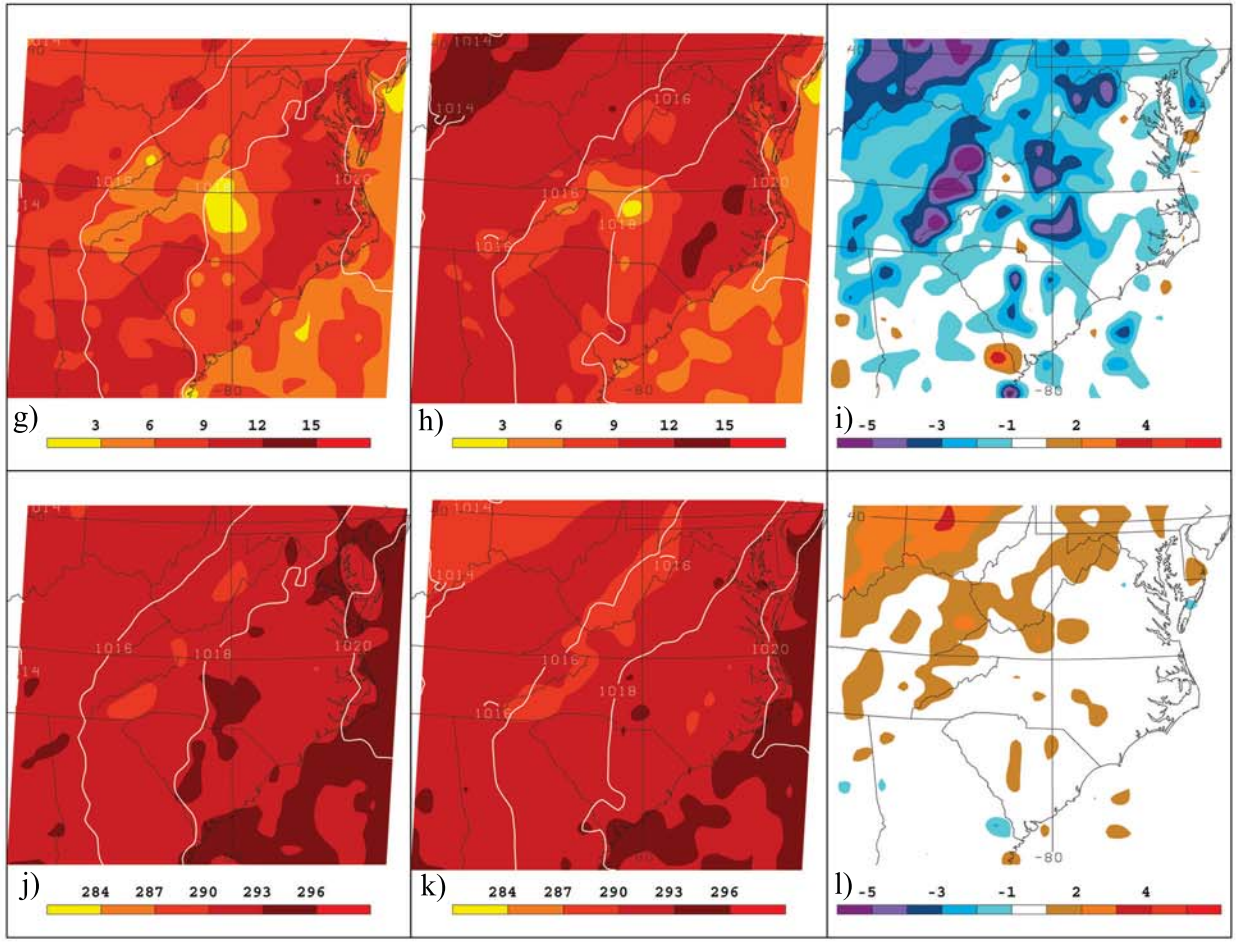


Figure 6.6. 30-hour forecast of a) and b): air temperature; c): a minus b; d) and e): 6-hour precipitation; f): d minus e; g) and h): dewpoint depression; i): g minus h; j) and k): dewpoint temperature; and l): j minus k, valid at 1800 UTC 30 July 2004. a), d), g), and j) are NOAH LSM images, while b), e), h), and k) are 5-layer soil model images. All temperatures plotted in Kelvin. Precipitation plotted in millimeters. Isobars contoured every 2 hPa where contoured.

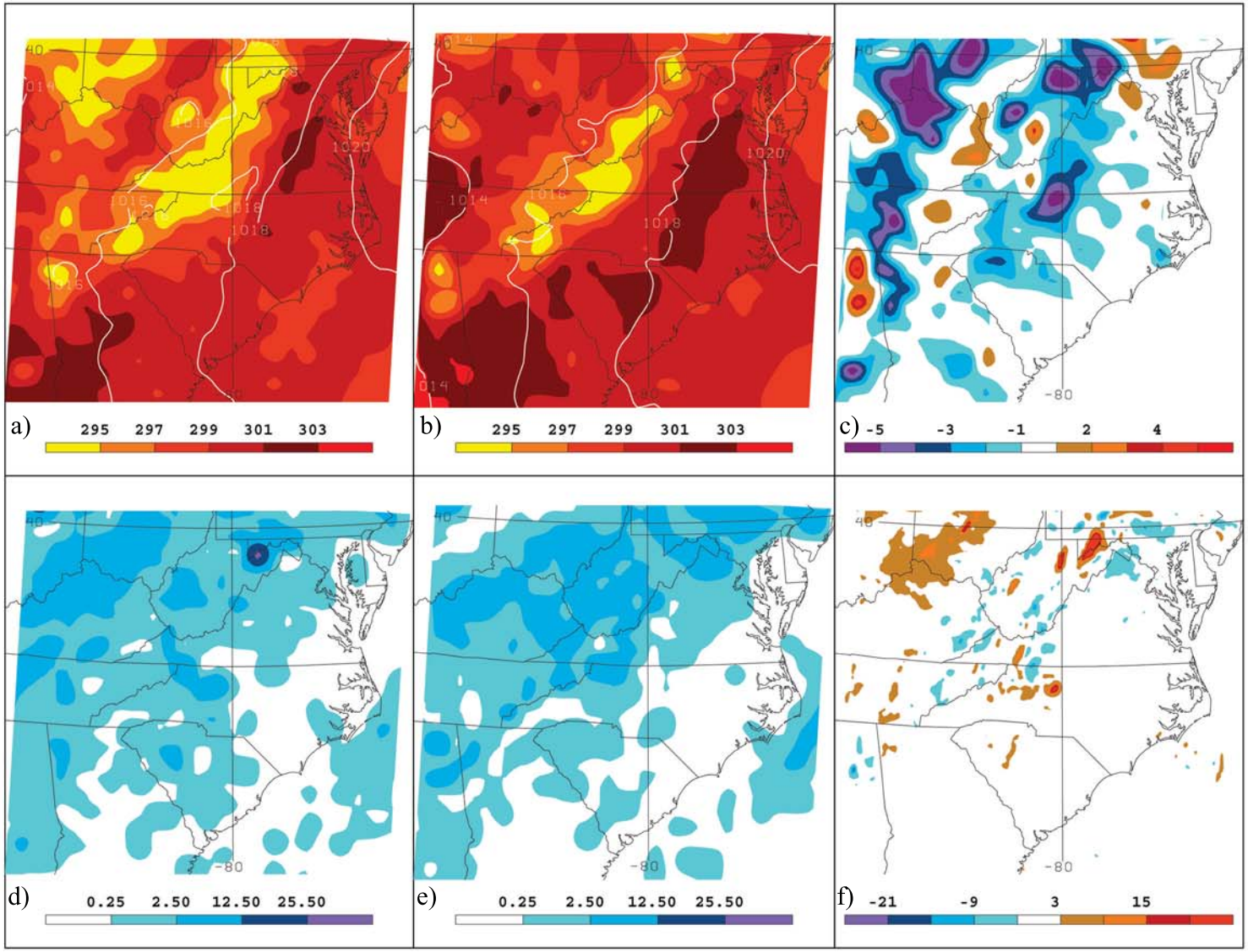
a)
295 297 299 301 303
b)
295 297 299 301 303
c)
-5 -3 -1 2 4
d)
0.25 2.50 12.50 25.50
e)
0.25 2.50 12.50 25.50
f)
-21 -9 3 15

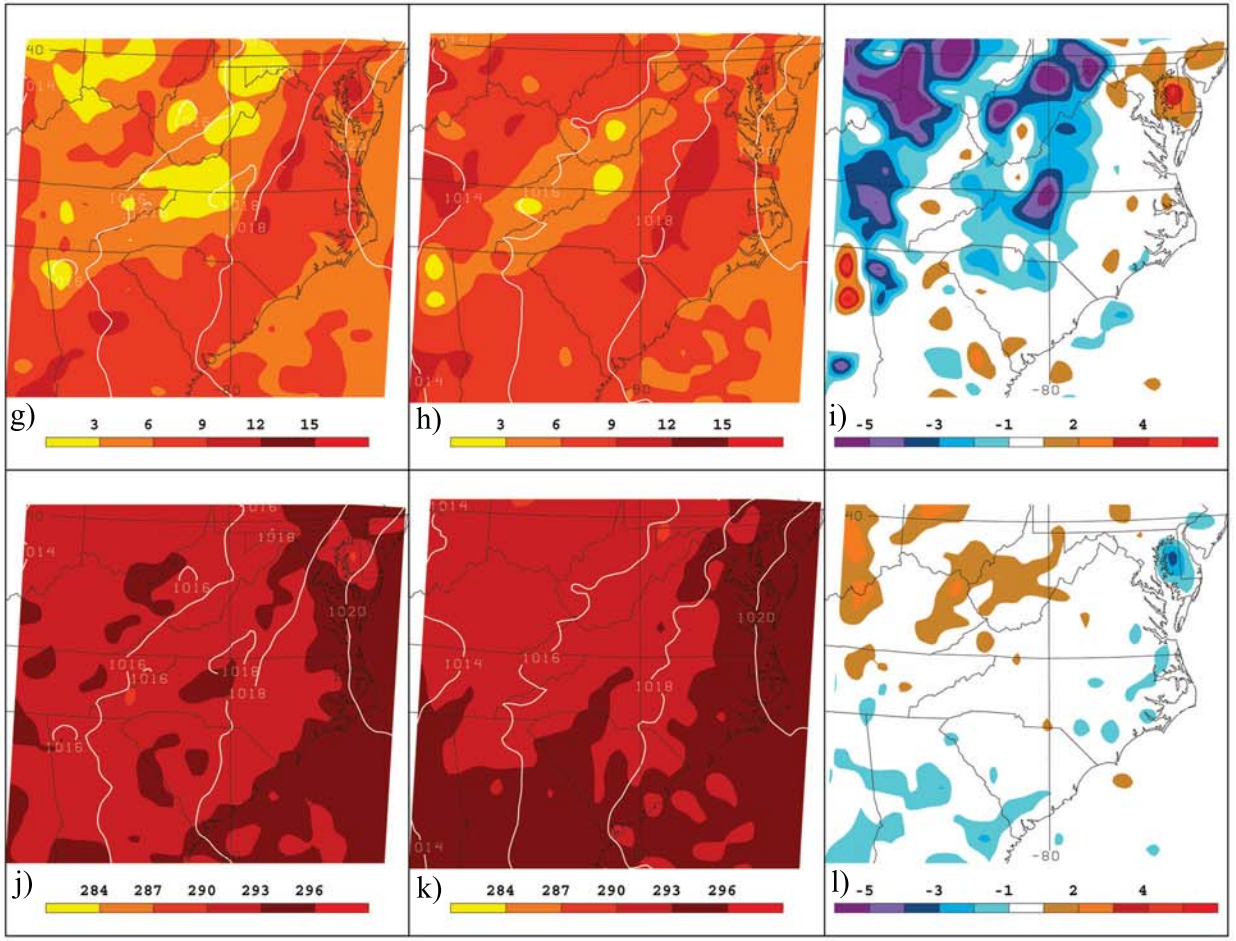


Figure 6.7. 36-hour forecast of a) and b): air temperature; c): a minus b; d) and e): 6-hour precipitation; f): d minus e; g) and h): dewpoint depression; i): g minus h; j) and k): dewpoint temperature; and l): j minus k, valid at 0000 UTC 31 July 2004. a), d), g), and j) are NOAH LSM images, while b), e), h), and k) are 5-layer soil model images. All temperatures plotted in Kelvin. Precipitation plotted in millimeters. Isobars contoured every 2 hPa where contoured.

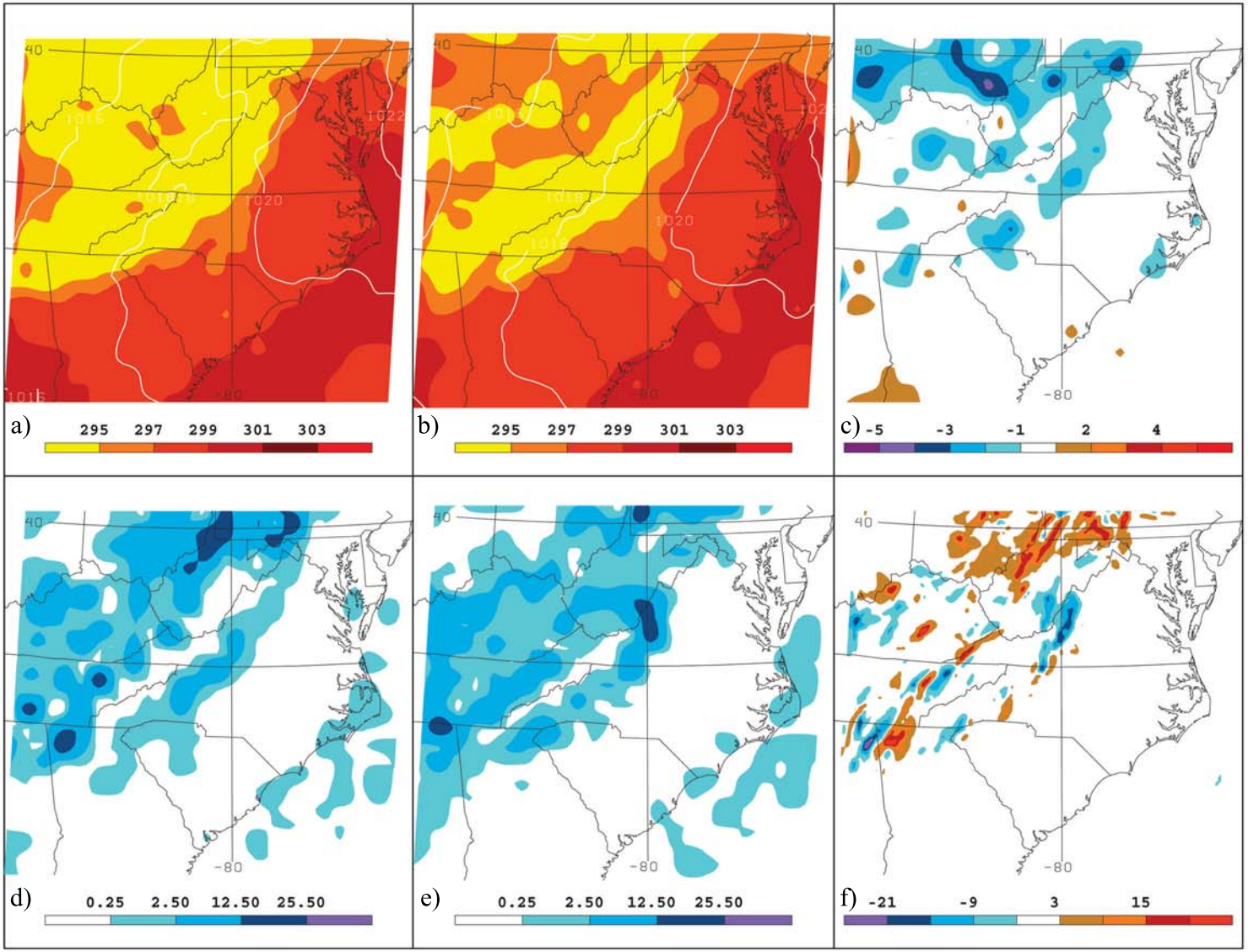
a)
295 297 299 301 303
b)
295 297 299 301 303
c)
-5 -3 -1 2 4
d)
0.25 2.50 12.50 25.50
e)
0.25 2.50 12.50 25.50
f)
-21 -9 3 15
40
-80

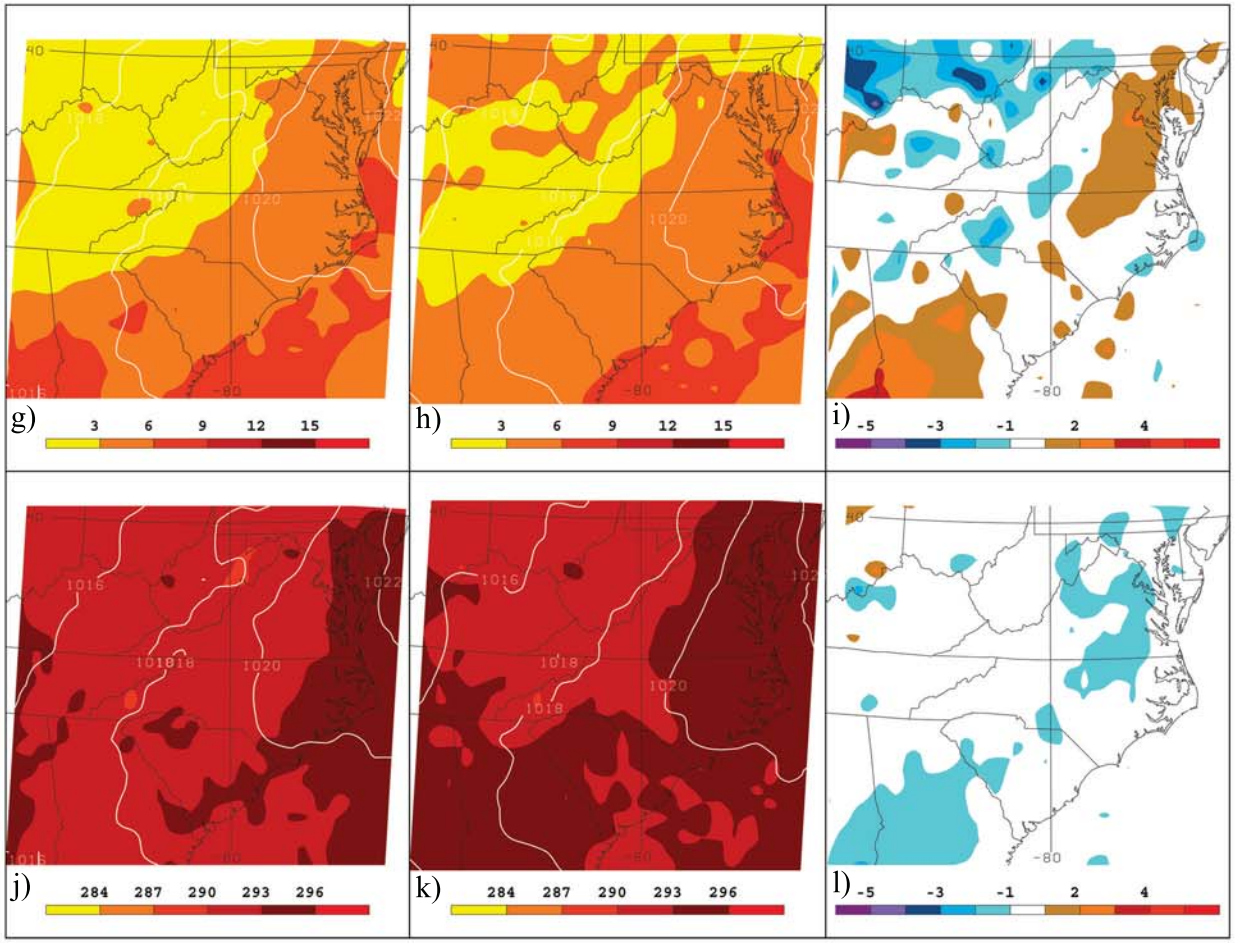


Figure 6.8. 42-hour forecast of a) and b): air temperature; c): a minus b; d) and e): 6-hour precipitation; f): d minus e; g) and h): dewpoint depression; i): g minus h; j) and k): dewpoint temperature; and l): j minus k, valid at 0600 UTC 31 July 2004. a), d), g), and j) are NOAH LSM images, while b), e), h), and k) are 5-layer soil model images. All temperatures plotted in Kelvin. Precipitation plotted in millimeters. Isobars contoured every 2 hPa where contoured.

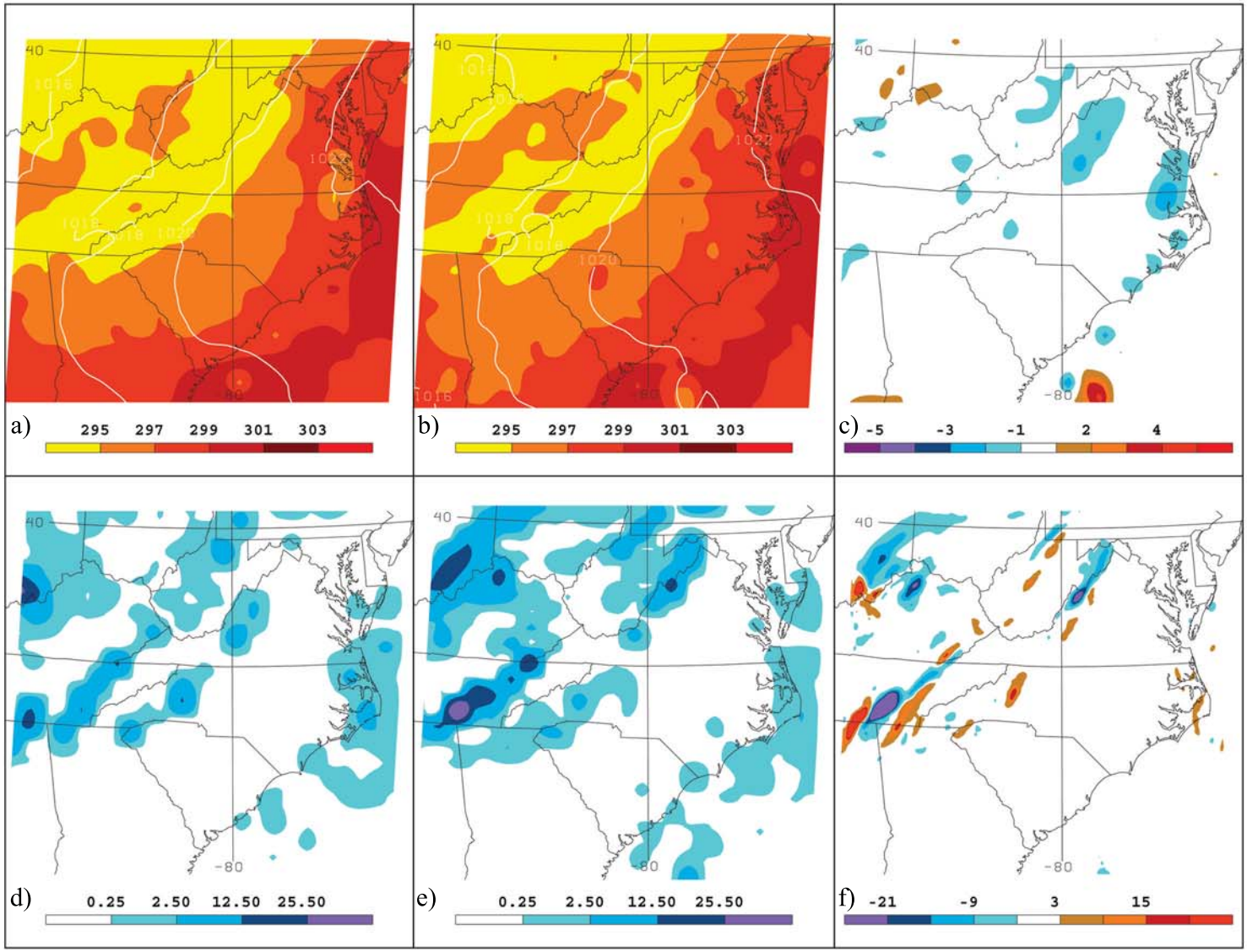
40
-80
a)
295 297 299 301 303
b)
295 297 299 301 303
c)
-5 -3 -1 2 4
d)
0.25 2.50 12.50 25.50
e)
0.25 2.50 12.50 25.50
f)
-21 -9 3 15

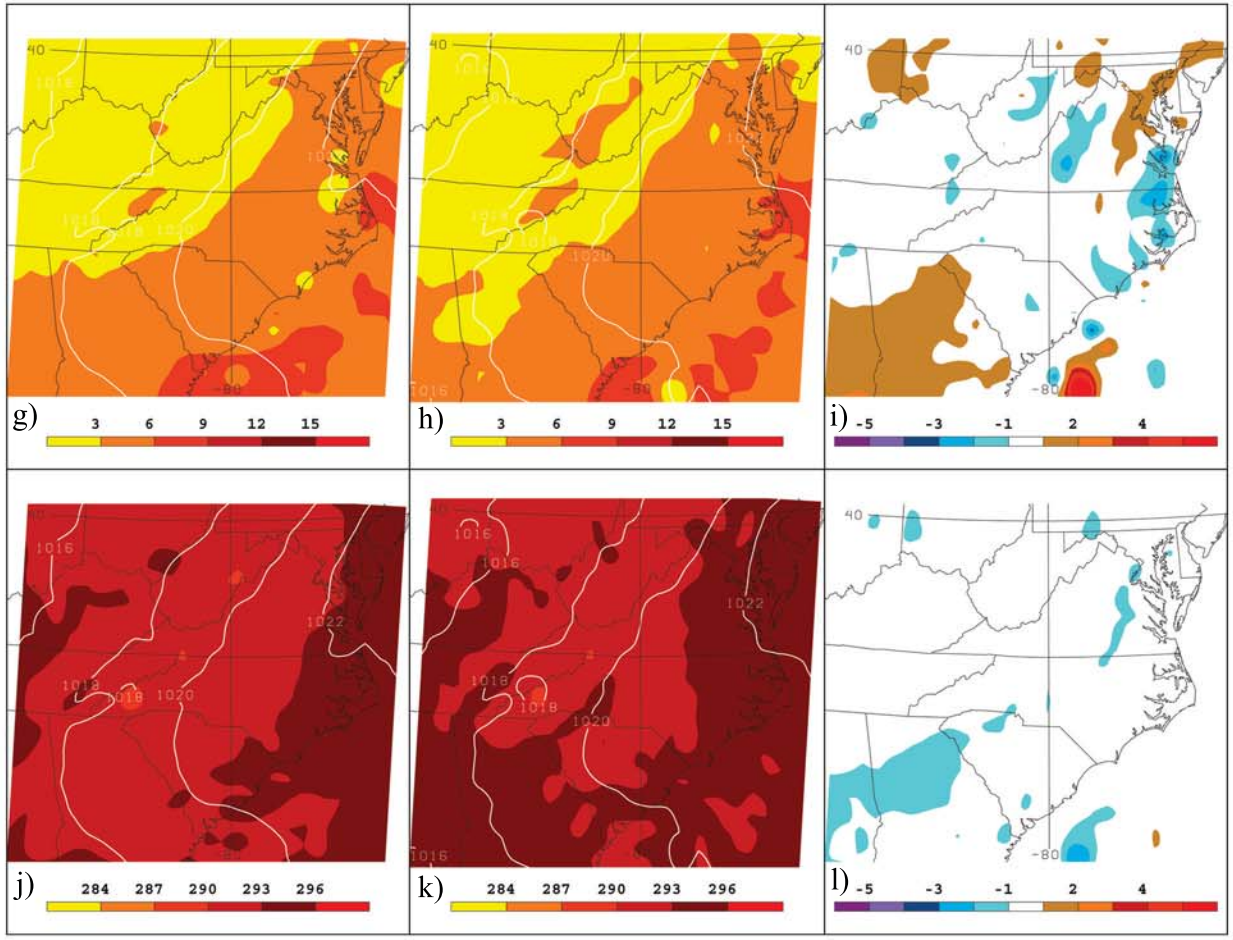


Figure 6.9. 48-hour forecast of a) and b): air temperature; c): a minus b; d) and e): 6-hour precipitation; f): d minus e; g) and h): dewpoint depression; i): g minus h; j) and k): dewpoint temperature; and l): j minus k, valid at 1200 UTC 31 July 2004. a), d), g), and j) are NOAH LSM images, while b), e), h), and k) are 5-layer soil model images. All temperatures plotted in Kelvin. Precipitation plotted in millimeters. Isobars contoured every 2 hPa where contoured.

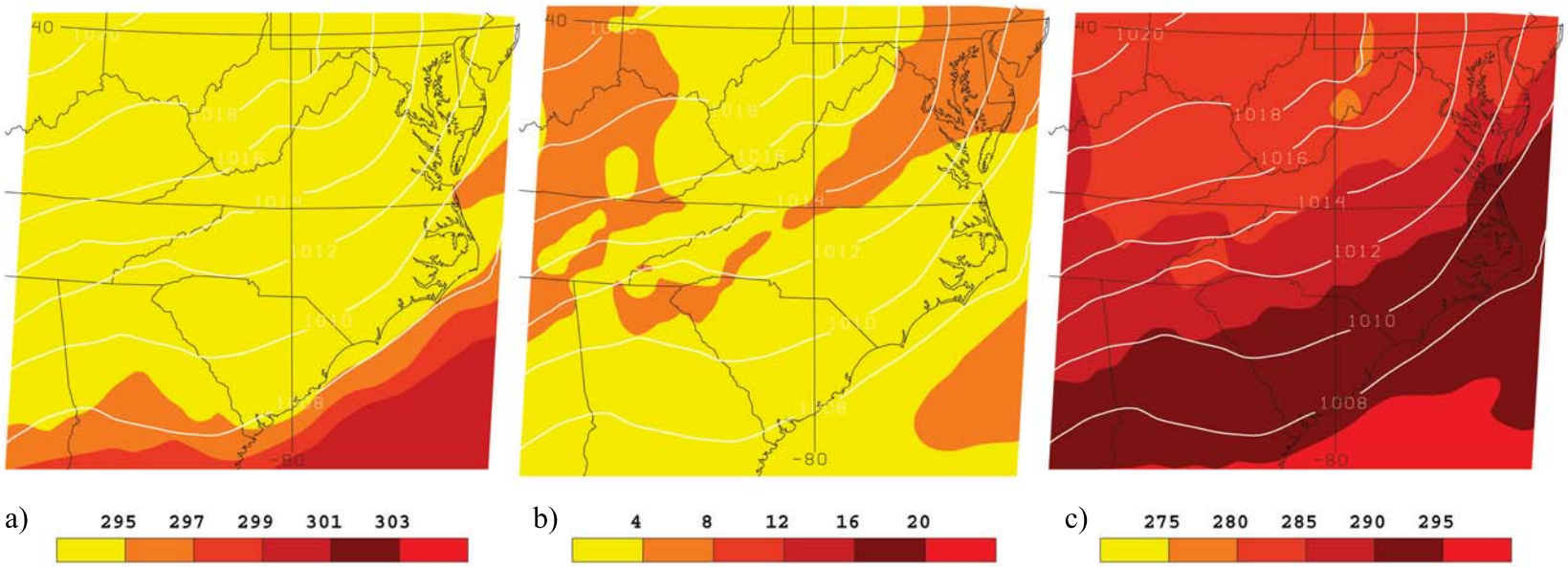


Figure 6.10. MM5 analysis of a) air temperature, b) dewpoint depression, and c) dewpoint temperature valid at 1200 UTC 6 August 2004. All values plotted in Kelvin. Isobars are plotted in white every 2 hPa in all panels.

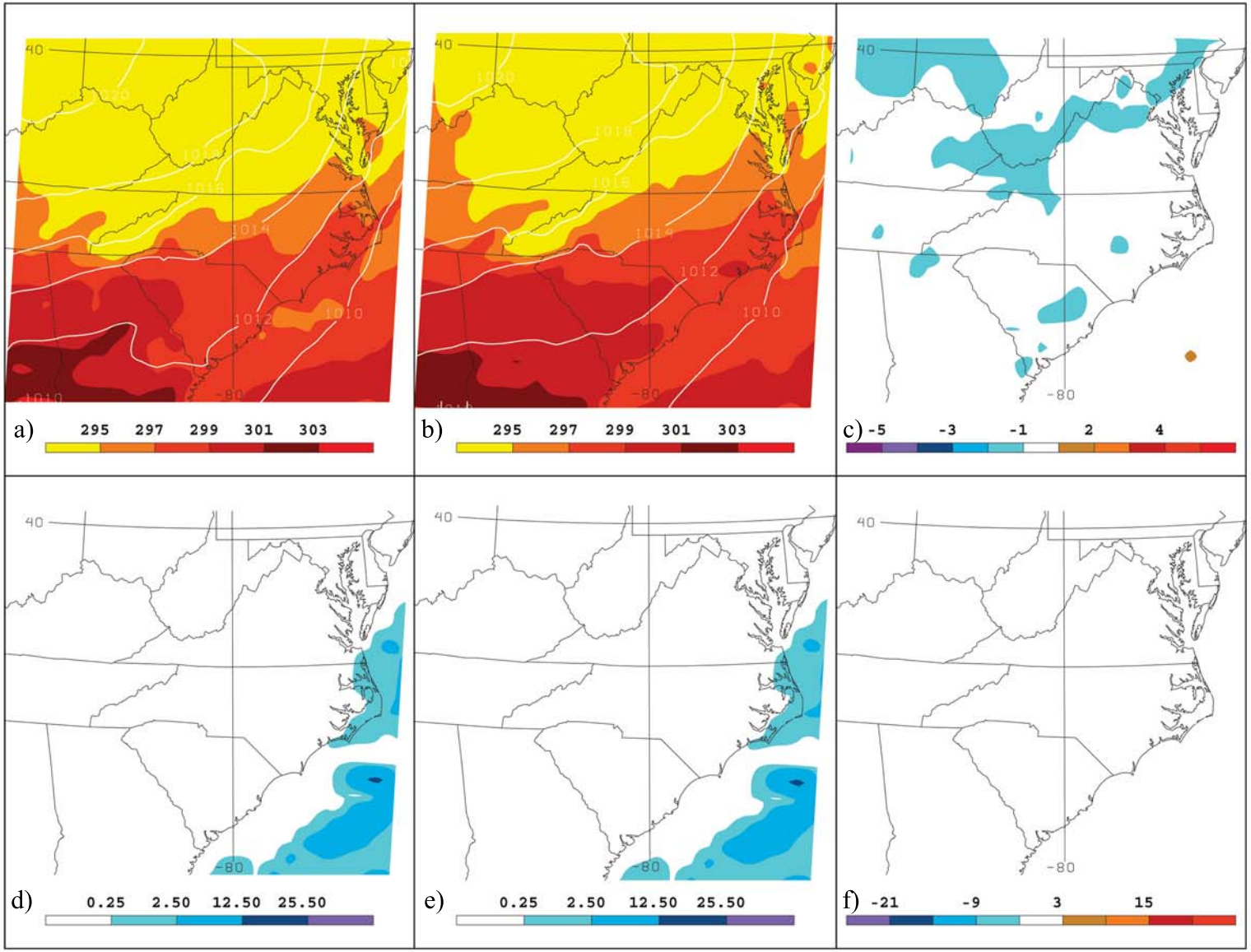
a)
295 297 299 301 303
b)
295 297 299 301 303
c) -5 -3 -1 2 4
d)
0.25 2.50 12.50 25.50
e)
0.25 2.50 12.50 25.50
f) -21 -9 3 15

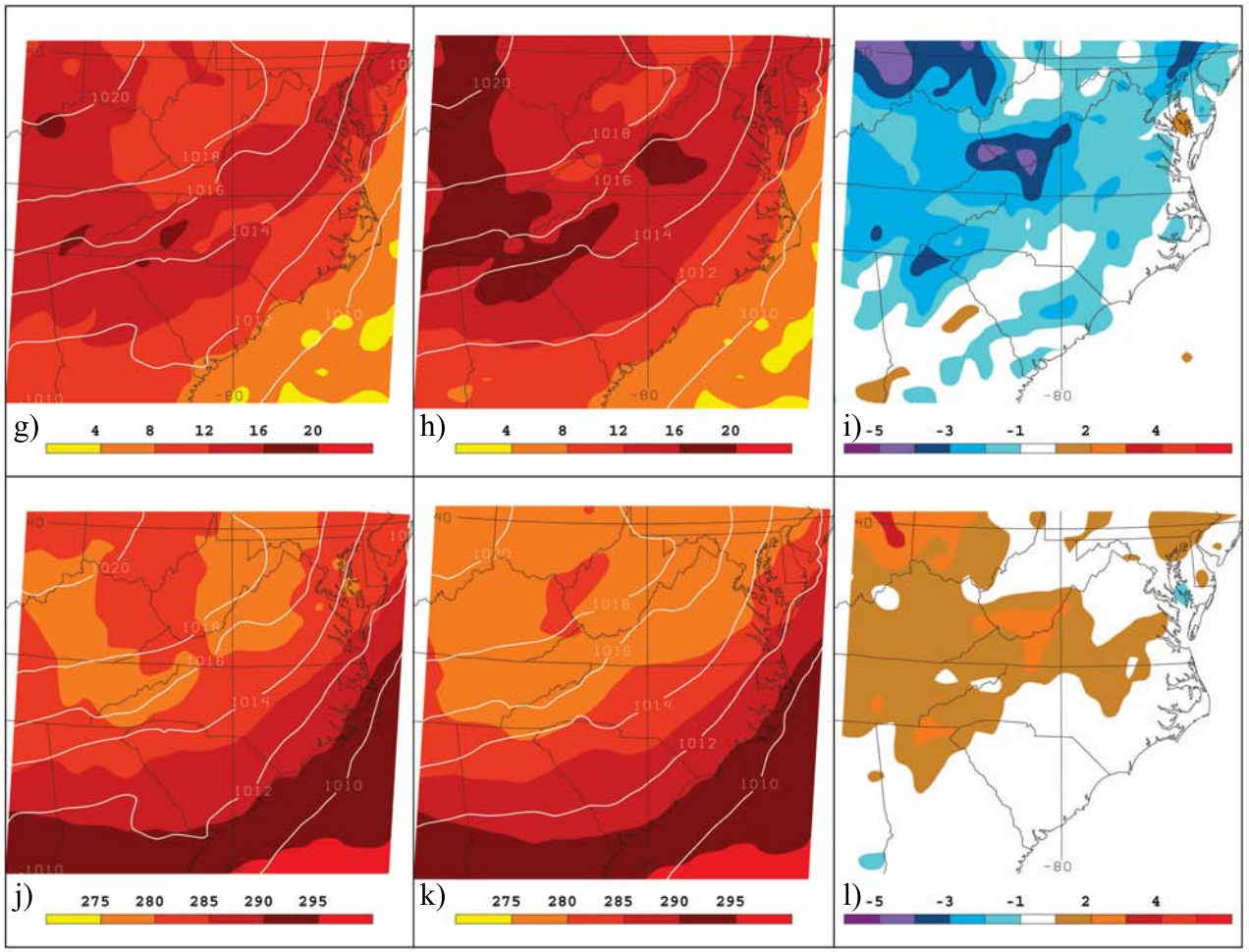


Figure 6.11. 6-hour MM5 forecasts of a) and b): air temperature; c): a minus b; d) and e): 6-hour precipitation; f): d minus e; g) and h): dewpoint depression; i): g minus h; j) and k): dewpoint temperature; and l): j minus k, valid at 1800 UTC 6 August 2004. All temperatures plotted in Kelvin. Precipitation plotted in millimeters. Isobars contoured every 2 hPa where contoured.

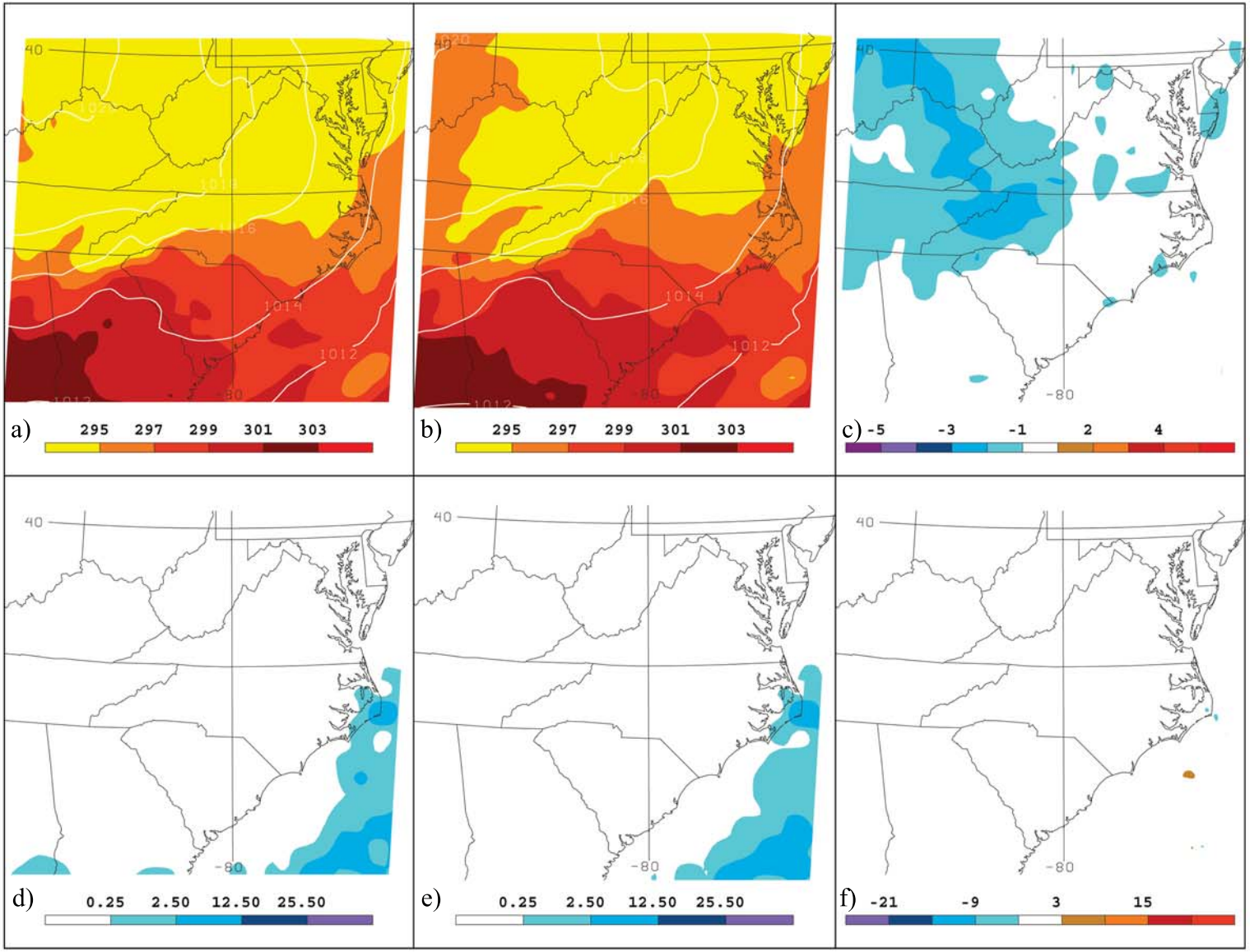
40
-80
1012
1014
a)
295 297 299 301 303
b)
295 297 299 301 303
c) -5 -3 -1 2 4
d)
0.25 2.50 12.50 25.50
e)
0.25 2.50 12.50 25.50
f) -21 -9 3 15

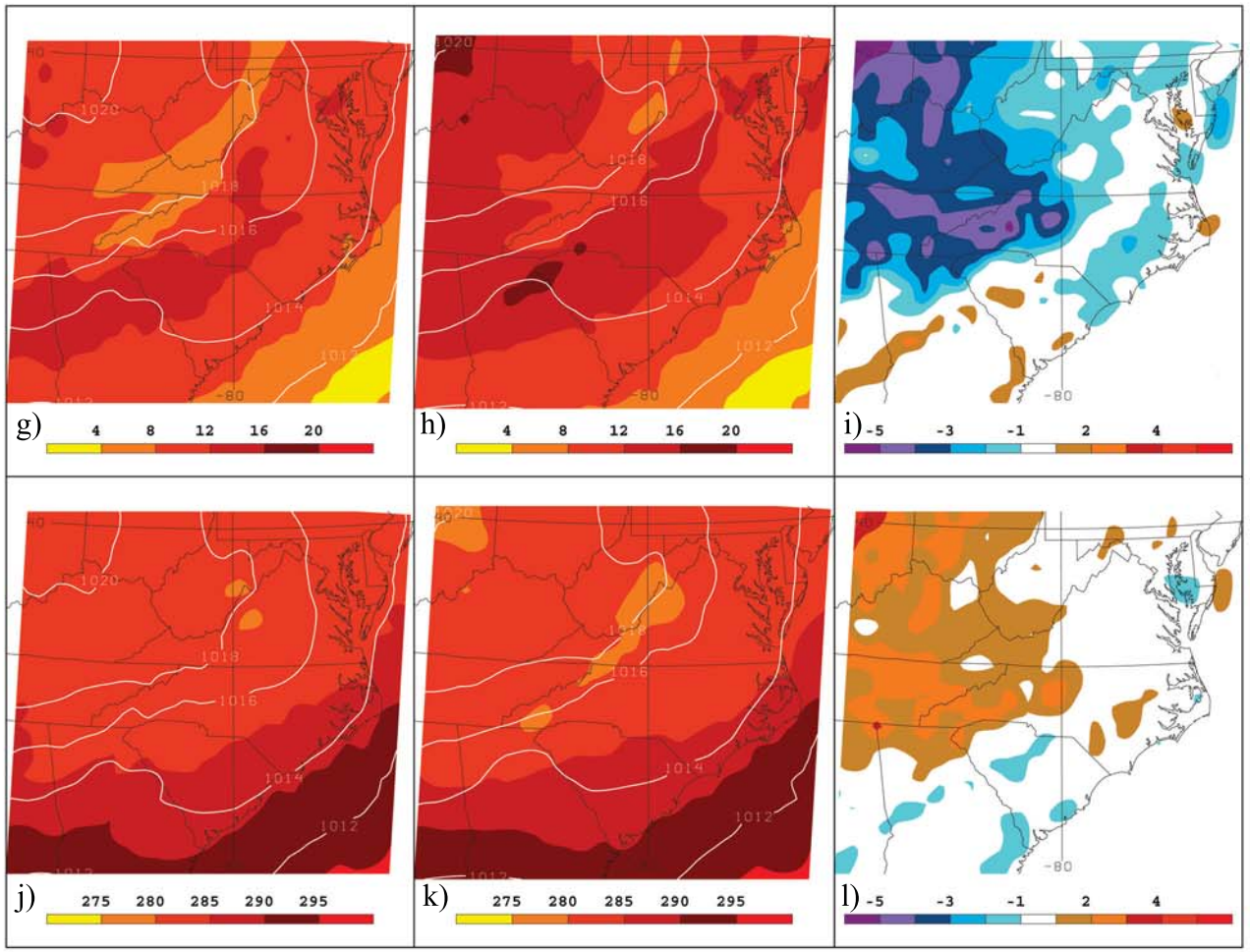


Figure 6.12. 12-hour MM5 forecasts of a) and b): air temperature; c): a minus b; d) and e): 6-hour precipitation; f): d minus e; g) and h): dewpoint depression; i): g minus h; j) and k): dewpoint temperature; and l): j minus k, valid at 0000 UTC 7 August 2004. All temperatures plotted in Kelvin. Precipitation plotted in millimeters. Isobars contoured every 2 hPa where contoured.

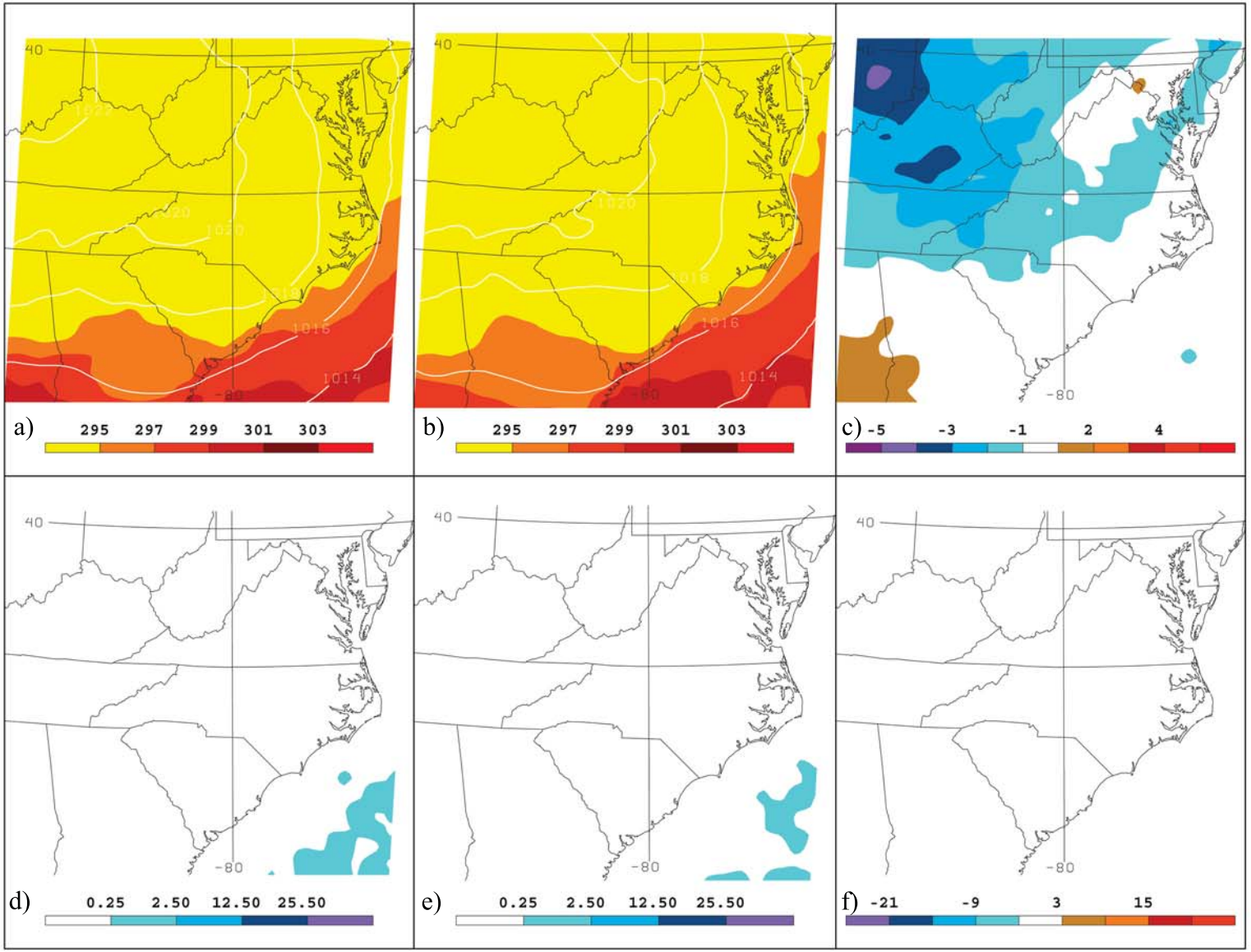
40
-80
1016
1014
a)
295 297 299 301 303
b)
295 297 299 301 303
c)
-5 -3 -1 2 4
d)
0.25 2.50 12.50 25.50
e)
0.25 2.50 12.50 25.50
f)
-21 -9 3 15

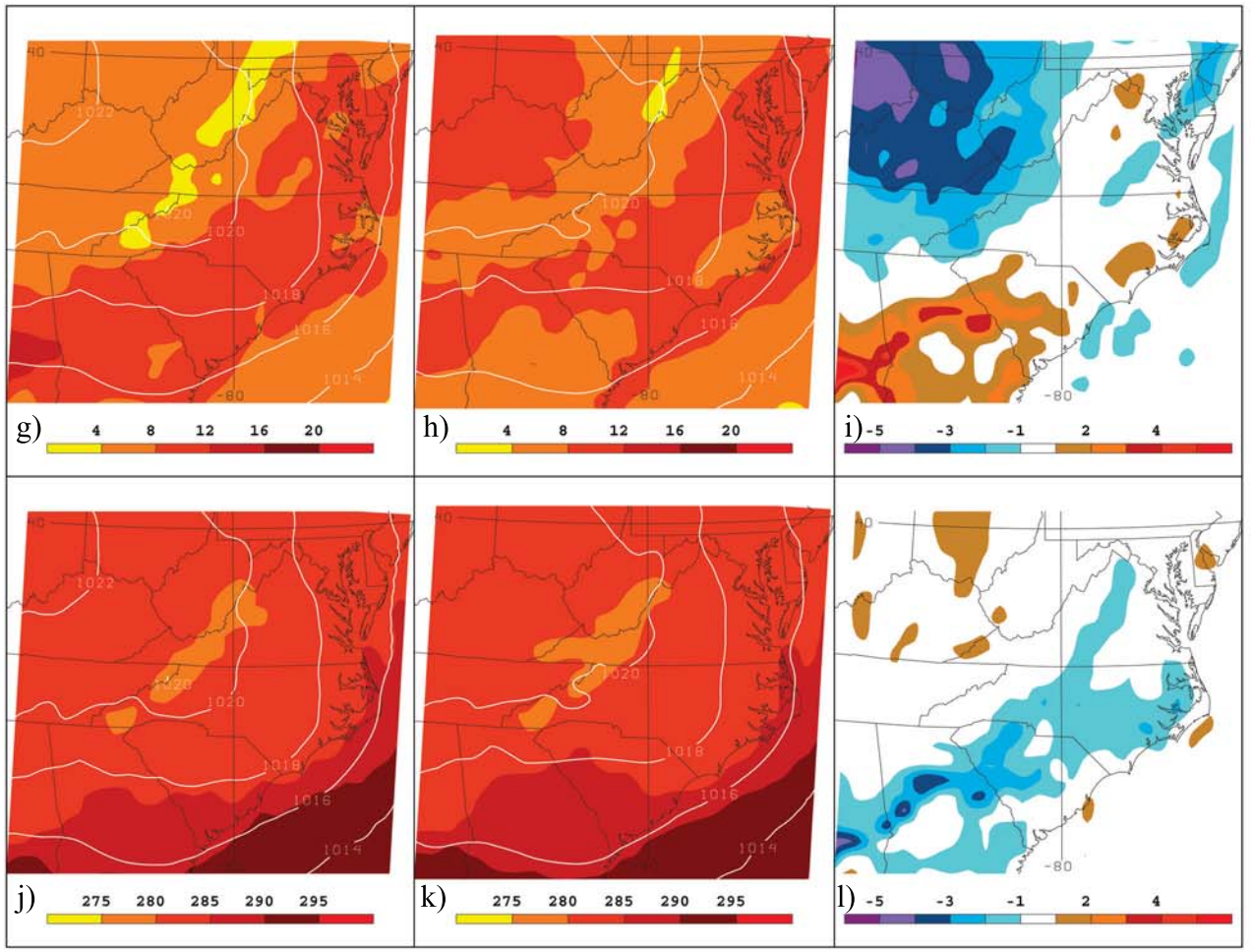


Figure 6.13. 18-hour MM5 forecasts of a) and b): air temperature; c): a minus b; d) and e): 6-hour precipitation; f): d minus e; g) and h): dewpoint depression; i): g minus h; j) and k): dewpoint temperature; and l): j minus k, valid at 0600 UTC 7 August 2004. All temperatures plotted in Kelvin. Precipitation plotted in millimeters. Isobars contoured every 2 hPa where contoured.

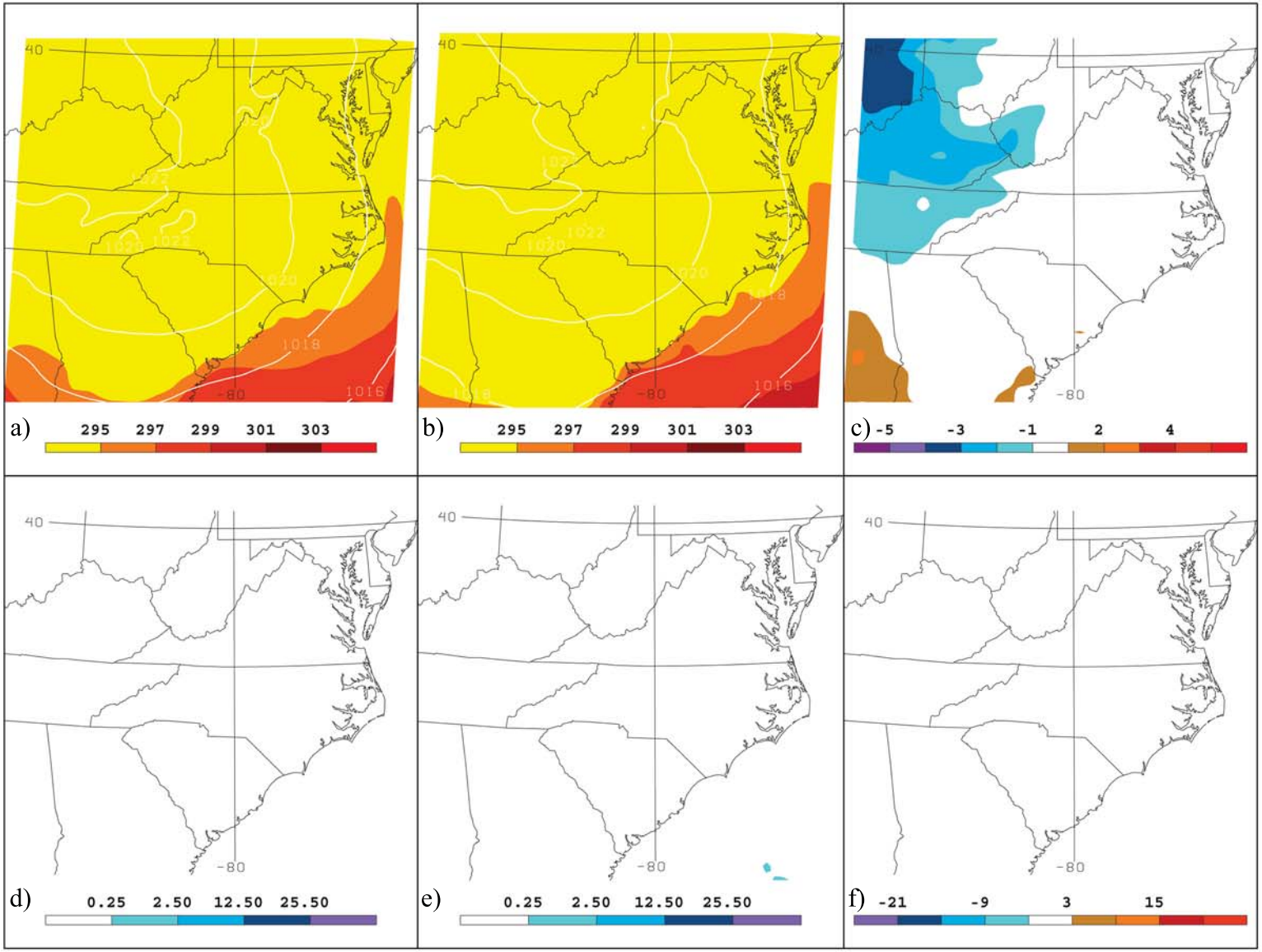
40
-80
1016
1018
1020
1022
a)
295 297 299 301 303
b)
295 297 299 301 303
c)
-5 -3 -1 2 4
d)
0.25 2.50 12.50 25.50
e)
0.25 2.50 12.50 25.50
f)
-21 -9 3 15

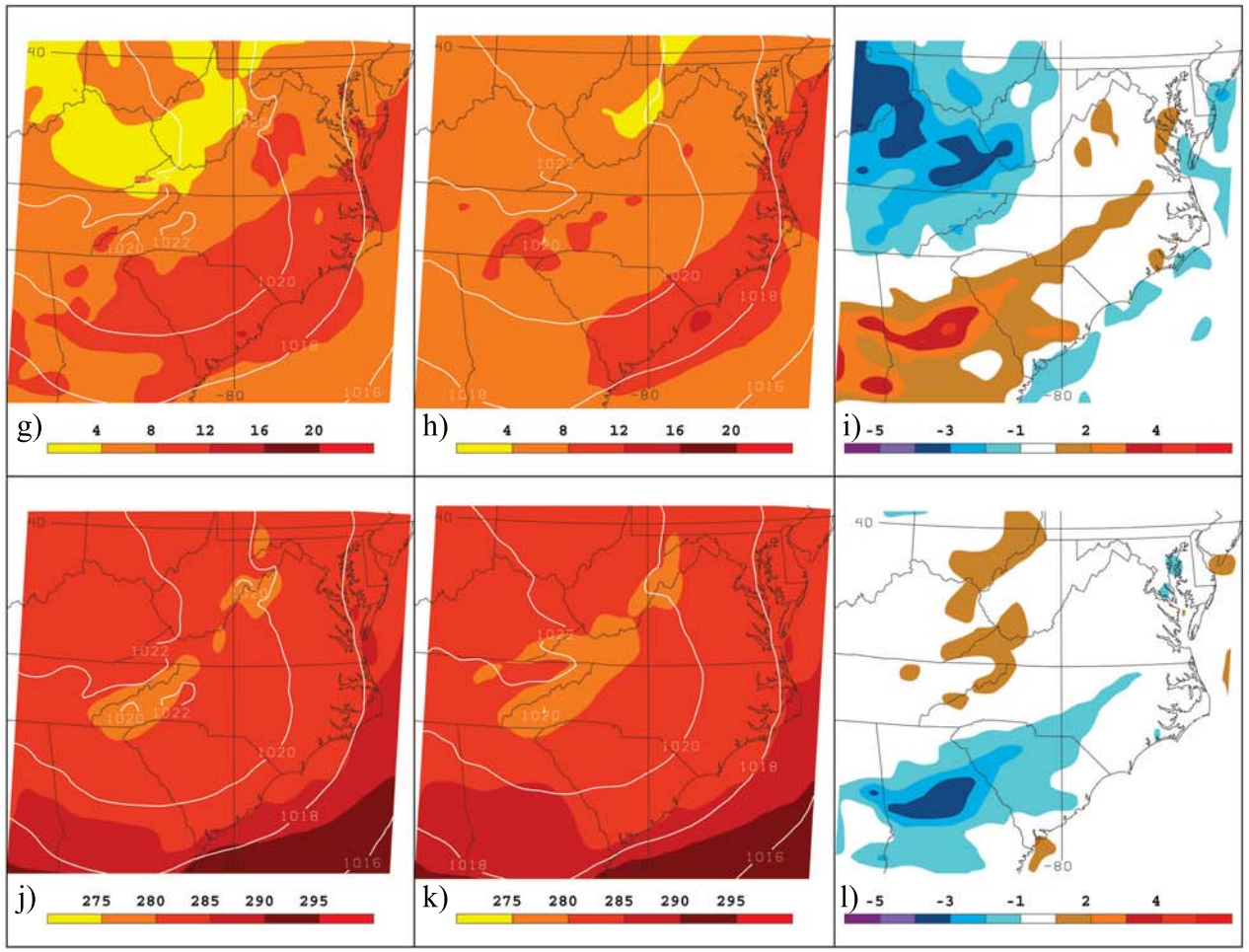


Figure 6.14. 24-hour MM5 forecasts of a) and b): air temperature; c): a minus b; d) and e): 6-hour precipitation; f): d minus e; g) and h): dewpoint depression; i): g minus h; j) and k): dewpoint temperature; and l): j minus k, valid at 1200 UTC 7 August 2004. All temperatures plotted in Kelvin. Precipitation plotted in millimeters. Isobars contoured every 2 hPa where contoured.

## 7. Conclusions and Future Work

The purpose of this study is to develop a weather-based epidemiological model for use as a decision aid to assist turfgrass managers in determining when to apply fungicides to prevent brown patch outbreaks. First, several existing epidemiological models, developed by Schumann et al. (1994) and Fidanza et al. (1996), were tested for their efficacy in North Carolina. Through the use of a variety of meteorological inputs, it was determined that neither epidemiological model would be accurate enough to be used in an operational disease-warning system. However, it was also determined that:

- It is likely that the installation of on-site weather observing equipment will not be necessary whenever an adequate epidemiological model is developed, because disease indices calculated using several off-site meteorological inputs correlated well with indices calculated using on-site meteorological inputs; and
- It is unclear whether the most accurate method of recording brown patch observations is to record the presence of a "smoke ring" once daily as activity, regardless of the size of the patch found, or to measure the incidence of the brown patch, and record activity when that incidence increases from one day to the next.

Data from two separate summers were subjected to several statistical and empirical analyses in an effort to develop a new epidemiological model for brown patch. The two statistical methods utilized in this study had very different base assumptions for their use. The autoregressive model worked under the assumption that brown patch activity was autocorrelated, or that the presence of disease on one day directly impacted the possibility of disease activity being observed the next day. The logistic regression procedure worked under exactly the opposite assumption: that brown patch activity was an independent event, and

activity on previous days had no bearing on the possibility of disease activity on the current day. Neither method was able to show a statistically significant link between any number of combinations of meteorological parameters and brown patch activity. Additionally, an attempt was made to use the assumption that brown patch thrives in hot, humid conditions in order to develop a criterion-based epidemiological model, similar to the $E_6$ index developed in F96. This method, too, was unable to outperform the $E_2$ index developed in F96. High false alarm ratios, regardless of the disease threshold chosen, led to low critical success indices. However, as previously noted, it is suspected that the disease observations themselves may be a source of error in this analysis.

Still working under the assumption that, at some base level, brown patch activity is connected to hot, humid conditions, a model sensitivity study was undertaken using the MM5 model to determine whether or not the prediction of near-surface parameters (such as air temperature and dewpoint) vary based on the parameterizations used for land-surface interaction. It was determined that differences in the way the land-surface models chosen (NOAH LSM vs. 5-layer soil model) calculate soil temperature and moisture content likely led to many of the differences noted between the model runs. In this study, the differences in forecasts of near-surface parameters resulting from altering the land-surface parameterization appear more likely to affect forecasts of epidemiological model output than would changing the source of the weather data.

Recommendations for future work are plentiful for this study. First, the most accurate methodology for collecting observations of disease activity must be determined, as this research showed that the current methodology may need alteration. One possible resolution to this problem would be to install a digital camera on-site that would

automatically photograph the turf at a given time interval (such as every half hour or hour). Image processing software could be used to automatically detect smoke rings, possibly leading to a better understanding of the time scale on which this phenomenon occurs. When this problem is solved, continued efforts to determine the meteorological conditions most favorable for disease activity must be undertaken. It may be even more important, however, to determine those meteorological conditions that are most unfavorable for brown patch activity. Such information would allow for adjustment of the criterion-based epidemiological model developed in this study, lowering false alarms ratios and perhaps leading to a more accurate epidemiological model.

Finally, the prediction of weather-based epidemiological models into the future will greatly increase the utility of such models. It is also important that turfgrass managers, and other end-users of the epidemiological models, have a proper understanding of the limitations these predictions. In this vein, and given the large differences that sometimes occur in model forecasts of near-surface parameters due to alterations of model physics (especially in convective regimes), it may be beneficial to develop an ensemble prediction of epidemiological model output. This would allow for quantification of the uncertainty spoken to earlier; information that would be beneficial for all users.

**8. List of References**

Amerson, P. A., 2001: Plant disease epidemiology. *The Plant Health Instructor*. DOI: 10.1094/PHI-A-2001-0524-01. [available online at http://www.apsnet.org/education/AdvancedPlantPath/Topics/Epidemiology/Epidemiology.htm]

Betts, A. K., 1986: A new convective adjustment scheme. Part I: Observation and theoretical basis. *Quart. J. Roy. Meteor. Soc.*, **112**, 677-691.

_____, and M. T. Miller, 1986: A new convective adjustment scheme. Part II: Single column tests using GATE wave, BOMEX, and Arctic air-mass data. *Quart. J. Roy. Meteor. Soc.*, **112**, 693-709.

Black, T. L., 1994: The new NMC mesoscale Eta Model: Description and forecast examples. *Wea. Forecasting.,* **9**, 265–279.

Bloom, J. R., and H. B. Couch, 1960: Influence of environment on diseases of turfgrass. I. Effect of nutrition, pH, and soil moisture on *Rhizoctonia* brown patch. *Phytopathology*, **50**, 532-535.

Box, G. E. P., and G. M. Jenkins, 1976: *Time Series Analysis: Forecasting and Control*. Holden-Day, San Francisco, CA.

Burpee, L. L., and L. G. Martin, 1992: Biology of *Rhizoctonia* species associated with turfgrass. *Plant Dis.*, **76**, 112-117.

Chen, F. and J. Dudhia, 2001: Coupling an advanced land-surface/hydrology model with the Penn State/NCAR MM5 modeling system. Part I: Model implementation and sensitivity. *Mon. Wea. Rev.*, **129**, 569-585.

Cox, D. R., and E. J. Snell, 1989: *The Analysis of Binary Data*. 2nd ed. Chapman and Hall, London, England.

Dahl, A. S., 1933: Effect of temperature on brown patch of turf. *Phytopathology*, **23**, 8.

desJardins, M. L., Brill, K. F., Jacobs, S., Schotz, S. S., and Bruehl, P., 1992: GEMPAK5 users manual version 5.1. NASA GSFC, National Meteorological Center, Unidata Program Center/UCAR, 267 pp.

Dickinson, L. S. 1930: The effect of air temperature on pathogenicity of *Rhizoctonia solani* parasitizing grasses on putting-green turf. *Phytopathology*, **20**, 597-608.

Dudhia, J., 1996: A multi-layer soil temperature model for MM5. Preprints, *6th PSU/NCAR Mesoscale Model Users' Workshop*, Boulder, CO, Mesoscale and Microscale Meteorology Division, NCAR. [Available on-line from http://www.mmm.ucar.edu/mm5/lsm/soil.pdf.]

_____, Y.-R. Guo, K. Manning, and W. Wang, 2000: PSU/NCAR Mesoscale Modeling System Tutorial Class Notes and User's Guide: MM5 Modeling System Version 3. [Available on-line from http://www.mmm.ucar.edu/mm5.]

Ek, M. B., K. E. Mitchell, Y. Lin, P. Grunmann, E. Rogers, G. Gayno, and V. Koren, 2003: Implementation of the upgraded Noah land-surface model in the NCEP operational mesoscale Eta model. *J. Geophys. Res.*, **108**, 8851, doi:10.1029/2002JD003296.

Fidanza, M. A., P. H. Dernoeden, and A. P. Grybauskas, 1996: Development and field validation of a brown patch warning model for perennial ryegrass turf. *Phytopathology*, **86**, 385-390.

Grell, G. A., Dudhia, J., and Stauffer, D. R., 1994: A description of the fifth-generation Penn State/NCAR Mesoscale Model (MM5). Tech. Note NCAR/TN-398+IA, National Center for Atmospheric Research, Boulder, CO, 122 pp.

Gross, M., J. Santini, I. Tikhonova, and R. Latin, 1998: The influence of temperature and leaf wetness duration on infection of perennial ryegrass by *Rhizoctonia solani*. *Plant Disease*, **86**, 1012-1016.

Hall, R., 1984: Relationship between weather factors and dollar spot of creeping bentgrass. *Can. J. Plant Sci.*, **64**, 167-174.

Hong, S. Y., and H. L. Pan, 1996: Nonlocal boundary layer vertical diffusion in a medium-range forecast model. *Mon. Wea. Rev.*, **124**, 2322-2339.

Jackson, N., 1994: Fungicide usage on golf course turf: The implications in a growing world market. *Proceedings of the Brighton Crop Protection Conference*: 857-864.

Janjic, Z. I., 1994: The step-mountain coordinate model: Further developments of the convection, viscous sublayer, and turbulence closure schemes. *Mon. Wea. Rev.,* **122**, 927–945.

Kerr, A., 1956: Factors influencing the development of brown patch in lawns of *Sagina procumbens* L. *Aust. J. Biol. Sci.*, **9**, 332-339.

Mesinger, F., 1984: A blocking technique for representation of mountains in atmospheric models. *Riv. Meteor. Aeronaut.*, **44**, 195-202.

North Carolina Department of Agriculture and Consumer Services. (2000) *North Carolina Turfgrass Survey*. Neas, K., & Smith, H., Eds. Raleigh, NC.

Nutter, F., H. Cole, Jr., and R. Schein, 1983: Disease forecasting system for warm weather Pythium blight of turfgrass. *Plant Disease*, **67**, 1126-1128.

Piper, C. V., and H. S. Coe, 1919: *Rhizoctonia* in lawns and pastures. *Phytopathology*, **9**, 89-92.

Reisner, J., Rasmussen, R. M., and Bruintjes, R. T., 1998: Explicit forecasting of supercooled liquid water in winter storms using the MM5 mesoscale model. *Quart. J. Roy. Meteor. Soc.,* **124B,** 1071-1108.

Rogers, E., D. G. Deaven, and G. J. DiMego, 1995: The regional analysis system for the operational "early" eta model: Original 80-km configuration and recent changes. *Wea. Forecasting*, **10**, 810-825.

Rowley, L. V., 1991: *Applied Epidemiology of* Rhizoctonia *spp. On Turfgrass*. MS Thesis, University of Massachusetts, Amherst, MA, 95 pp.

SAS Institute, cited 2005: SAS OnlineDoc, version 8. [Available at http://v8doc.sas.com/sashtml/]

Schumann, G., B. Clarke, L. Rowley, and L. Burpee, 1994: Use of environmental parameters and immunoassays to predict *Rhizoctonia* blight and schedule fungicide applications on creeping bentgrass. *Crop Protection*, **13**, 211-218.

Smiley, R., P. Dernoeden, and B. Clarke, 1992: *Compendium of Turfgrass Diseases*. 2nd ed. American Phytopathological Scoeity, St. Paul, MN.

Tredway, L., G. Lackmann, D. Niyogi, and R. Palmieri, 2004: What's the Forecast for Turfgrass Disease Modeling? *Turfgrass Trends*, Aug. 2004 [Available online at http://www.turfgrasstrends.com/turfgrasstrends/article/articleDetail.jsp?id=119613].

Vanderplank, J. E., 1963. *Plant Diseases: Epidemics and Control*. Academic Press, New York.

Zadoks, J. C. and R. D. Schein, 1979: *Epidemiology and Plant Disease Management*. Oxford University Press, New York.